

RICE UNIVERSITY

**Promotion and Control of Angiogenic Activity
in Poly(ethylene glycol) Diacrylate Hydrogels
for Tissue Engineering Applications**

by

Julia Elizabeth Barbick

A THESIS SUBMITTED
IN PARTIAL FULFILLMENT OF THE
REQUIREMENTS FOR THE DEGREE

Doctor of Philosophy

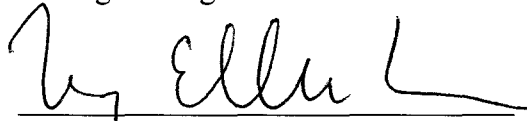
APPROVED, THESIS COMMITTEE:



Jennifer L. West
Cameron Professor, Chair
Bioengineering



K. Jane Grande-Allen, Associate Professor
Bioengineering



Mary Ellen Lane, Assistant Professor
Biochemistry and Cell Biology

HOUSTON, TEXAS
SEPTEMBER 2009

UMI Number: 3421157

All rights reserved

INFORMATION TO ALL USERS

The quality of this reproduction is dependent upon the quality of the copy submitted.

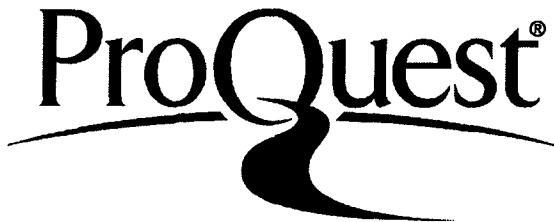
In the unlikely event that the author did not send a complete manuscript and there are missing pages, these will be noted. Also, if material had to be removed, a note will indicate the deletion.



UMI 3421157

Copyright 2010 by ProQuest LLC.

All rights reserved. This edition of the work is protected against unauthorized copying under Title 17, United States Code.



ProQuest LLC
789 East Eisenhower Parkway
P.O. Box 1346
Ann Arbor, MI 48106-1346

ABSTRACT

Promotion and Control of Angiogenic Activity in Poly(ethylene glycol) Diacrylate Hydrogels for Tissue Engineering Applications

by

Julia Elizabeth Barbick

Promotion and control of angiogenic activity have been achieved by covalently linking an angiogenic-signaling protein or peptide to poly(ethylene glycol) diacrylate hydrogels, thereby yielding a system which can be used to develop vascularized, functional engineered tissues. The field of tissue engineering has the capability of providing greatly needed biological organs and tissues for transplantation therapy. In living tissues of physiologically relevant size, metabolically active cells far from a nutrient source undergo necrosis when starved of oxygen and vital nutrients, but the incorporation of microvasculature would allow the production of functional tissues larger than 200 μm , the diffusion limit of oxygen through tissue. By combining a supporting matrix material, signaling factors, and cells, an environment has been created to support the formation and control of endothelial tubes. Poly(ethylene glycol) (PEG)-based hydrogels, which are hydrophilic and resistant to protein adsorption and subsequent non-specific cell adhesion, were modified to contain cell-adhesive ligands and growth factors to support cell and tissue function. Human endothelial cells were cultured in these systems *in vitro*. Covalent immobilization of vascular endothelial growth factor (VEGF) was shown to promote endothelial cell angiogenic activity, including migration, cell-cell

contact formation, and tubule formation, in PEG hydrogels in two and three dimensions. Furthermore, patterning the micron-scale spatial presentation of cell-adhesive ligands and VEGF controlled and accelerated tubule formation. Endothelial tubules formed on restricted patterns less than 70 μm wide showed increased expression of angiogenic receptors VEGFR1, VEGFR2, and EphA2, in addition to increased production and secretion of laminin, a tubule-associated extracellular matrix protein. The incorporation of QK, a synthetic angiogenic peptide, was also shown to promote endothelial cell proliferation and tubulogenesis in two and three dimensions *in vitro* at levels comparable to those achieved through signaling by VEGF. This work improves upon previous research on angiogenic growth factor release from tissue engineering matrices by showing that localized, covalently-bound signaling can promote angiogenesis, thereby providing an engineered, predictable response in a local environment without systemic effects. Additionally, these findings provide a valuable method to incorporate capillary networks throughout tissue engineering matrices to support the continued development of functional tissue-engineered products for clinical use.

ACKNOWLEDGEMENTS

My gratitude is extended to my research advisor, Dr. Jennifer West, and committee members, Dr. Jane Grande-Allen and Dr. Mary Ellen Lane. I am honored and humbled to be working with you on my little part of such a large endeavor. Thank you for supporting my research interests and aspirations. I am truly lucky to be doing exactly what I wanted from the beginning and to have excellent female role models in the fields of engineering and science.

Extreme gratefulness also is given to the knowledgeable and helpful graduate students, post doctoral researchers, and lab technicians who have worked alongside me in our group. Thank you for helping me find new solutions through brain-storming sessions, being patient, and supporting my efforts. Special recognition is given to Dr. James Moon, Stephanie Nemir, and Jennifer Saik, who have worked with me most closely.

My interest in engineering, science, and continued discovery is due to my parents. Thank you for being extremely supportive and loving. I know that most of my success is because you taught me how to be successful.

My husband, Dave, supported my efforts in graduate school and made my life much more pleasurable by standing by me for the past four years. Thank you for following me to Houston, proposing, and marrying me. Now it's time to go home.

This research was supported by a National Science Foundation Graduate Research Fellowship and grants from the National Institute of Health.

TABLE OF CONTENTS

ABSTRACT.....	ii
ACKNOWLEDGEMENTS.....	iv
Chapter 1 Introduction.....	1
CURRENT CLINICAL NEEDS AND SUCCESSES IN TISSUE ENGINEERING....	1
<i>Clinically successful avascular engineered tissues</i>	4
ANGIOGENESIS	7
<i>Initiation</i>	8
<i>Stabilization of Capillaries</i>	14
<i>Vascular Endothelial Growth Factor</i>	15
<i>VEGF Receptors</i>	18
<i>VEGF Mimicking Peptide</i>	21
<i>Summary: Angiogenesis</i>	23
TISSUE ENGINEERING MATRIX MODIFICATIONS TO PROMOTE	
ANGIOGENESIS	24
<i>Growth factor-incorporated matrices</i>	24
<i>Scaffold Material</i>	26
<i>Patterned Ligand Presentation to Control Cell and Tissue Functionality</i>	31
<i>Summary</i>	35
Chapter 2 Covalently immobilized PEG-VEGF promotes endothelial tubulogenesis in	
PEGDA hydrogels	37
INTRODUCTION	37
MATERIALS AND METHODS.....	41
<i>Cell Culture</i>	41
<i>Preparation and Purification of Poly(ethylene glycol) Diacrylate (PEGDA)</i>	41
<i>Preparation and Purification of PEG-succinimidyl carbonate (PEG-SMC)</i>	42
<i>Preparation and Purification of PEG-RGDS</i>	43
<i>Synthesis of Collagenase-Degradable PEG-PQ-PEG</i>	45
<i>Synthesis of PEG-VEGF</i>	45
<i>Bioactivity Assay</i>	46
<i>Formation of PEGDA Hydrogels</i>	47
<i>Surface Modification of PEGDA Hydrogels</i>	47
<i>Quantification of Surface-Immobilized VEGF and RGDS</i>	48
<i>Endothelial Tubule Formation</i>	49
<i>Formation of Three-dimensional Proteolytically Degradable PEG Hydrogels</i>	50
<i>Timelapse Study of Endothelial Tubulogenesis in Three-dimensional Degradable</i>	
<i>PEG Hydrogels</i>	50
<i>VEGF Release Study</i>	51
<i>Chorioallantoic Membrane Assay</i>	52
RESULTS	53
<i>Polymer Characterization</i>	53
<i>Bioactivity of PEG-VEGF</i>	56
<i>Quantification of PEG-VEGF and PEG-RGDS on the Surface of Hydrogels</i>	57

<i>Surface-immobilized VEGF Promotes Tubulogenesis</i>	57
<i>Immobilized VEGF in 3D Degradable Hydrogels Promotes Cell Motility, Cell-Cell Contact Formation, and Tubulogenesis</i>	61
<i>VEGF Release</i>	68
<i>CAM Assay</i>	69
DISCUSSION	71
CONCLUSIONS	76
Chapter 3 Micron-scale Spatially Patterned, Covalently Immobilized VEGF on Hydrogels Accelerates Endothelial Tubulogenesis and Increases Cellular Angiogenic Responses	78
INTRODUCTION	78
<i>Micron-scale Patterning Techniques</i>	82
MATERIALS AND METHODS	87
<i>Cell Culture</i>	87
<i>Preparation and Purification of Poly(ethylene glycol) Diacrylate (PEGDA)</i>	87
<i>Preparation and Purification of Acryl-PEG-Succinimidyl Carbonate</i>	88
<i>Preparation and Purification of PEG-RGDS</i>	89
<i>Synthesis of PEG-VEGF</i>	89
<i>Synthesis of PEG-RGDS-Fluor</i>	90
<i>Formation of PEGDA Hydrogels</i>	90
<i>Laser Scanning Lithography Patterning of Ligand Surface Immobilization</i>	91
<i>Quantification of Surface-Immobilized VEGF and RGDS</i>	93
<i>Endothelial Tubule Formation and Quantification of Angiogenic Markers</i>	94
RESULTS	97
<i>Polymer Characterization</i>	97
<i>Photolithographic Patterning of Ligand Surface Immobilization</i>	97
<i>Endothelial Response to Patterned PEG-RGDS and PEG-VEGF</i>	98
<i>Cell-surface Markers and Protein Expression</i>	105
DISCUSSION AND CONCLUSIONS	109
Chapter 4 An Immobilized VEGF Fragment, PEG-KLTWQELYQLKYKGI, Promotes Microvasculature Formation in Poly(ethylene glycol) Diacrylate Hydrogels	111
INTRODUCTION	111
MATERIALS AND METHODS	115
<i>Cell Culture</i>	115
<i>Preparation and Purification of Poly(ethylene glycol) Diacrylate (PEGDA)</i>	115
<i>Preparation and Purification of PEG-succinimidyl carbonate (PEG-SMC)</i>	116
<i>Preparation and Purification of PEG-QK</i>	116
<i>Preparation and Purification of PEG-RGDS</i>	117
<i>Synthesis of Collagenase-Degradable PEG-PQ-PEG</i>	117
<i>Synthesis of PEG-VEGF</i>	118
<i>Bioactivity Assay</i>	118
<i>Formation of PEGDA Hydrogels</i>	119
<i>Surface Modification of PEGDA Hydrogels</i>	120
<i>Quantification of Surface-Immobilized QK, VEGF, and RGDS</i>	120
<i>Endothelial Tubule Formation</i>	121
<i>Formation of Three-dimensional Proteolytically Degradable PEG Hydrogels</i>	122

<i>Time lapse Study of Endothelial Tubulogenesis in Three-dimensional Degradable PEG Hydrogels</i>	123
<i>Zymography Analysis of MMPs Present in 3D Time Lapse Culture Medium</i>	124
RESULTS	125
<i>Polymer Characterization</i>	125
<i>Bioactivity of PEG-QK Determined by Pro-mitotic Effects</i>	125
<i>Quantification of PEG-QK, PEG-VEGF, and PEG-RGDS on the Surface of Hydrogels</i>	127
<i>Surface-immobilized VEGF Promotes Tubulogenesis</i>	127
<i>Immobilized QK in 3D Collagenase-Degradable Hydrogels Promotes Tubulogenesis and Cell-Cell Contact Formation</i>	132
<i>Zymography Analysis of MMPs Present in 3D Time lapse Culture Medium</i>	140
DISCUSSION AND CONCLUSIONS	142
Chapter 5 Conclusions and Future Directions	146
THESIS SUMMARY	146
CONCLUSIONS.....	147
FUTURE DIRECTIONS	151
References.....	156

List of Figures

FIGURE 1-1 TISSUE ENGINEERING USES A MULTI-PART METHOD OF COMBINING CELLS, SIGNALS, AND MATRIX	2
FIGURE 1-2 TOP LEFT) HISTOLOGY SHOWING ~1415 μM HT29 SPHEROID WITH NECROTIC CORE AT 18 D. TOP RIGHT) HISTOLOGY SHOWING ~1480 μM Co112 SPHEROID WITH NECROTIC CORE AT 24 D. PO_2 MICROELECTRODE PROFILES OF TUMOR CELL SPHEROIDS. BOTTOM LEFT) HT29 SPHEROIDS OF DIAMETER > 2000 μM . BOTTOM RIGHT) Co112 SPHEROIDS OF 1000-2000 μM . ARROWS SHOW THE SURFACE OF THE SPHEROID. NOTE THE DRASTIC DROP IN OXYGEN AVAILABILITY INSIDE TISSUE SPHEROIDS. FROM [SUTHERLAND 1986].	3
FIGURE 1-3 DERMAGRAFT IS A CLINICALLY AVAILABLE TISSUE ENGINEERED PRODUCT. BECAUSE THE GRAFT IS THIN, CELLS CAN RELY ON DIFFUSION FOR TRANSPORT OF NUTRIENTS, OXYGEN, AND WASTE. FROM [WWW.ADVANCEDBIOHEALING.COM].	4
FIGURE 1-4 CAPILLARY BEDS CONNECT ARTERIAL AND VENOUS VASCULATURE, ENSURING CONVECTIVE TRANSPORT OF NUTRIENTS AND OXYGEN THROUGHOUT TISSUES. ANGIOGENESIS, THE FORMATION OF THESE CAPILLARIES, OCCURS NATURALLY IN THE BODY IN RESPONSE TO BIOCHEMICAL SIGNALS. FROM [ESTRELLAMOUNTAIN.EDU].	7
FIGURE 1-5 CAPILLARY NETWORKS FORMED UNDER NORMAL CONDITIONS ARE “PATTERNED” BY THE BODY TO OPTIMIZE TRANSPORT. FROM [JAIN 2005].	7
FIGURE 1-6 BLOOD VESSEL TYPES ORIGINATE FROM (A) ENDOTHELIAL TUBES, WHICH ARE STABILIZED BY PERICYTES AND BASEMENT MEMBRANE TO FORM (B) CAPILLARIES. CAPILLARIES CAN REMODEL INTO (C) LARGER VESSELS, WHICH REQUIRE MORE STRENGTH, DERIVED FROM SMOOTH MUSCLE CELLS AND FIBROUS TISSUE. FROM [JAIN 2003].	8
FIGURE 1-7 NEW CAPILLARIES FORM WHEN PRE-EXISTING CAPILLARY ENDOTHELIAL CELLS SPROUT IN RESPONSE TO CHEMOKINES SECRETED BY HYPOXIC CELLS (ADAPTED FROM [GERHART 2005]).	8
FIGURE 1-8 THE PLASMINOGEN ACTIVATOR-PLASMIN SYSTEM LEADS TO CONTROLLED CELL-MEDIATED DEGRADATION OF ECM PROTEINS.	12
FIGURE 1-9 PROTEIN STRUCTURE OF VEGF_{165} . FROM [MULLER 1997]. VEGF_{165} IS A HOMODIMER WITH MW ~40 kDa. ALTERNATIVE GENE SPLICING OF THE VEGF GENE YIELDS SEVERAL ISOTOPES, WHICH ALL FORM HOMODIMERS OF VARYING BIOACTIVITY LEVELS.	16
FIGURE 1-10 LIGAND-RECEPTOR INTERACTIONS WITHIN THE VEGF FAMILY ARE PART OF A COMPLEX REGULATORY SYSTEM. FROM [ZACHARY 2005].	19
FIGURE 1-11 VEGFR-2, VEGFR-1, AND NEUROPOLIN-1 BIND VEGF_{165} , LEADING TO INITIATION AND REGULATION OF ANGIOGENESIS. FROM [ZACHARY 2005].	20
FIGURE 1-12 INTEGRINS, VEGFR-2, AND VE-CADHERIN BINDING INITIATE INTRACELLULAR SIGNALING PATHWAYS DURING ANGIOGENESIS. FROM [ZACHARY 2005].	20
FIGURE 1-13 CONFORMATION OF QK. SUPERPOSITION OF 20 QK PEPTIDES [D'ANDREA 2005]. QK WAS DESIGNED TO ASSUME AN α -HELIX CONFORMATION IN SOLUTION.	21
FIGURE 1-14 BINDING OF IODINATED VEGF WITH CELL MEMBRANE EXTRACT WHEN IN COMPETITION WITH QK. INCREASING AMOUNTS OF QK DECREASE VEGF BINDING, INDICATING COMPETITIVE BINDING.	22
FIGURE 1-15 PECAM STAINING OF ENDOTHELIAL TUBES FORMED ON MATRIGEL WITH QK OR VEGF (100 NG/ML) IN MEDIUM. BOTH FIGURES FROM [D'ANDREA 2005].	22
FIGURE 1-16 POLY(ETHYLENE GLYCOL) DIACRYLATE. CARBONS PARTICIPATING IN DOUBLE BONDS IN ACRYLATE GROUPS AT ENDS OF CHAIN ARE REACTIVE TO FORM CROSSLINKS IN A FREE RADICAL-INITIATED POLYMERIZATION SCHEME.	28
FIGURE 1-17 IDEALIZED NETWORK CROSSLINKING OF PEGDA CHAINS. CROSSLINKING OCCURS BETWEEN THE CARBONS IN THE ACRYLATE GROUPS AT THE END OF EACH POLYMER CHAIN. FROM [PADMAVATHI 1996].	29
FIGURE 1-18 BIOMIMETIC PEG HYDROGELS CAN CONTAIN PROTEOLYTICALLY-DEGRADABLE SEQUENCES AND COVALENTLY LINKED CELL INTEGRIN LIGANDS AND GROWTH FACTORS. CELLS CAN BE ENCAPSULATED AT THE TIME OF HYDROGEL FORMATION DUE TO THE BIOCOMPATIBLE PHOTOPOLYMERIZATION PROCESS.	30
FIGURE 1-19 PHOTOLITHOGRAPHIC PATTERNING REQUIRES A MASK TO CONTROL EXPOSURE OF LIGHT TO THE PHOTO-SENSITIVE SUBSTRATE BELOW.	32

FIGURE 1-20 A) PHOTOPOLYMERIZATION OF SURFACE-IMMOBILIZED LIGANDS VIA SINGLE-PHOTON EXCITATION PROVIDED BY CONFOCAL MICROSCOPY. B) EXCITATION IS MOST PRECISE AT THE FOCAL PLANE (FROM JORDAN MILLER).....	33
FIGURE 1-21 ENDOTHELIAL CELLS FORMED TUBE-LIKE STRUCTURES WITH LUMENS (ARROWS) ON LINES OF PATTERNED SURFACE-ADSORBED FIBRONECTIN WITH LINE WIDTH OF 10 μm BUT NOT 30 μm . FROM [DIKE 1999].....	34
FIGURE 2-1 RELEASE OF GROWTH FACTORS COMPARED TO MATRIX-BOUND SEQUESTERING. RELEASE LEADS TO A SINK EFFECT IN WHICH GROWTH FACTOR CONCENTRATION IS QUICKLY DECREASED WITHIN THE MATRIX, AND GROWTH FACTORS CONTINUE TO DIFFUSE TO OTHER, UNWANTED AREAS IN THE BODY. IN CONTRAST, MATRIX BOUND GROWTH FACTORS REMAIN LOCALIZED, AT ENGINEERED CONCENTRATIONS TO YIELD DESIRED EFFECTS.....	40
FIGURE 2-2 PEGDA SYNTHESIS OCCURS THROUGH A REACTION OF POLY(ETHYLENE GLYCOL) AND ACRYLOYL CHLORIDE. THE PRODUCT IS A PEG CHAIN WITH REACTIVE END GROUPS THAT ALLOW CROSSLINKING OF CHAINS INTO NETWORKS.....	42
FIGURE 2-3 PEG-NHS REACTION WITH PEPTIDE RGDS. THE NHS END GROUP ON THE PEG CHAIN LEAVES, ALLOWING COVALENT BINDING TO A FREE AMINE IN THE PEPTIDE, YIELDING A PEG-PEPTIDE MOLECULE.	44
FIGURE 2-4 PEG-SMC REACTION WITH VEGF PROTEIN. THE REACTION YIELDS A PEG-PROTEIN MOLECULE.	46
FIGURE 2-5 GEL PERMEATION CHROMATOGRAPHY ANALYSIS OF PEG-RGDS CONJUGATION. BLACK LINE, WITH PEAK AT 7 SHOWS MOLECULAR WEIGHT DISTRIBUTION OF CONJUGATED PEG-RGDS. RED LINE WITH MAIN PEAK AT 7.5 SHOWS MOLECULAR WEIGHT DISTRIBUTION OF PEG-NHS. SUCCESSFUL CONJUGATION IS SHOWN BY A SHIFT IN THE PEAK, INDICATING INCREASE IN MOLECULAR WEIGHT, AND LACK OF PEG-NHS PEAK IN PEG-RGDS SAMPLE.....	54
FIGURE 2-6 GEL PERMEATION CHROMATOGRAPHY ANALYSIS OF PEG-PQ-PEG. SHIFT OF PEAK TO LEFT INDICATES INCREASE OF MOLECULAR WEIGHT AND HYDRODYNAMIC SIZE OF POLYMER WITH PEPTIDE.	55
FIGURE 2-7 WESTERN BLOT OF PEGYLATED VEGF COMPARED TO NATIVE VEGF SHOWS A SUBSTANTIAL INCREASE IN MOLECULAR WEIGHT, INDICATING PEGYLATION OF THE PROTEIN.	55
FIGURE 2-8 PROLIFERATION OF HUVEC CELLS IN RESPONSE TO SOLUBLE PEG-VEGF. MEDIUM CONTAINING SOLUBLE PEG-VEGF PROMOTED AN INCREASE IN CELL NUMBER AS COMPARED TO THE NO VEGF CONTROL. PEG-VEGF SHOWED STATISTICALLY SIMILAR RESULTS TO UNPEGYLATED VEGF. * $p < 0.01$, ** $p < 0.05$	56
FIGURE 2-9 A) BRANCHING ENDOTHELIAL TUBULE NETWORKS FORMED ON THE SURFACE OF HYDROGELS MODIFIED WITH RGDS AND VEGF AT 19 D. B) FEWER TUBULES FORMED ON HYDROGELS MODIFIED WITH RGDS ONLY AT 19 D. SCALE BAR = 500 μm	59
FIGURE 2-10 ENDOTHELIAL TUBE ON HYDROGEL SURFACE STAINED WITH PHALLOIDIN (RED) AND DAPI (BLUE). WHITE LINE INDICATES CROSS-SECTIONAL VIEW IN FIGURE 2-11.	60
FIGURE 2-11 CROSS-SECTION OF TUBE STRUCTURE ON THE SURFACE OF HYDROGEL. ARROW POINTS TO TUBE STRUCTURE RISING ABOVE PLANE OF SURROUNDING SPREAD CELLS.	60
FIGURE 2-12 QUANTIFICATION OF TUBULOGENESIS SHOWS A SIGNIFICANT ENDOTHELIAL CELL RESPONSE TO IMMOBILIZED VEGF ON THE SURFACE OF PEGDA HYDROGELS. HYDROGELS MODIFIED WITH VEGF AND RGDS WERE CULTURED IN VEGF-FREE MEDIA. ERROR BARS SHOW STANDARD DEVIATION. (ANOVA $p < 0.01$, TUKEY'S LEAST SIGNIFICANT DIFFERENCE BETWEEN VEGF GROUP AND BOTH RGDS GROUPS $p < 0.05$).....	61
FIGURE 2-13 TIME SERIES OF CONFOCAL IMAGES ILLUSTRATING CELL BEHAVIOR IN 3D COLLAGENASE-DEGRADABLE PEG HYDROGELS. WHITE ARROWS POINT TO CELL MIGRATION AND CELL-CELL CONTACT FORMATION. YELLOW ARROWS SHOW PATHS OF CELL MIGRATION AND TUBULE FORMATION. CELLULAR MIGRATION, CELL-CELL CONTACT FORMATION, AND BRANCHING TUBE FORMATION INSIDE COLLAGENASE-DEGRADABLE PEGDA HYDROGELS MODIFIED WITH PEG-VEGF AND RGDS. SCALE BAR = 100 μm	63
FIGURE 2-14 TIME SERIES OF CONFOCAL IMAGES ILLUSTRATING CELL BEHAVIOR IN 3D COLLAGENASE-DEGRADABLE PEG HYDROGELS. WHITE ARROWS POINT TO CELL MIGRATION AND CELL-CELL CONTACT FORMATION. YELLOW ARROWS AND LINES SHOW PATHS OF CELL MIGRATION AND TUBULE FORMATION. ACCELERATED ANGIOGENIC ACTIVITY AND HYDROGEL DEGRADATION IN RESPONSE TO A 5-FOLD INCREASE IN ATTACHED PEG-VEGF. SCALE BAR = 100 μm	64

FIGURE 2-15 TIME SERIES OF CONFOCAL IMAGES ILLUSTRATING CELL BEHAVIOR IN 3D COLLAGENASE-DEGRADABLE PEG HYDROGELS. LESS CELLULAR ACTIVITY IN HYDROGELS MODIFIED WITH RGDS ONLY. SCALE BAR = 100 μ M.	65
FIGURE 2-16 THREE-DIMENSIONAL CONFOCAL IMAGE OF ENDOTHELIAL TUBE STRUCTURES FORMED AT 27 H IN 3D COLLAGENASE-DEGRADABLE PEG HYDROGELS MODIFIED WITH VEGF AND RGDS. CELLULAR STRUCTURES WERE STAINED WITH DAPI (BLUE) AND PHALLOIDIN (RED) TO VISUALIZE CELL NUCLEI AND ACTIN FILAMENTS, RESPECTIVELY. SCALE BAR = 20 μ M.	66
FIGURE 2-17 QUANTIFICATION OF ANGIOGENIC ACTIVITY IN 3D COLLAGENASE-DEGRADABLE PEG HYDROGELS SHOWS A SIGNIFICANT ENDOTHELIAL CELL MIGRATION AND CELL-CELL CONTACT RESPONSE TO IMMOBILIZED VEGF (400 PMOL/ML) BOUND WITHIN THE HYDROGEL. HYDROGELS WERE CULTURED IN VEGF-FREE MEDIA. ERROR BARS SHOW STANDARD DEVIATION. (* $p < 5.45 \times 10^{-7}$, ** $p < 0.006$).	67
FIGURE 2-18 VEGF RELEASE PROFILE OF PEGDA HYDROGELS INITIALLY CONTAINING 2 μ G VEGF SHOWS AN INITIAL BURST WITHIN THE FIRST 8 HOURS. THIS RELEASE PROFILE ALLOWS THE HYDROGEL TO PROVIDE AN INITIAL LARGER DOSE OF GROWTH FACTOR SIGNALING, FOLLOWED BY A SLOW, LONG LASTING RELEASE OF SIGNALING TO SURROUNDING TISSUE.	69
FIGURE 2-19 MICROGRAPHS OF CAM MICROVASCULATURE RESPONSE TO HYDROGELS. A) CONTROL GEL, NO VEGF. B, C, D) VEGF-LOADED HYDROGELS. THE CAM ANGIOGENIC RESPONSE TO RELEASED VEGF FROM PEGDA HYDROGELS PROMOTES GROWTH OF NATIVE CAPILLARIES TOWARDS THE HYDROGEL. 6.4X MAGNIFICATION.	70
FIGURE 3-1 CAPILLARY NETWORKS FORMED UNDER NORMAL CONDITIONS ARE “PATTERNED” BY THE BODY TO OPTIMIZE TRANSPORT. FROM [JAIN 2005].	79
FIGURE 3-2 NEW CAPILLARIES FORM WHEN PRE-EXISTING CAPILLARY ENDOTHELIAL CELLS SPROUT IN RESPONSE TO CHEMOKINES SECRETED BY HYPOXIC CELLS (ADAPTED FROM [GERHART 2005]).	79
FIGURE 3-3 PHOTOLITHOGRAPHIC PATTERNING REQUIRES A MASK TO CONTROL EXPOSURE OF LIGHT TO THE PHOTO-SENSITIVE SUBSTRATE BELOW.	83
FIGURE 3-4 PROCESS OF MICROCONTACT PRINTING [FROM WHITESIDES 2001]. “STAMP AND INK” METHOD OF CREATING MICRON-SCALE PATTERN ON SILICON OR GLASS SURFACES. THIS PROCESS IS MOST SUCCESSFUL ON HARD SURFACES, WHICH DO NOT MIMIC ELASTIC PROPERTIES OF NATURAL EXTRACELLULAR MATRIX.	84
FIGURE 3-5 EXCITATION PROVIDED BY SINGLE-PHOTON LASER. THE EXCITATION AND SUBSEQUENT PHOTOPOLYMERIZATION IS CONTROLLED BY ALIGNING THE FOCAL PLANE OF THE LASER BEAM WITH THE INTERFACE OF THE HYDROGEL AND POLYMER SOLUTION. NO MASK OR STAMP IS USED, THEREBY ALLOWING FACILE ADJUSTMENT OF PATTERNS VIA SOFTWARE (FROM JORDAN MILLER).	86
FIGURE 3-6 SCHEMATIC OF PATTERNED SURFACE MODIFICATION PROCESS OF PEG HYDROGELS. HYDROGEL DISKS WERE PLACED ON TOP OF SURFACE-MODIFYING POLYMER SOLUTION. A LASER WAS FOCUSED ONTO THE INTERFACE OF THE HYDROGEL DISK AND POLYMER SOLUTION BY UTILIZING CONFOCAL MICROSCOPY. THE LASER WAS SCANNED ACROSS USER-DEFINED REGIONS OF INTEREST TO CONTROL PHOTOPOLYMERIZATION AND SUBSEQUENT SURFACE MODIFICATION TO RESTRICTED AREAS.	92
FIGURE 3-7 PATTERNED REGIONS OF INTEREST USED TO COMMAND LASER SCANNING SOFTWARE ON ZEISS LIVE 5 OR LSM 510 CONFOCAL MICROSCOPES. PHOTOPOLYMERIZATION WAS LOCALIZED TO THESE REGIONS OF INTEREST, THUS ENSURING PATTERNED AREAS OF RGDS AND VEGF ON THE SURFACE OF HYDROGELS.	93
FIGURE 3-8 CONFOCAL IMAGES OF LSL PATTERNS, WITH ATTACHED AND FLUORESCENTLY LABELED CELLS. LSL PATTERNS ARE FLUORESCENT DUE TO INCORPORATION OF FLUORESCENT EOSIN Y, USED AS THE PHOTOINITIATOR FOR THE POLYMERIZATION CROSSLINKING REACTION BETWEEN THE PEGDA HYDROGEL BASE AND THE PEG-RGDS AND PEG-VEGF MODIFYING THE SURFACE. SCALE BAR = 100 μ M.	98
FIGURE 3-9 PHASE CONTRAST IMAGE OF PATTERNED ENDOTHELIAL CELLS. CELLS PATTERNED ON ~10 μ M LINES OF RGDS AND VEGF FORMED CAPILLARY-LIKE STRUCTURES BY DAY 2, WHILE THOSE ALLOWED TO SPREAD TO ~100 μ M REMAINED IN A COBBLESTONE MORPHOLOGY. SCALE BAR = 100 μ M.	100
FIGURE 3-10 QUANTIFICATION OF TUBULE FORMATION BY DAY 2 ON PATTERNED AREAS. WIDTH OF AREA OF ATTACHED CELLS ACTS AS A SWITCH TO PROMOTE TUBULE FORMATION, WITH TUBULES FORMING ONLY ON AREAS LESS THAN 100 μ M.	101

FIGURE 3-11 QUANTIFICATION OF THE EFFECT OF PATTERN SIZE ON TUBULE FORMATION. ALL PATTERNED LINES LESS THAN 35 μm PROMOTED TUBULE FORMATION. AS THE PATTERN SIZE INCREASES, THE PERCENTAGE OF PATTERNS THAT PROMOTE TUBULE FORMATION DECREASES. FOR PATTERNS BETWEEN 35 AND 70 μm , PATTERNS WITH RGDS AND VEGF PROMOTE MORE TUBULE FORMATION THAN RGDS ONLY. ERROR BARS SHOW STANDARD DEVIATION ($\text{SD}=\text{SQUARE ROOT}(\text{PQ}/\text{N})$, WHERE P=PROPORTION OF SUCCESS, Q=PROPORTION OF FAILURE, N=SAMPLE SIZE). STATISTICAL DIFFERENCES ($\text{p}<0.01$) BETWEEN ALL GROUPS EXCEPT GROUPS SHOWING 100% TUBULE FORMATION (RGDS, RGDS & VEGF 1-35 μm).	101
FIGURE 3-12 ENDOTHELIAL CELLS PATTERNED TO FORM BRANCHING UNIT. SCALE BAR = 100 μm .	102
FIGURE 3-13 VOLUME RENDERINGS. THREE DIMENSIONAL IMAGES OF ENDOTHELIAL TUBULES FORMED ON THIN PATTERNED LINES OF RGDS AND VEGF. THESE IMAGES SUGGEST THAT THE TUBULE HAS BEGUN TO DETACH FROM THE HYDROGEL, WHICH MAY BE PART OF THE TUBULOGENIC PROCESS. IMAGES ALSO SHOW VACUOLE FORMATION IN SURROUNDING CELLS ATTACHED TO THIN LINES, WHICH IS AN EARLIER STEP BEFORE TUBULOGENESIS.	103
FIGURE 3-14 VOLUME RENDERING. THREE DIMENSIONAL IMAGE OF ENDOTHELIAL TUBE FORMED ON THIN PATTERNED LINE OF RGDS ONLY. ALTHOUGH SOME TUBULE-LIKE STRUCTURES FORMED BY DAY 2 ON RGDS ONLY LINES, NO PATENT LUMENS WERE OBSERVED.	103
FIGURE 3-15 VISUALIZATION OF ACTIN FILAMENTS (RED) IN TUBULE FORMED ON PATTERNED RGDS AND VEGF. A) TOP VIEW AND CROSS-SECTION OF TUBULE SHOWS LUMEN. B) TOP VIEW AND CROSS-SECTION OF CELL FORMING VACUOLE. RED LINE SHOWS REGION OF CROSS-SECTION.	104
FIGURE 3-16 VISUALIZATION OF ACTIN FILAMENTS (RED) AND DAPI (BLUE) IN TUBULES FORMED ON PATTERNED RGDS ONLY. CELLS CULTURED ON ONLY RGDS WERE NOT OBSERVED TO FORM TUBULES WITH CONTINUOUS LUMENS. SCALE BAR = 10 μm . RED LINES SHOWS REGION OF CROSS-SECTION.	104
FIGURE 3-17 CONFOCAL IMAGES OF FLUORESCENT IMMUNOCYTOCHEMISTRY. CELLS ON BOTH THIN AND THICK PATTERNED LINES ON THE SAME SAMPLE WERE FIXED AT DAY 2 AND STAINED EITHER FOR A & B) VEGFR1 (WHITE), C&D) VEGFR2 (GREEN), AND EPHA7 (RED) OR E & F) FIBRONECTIN (WHITE), G & H) LAMININ (RED), AND PECAM (GREEN). BACKGROUND SIGNALS ARISE FROM INCORPORATED EOSIN Y, WHICH WAS USED AS THE PHOTOINITIATOR; THE BACKGROUND SIGNAL WAS SUBTRACTED BEFORE QUANTIFICATION.	107
FIGURE 3-18 ANALYSIS OF PROTEIN EXPRESSION OF SIX ANGIOGENIC PROTEINS AND CELL SURFACE RECEPTORS EXPRESSED BY ENDOTHELIAL CELLS ON PATTERNED LINES AT DAY 2. FLUORESCENT IMMUNOCYTOCHEMISTRY IMAGES WERE ANALYZED FOR INTENSITY OF PIXELS IN IMAGES TO QUANTIFY EXPRESSION OF ANGIOGENIC CELL SURFACE RECEPTORS AND PROTEINS. INCREASED EXPRESSION WAS DETERMINED FOR VEGFR1, VEGFR2, EPHA7, AND LAMININ. * $\text{p}<0.05$ USING STUDENT'S T-TEST COMPARISON BETWEEN THIN AND WIDE LINES WITHIN EACH MARKER CATEGORY.	108
FIGURE 4-1 CONFORMATIONAL STRUCTURE OF QK IN WATER FROM [D'ANDREA 2005]. THE DESIGNED PEPTIDE ASSUMES AN α -HELIX CONFORMATION, WHICH IS REQUISITE FOR ITS BIOACTIVITY.	112
FIGURE 4-2 BIOACTIVITY OF PEG-QK WAS DETERMINED BY MEASURING ITS PRO-MITOTIC EFFECTS ON ENDOTHELIAL CELLS. PEG-QK SHOWED STATISTICALLY SIMILAR RESULTS TO VEGF IN PROMOTING CELL PROLIFERATION, AS DETERMINED BY CELL NUMBER AFTER TREATMENT. CELLS WERE TREATED WITH EGM-2 MEDIUM WITHOUT VEGF AND FGF, WITH ADDED PEG-QK, QK, OR VEGF FOR 4 H. CELLS WERE THEN CULTURED IN EGM-2 MEDIUM WITHOUT VEGF AND FGF FOR 2 D. CELLS WERE STAINED WITH HOECHST 33342 NUCLEAR DYE AND IMAGED. CELL NUMBER WAS ANALYZED, AND ANOVA, FOLLOWED BY TUKEY'S LEAST SIGNIFICANT DIFFERENCE POST-HOC ANALYSIS SHOWED SIGNIFICANT DIFFERENCES BETWEEN EXPERIMENTAL GROUPS (* $\text{p}<0.05$, ** $\text{p}<0.01$).	126
FIGURE 4-3 A) BRANCHING ENDOTHELIAL TUBULE NETWORKS FORMED ON THE SURFACE OF HYDROGELS MODIFIED WITH RGDS AND QK AT 5 D. B) FEWER TUBULES FORMED ON HYDROGELS MODIFIED WITH RGDS ONLY AT 5 D.	129
FIGURE 4-4 SURFACE ENDOTHELIAL TUBULE FORMATION AT DAY 5 ON THE SURFACE OF MODIFIED PEGDA HYDROGELS. PEG-QK PROMOTED AN ACCELERATION OF TUBULE FORMATION COMPARED TO PEG-VEGF. * $\text{p}<0.05$ BETWEEN GROUPS, FOLLOWING ANOVA AND TUKEY'S LEAST SIGNIFICANT DIFFERENCE ANALYSIS.	130

FIGURE 4-5	CONFOCAL IMAGES OF TUBULE NETWORKS ON THE SURFACE OF PEG-QK GELS. CELLS WERE LABELED WITH PHALLOIDIN (RED) AND DAPI (BLUE) TO VISUALIZE ACTIN CYTOSKELETON AND NUCLEI, RESPECTIVELY. TUBULES WERE CONFIRMED TO RISE ABOVE THE PLANE OF SPREAD CELLS ON THE HYDROGEL SURFACE. LOW LEVELS OF DAPI AND PHALLOIDIN ARE SEEN IN BACKGROUND FROM SPREAD CELLS.	131
FIGURE 4-6	TIME SERIES OF CONFOCAL IMAGES ILLUSTRATING CELL BEHAVIOR IN 3D COLLAGENASE-DEGRADABLE PEG HYDROGELS. WHITE ARROWS POINT TO CELL MIGRATION, CELL-CELL CONTACT FORMATION, AND TUBULE FORMATION. YELLOW ARROWS AND LINES SHOW PATH OF CELL MIGRATION AND NETWORK FORMATION. CELLULAR MIGRATION, CELL-CELL CONTACT FORMATION, AND BRANCHING TUBE FORMATION INSIDE COLLAGENASE-DEGRADABLE	133
FIGURE 4-7	TIME SERIES OF CONFOCAL IMAGES ILLUSTRATING CELL BEHAVIOR IN 3D COLLAGENASE-DEGRADABLE PEG HYDROGELS. WHITE ARROWS POINT TO CELL MIGRATION, CELL-CELL CONTACT FORMATION, AND TUBULE FORMATION. YELLOW LINES SHOW PATH OF NETWORK FORMATION. ANGIOGENIC ACTIVITY IN RESPONSE TO A 5-FOLD INCREASE IN ATTACHED PEG-QK. SCALE BAR = 50 μ M	134
FIGURE 4-8	TIME SERIES OF CONFOCAL IMAGES ILLUSTRATING CELL BEHAVIOR IN 3D COLLAGENASE-DEGRADABLE PEG HYDROGELS. WHITE ARROWS POINT TO CELL MIGRATION, CELL-CELL CONTACT FORMATION, AND TUBULE	135
FIGURE 4-9	TIME SERIES OF CONFOCAL IMAGES ILLUSTRATING CELL BEHAVIOR IN 3D COLLAGENASE-DEGRADABLE PEG HYDROGELS. LESS CELLULAR ACTIVITY IN HYDROGELS MODIFIED WITH RGDS ONLY. SCALE BAR = 50 μ M.	136
FIGURE 4-10	PEG-QK AND PEG-VEGF PROMOTE ENDOTHELIAL TUBULE NETWORK FORMATION IN 3D COLLAGENASE-DEGRADABLE HYDROGELS, BUT PEG-RGDS DOES NOT. ASTERISK SIGNIFIES STATISTICAL SIGNIFICANCE OF $p < 0.05$ BETWEEN QK GROUPS AND RGDS AS WELL AS VEGF AND RGDS. COMPARISONS WERE MADE BETWEEN RESULTS FROM THE SAME TIME POINT (22 H v 22 H AND 32 H v 32 H). THE DROP IN TUBULE LENGTH WITHIN THE VEGF EXPERIMENTAL GROUP BETWEEN 22 H AND 32 H WAS ALSO STATISTICALLY SIGNIFICANT ($*p < 0.05$). THE DROPS IN TUBULE LENGTH IN THE QK GROUPS WERE NOT STATISTICALLY SIGNIFICANT.	138
FIGURE 4-11	CELL-CELL CONTACT FORMATION MAY RESPOND TO INCLUSION OF QK OR VEGF. RESULTS OF CELL-CELL CONTACT FORMATION FOLLOW TRENDS OF TUBULE LENGTH, SUGGESTING A RELATIONSHIP BETWEEN THE TWO. NO GROUP HAD SIGNIFICANTLY MORE CELL-CELL CONTACTS FORMED DURING THE EXPERIMENTAL OBSERVATION FROM 2-32 H.	138
FIGURE 4-12	SEVERAL DOWNSTREAM PATHWAYS EXIST AFTER VEGFR-2 DIMERIZATION. PHOSPHORYLATION OF SPECIFIC TYROSINE RESIDUES DETERMINES WHICH PATHWAYS ARE ACTIVATED. ACTIVATION OF THE PATHWAY FOR GENE EXPRESSION, DIFFERENTIATION, PROLIFERATION, AND TUBE FORMATION, AS OBSERVED WITH PEG-QK, IS THE RESULT OF PHOSPHORYLATION OF Y1175, THE MOST IMPORTANT TYROSINE RESIDUE [SIEKMANN 2008]. OTHER PATHWAYS LEAD TO MIGRATION AND ACTIN REMODELING, WHICH WOULD BE RESPONSIBLE FOR CELL-CELL CONTACT FORMATION. ADAPTED FROM [SIEKMANN 2008].	139
FIGURE 4-13	ZYMOGRAM OF MMPs PRESENT IN CULTURE MEDIUM FROM 3D COLLAGENASE-DEGRADABLE HYDROGELS WITH ENCAPSULATED ENDOTHELIAL CELLS. MMPs WERE RUN ON A GELATIN GEL, THEREBY ALLOWING VISUALIZATION OF PRO- AND ACTIVE FORMS OF MMP-2 AND MMP-9, BOTH OF WHICH ARE ACTIVE DURING ANGIOGENESIS.	140
FIGURE 5-1	PEG-VEGF HAS BEEN USED IN A MURINE CORNEA MODEL BASED ON WORK REPORTED IN THIS THESIS. RESULTS SHOW THAT THE INCORPORATION OF RELEASED VEGF AND PEG-VEGF IN COLLAGENASE-DEGRADABLE HYDROGELS PROMOTES INFILTRATION OF SURROUNDING CAPILLARIES FROM THE CORNEA LIMBUS. MICROVASCULATURE IS VISUALIZED BY USING GENETICALLY ALTERED MICE WITH FLUORESCENT ENDOTHELIAL CELLS. FROM [MOON 2009].	153

List of Tables

TABLE 1-1 AMINO ACID SEQUENCES OF VEGF-VEGFR1 BINDING SITE AND QK SYNTHETIC PEPTIDE. FROM [D'ANDREA 2005].....	22
TABLE 4-1 PEPTIDE SEQUENCE COMPARISON OF VEGF15, WHICH IS THE EXACT VEGFR1 BINDING SEQUENCE FOUND IN VEGF165, AND QK, WHICH IS THE PEPTIDE WITH SOME AMINO ACID SUBSTITUTIONS TO ENSURE AN α -HELIX CONFORMATION IN WATER.	112

Chapter 1 Introduction

CURRENT CLINICAL NEEDS AND SUCCESSES IN TISSUE ENGINEERING

In 2006, 130,527 patients were on the organ transplant wait list in the United States. Although 28,291 organs were transplanted, 7,191 patients died while waiting for an available acceptable organ [U.S. Organ Procurement and Transplantation Network 2007]. The supply of organs through organ donation clearly does not meet the demand. The supply of available transplantable organs and tissues could be augmented by manufacturing functional tissues, with a goal of surpassing current standards of allograft transplantation, by reducing graft rejection and possible disease transmission associated with donated organ transplants.

The field of tissue engineering aims to generate functional tissues and organs in the lab for replacement therapy. To achieve this end, tissue engineers generally use a multi-part method of combining cells, signals, and matrix material (Figure 1-1). Appropriate cells may be harvested from the patient or a healthy donor via biopsy. Incorporated signals to cells could be chemical, biological, mechanical, or electrical, or more likely, a tissue-specific combination of these. The types of materials used for matrices can be natural, synthetic, or a mixture. This combination of materials provides an environment for tissue to grow successfully into functional tissue that can perform metabolic and tissue-specific functions when transplanted into the body.

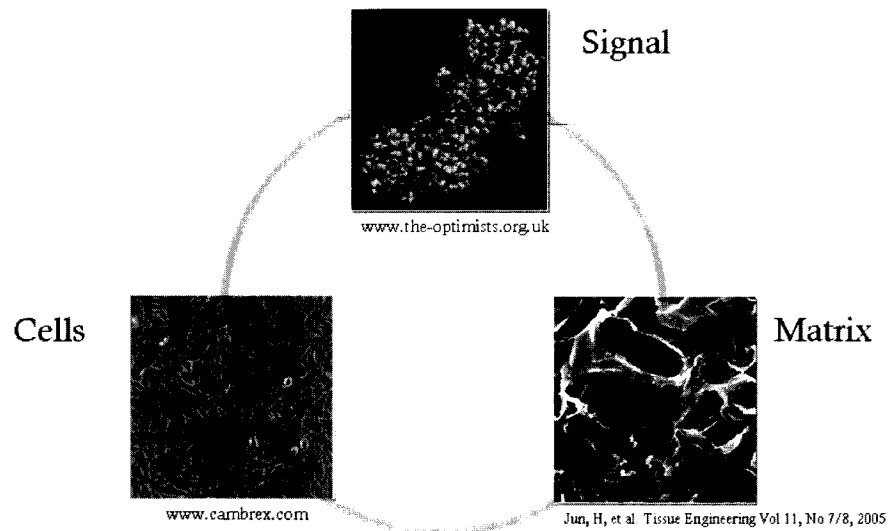


Figure 1-1 Tissue engineering uses a multi-part method of combining cells, signals, and matrix materials to create functional tissues.

Current clinical achievements in tissue engineering include skin [Marston 2003], commercially available as Dermagraft [www.advancedbiohealing.com], and bladder [Atala 2006]. It should be noted, however, that these engineered tissues are successful only because they are thin and can rely on diffusion rather than vascularization for transport of nutrients, oxygen, and waste. Some avascular tissues such as cartilage can be produced without microvasculature [carticel.com, Behrens 2006]; however, most other tissues require vasculature. *In vivo*, cells are generally within 100 μm of a capillary [Sieminski 2005] so that they receive adequate nutrients and oxygen. Microvasculature is required for tissues larger than 200 μm [Jain 2005]; otherwise cells undergo necrosis caused by low nutrient and oxygen supply in addition to build-up of waste products due to the diffusion limits of these molecules in tissue. Sutherland et al. showed that the partial pressure of oxygen drops rapidly from the surrounding medium to the center of

tumor cell spheroids (Figure 1-2). Depending on cell metabolism and oxygen requirements, the partial pressure of oxygen (PO_2) drops by 50% within the outside 50-100 μm -wide rim of spheroids [Sutherland 1986].

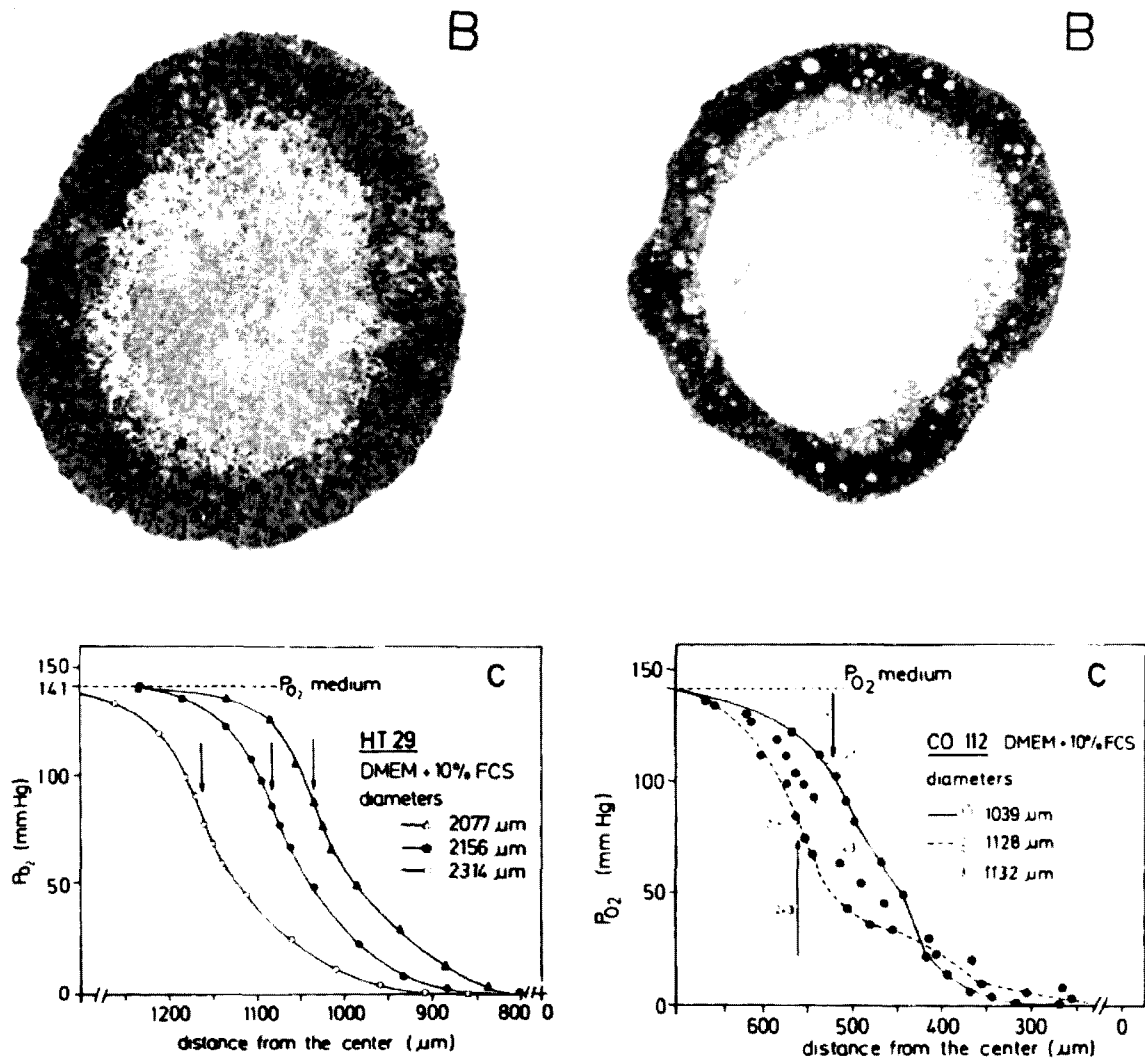


Figure 1-2 Top left) Histology showing ~1415 μm HT29 spheroid with necrotic core at 18 d. Top right) Histology showing ~1480 μm Co112 spheroid with necrotic core at 24 d. PO_2 microelectrode profiles of tumor cell spheroids. Bottom left) HT29 spheroids of diameter > 2000 μm . Bottom right) Co112 spheroids of 1000-2000 μm . Arrows show the surface of the spheroid. Note the drastic drop in oxygen availability inside tissue spheroids. From [Sutherland 1986].

Since tissues cannot depend solely on diffusion for transport, microvascularization must be considered a requirement for three-dimensional engineered tissues; however, the incorporation of microvascularization in engineered tissues is currently a roadblock to successfully engineering functional tissues. Meeting the challenge of microvascularization will allow the acceleration of tissue engineering technologies. The work presented in this thesis outlines several strategies to incorporate such microvascular networks into tissue engineered products. Understanding the functionality of avascular engineered tissues transplanted into patients and subsequent clinical outcomes provides insight into the potential applications of vascularized engineered tissues.

Clinically successful avascular engineered tissues



Figure 1-3 Dermagraft is a clinically available tissue engineered product. Because the graft is thin, cells can rely on diffusion for transport of nutrients, oxygen, and waste. From [www.advancedbiohealing.com].

As noted, avascular tissues, including the bladder wall and thin layers of dermal tissue (Figure 1-3), have been transplanted into human patients. These tissues have yielded improvements in patient outcome, yet full functionality is yet to be achieved. Engineered bladder tissues were successfully implanted in young humans (age 4-19 yr) requiring augmentive cystoplasty [Atala 2006]. Cells from each patient were taken as a biopsy, grown in culture, and seeded on a bladder-shaped collagen-polyglycolic acid scaffold. The engineered tissue was cultured for 7 weeks

before implantation. The constructs were 2 mm in width, which is thicker than what can be supported by diffusion alone [Atala 2006]. During surgery, omentum, a double layer of peritoneum connecting abdominal organs [Bantam Medical Dictionary], was wrapped around the implanted tissue. Due to its rich blood supply, omentum is used in plastic surgery to support vascularization of flaps and grafts. Bladder function was followed for 22-61 months with favorable results. Engineered constructs that were wrapped in omentum yielded better mechanical results than those without the covering, presumably from better transport of nutrients and oxygen to the construct from direct contact with the omentum and its blood supply [Atala 2006].

Another engineered tissue, Dermagraft, is an engineered dermal graft composed of neonatal fibroblasts cultured on a synthetic bioabsorbable polyglactin matrix [Marston 2003, www.advancedbiohealing.com]. The seeded fibroblasts secrete collagen, other extracellular matrix (ECM) components, and growth factors, which are incorporated into the graft. The neonatal cells used in the graft have undeveloped HLA surface markers and were therefore chosen because they are not expected to promote a rejection immune response. The product is stored via cryopreservation, but contains living, metabolically-active cells upon thawing and application. Marston et al. showed that weekly applications of Dermagraft significantly increased wound closure in diabetic foot ulcers during a 12 week study. In the 245-patient, 35-center single-blinded study, graft rejection was not observed [Marston 2003]. In this case, the events of wound healing, which involve active formation of capillaries, most likely led to the body infiltrating the avascular tissue with vasculature. In unhealthy patients who may be suffering from

several pathologies including slow wound healing, relying on host vascularization of thick engineered tissues is not a viable option.

To provide better function of these promising therapeutics, tissue engineered products must be vascularized. Tissue engineering technologies have produced pioneering successes in engineered tissues in the clinical setting; however, these tissues relied on nutrients and oxygen from surrounding blood supplies in the host. The field of tissue engineering has widely accepted that microvascularization, the formation of blood capillary networks, is and will be a requirement for certain functional engineered tissues. Furthermore, *in vitro* microvascularization allows quality control of the product before implantation, whereas relying on post-operative microvascularization in the body introduces an increased risk of transplant failure. The work presented in this thesis shows that *in vitro* microvascularization of engineered tissues may be achieved by mimicking the natural process of capillary formation *in vivo*, angiogenesis. The study of angiogenesis provides useful information about natural signals and cell types which could be incorporated into tissue engineering scaffolds.

ANGIOGENESIS

Angiogenesis is the formation of capillaries from pre-existing capillaries or capillary cells *in vivo*. Capillaries form networks to allow transport of nutrients, oxygen, and waste throughout tissue, connecting arterial and

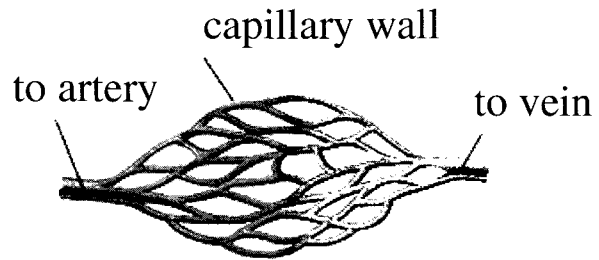


Figure 1-4 Capillary beds connect arterial and venous vasculature, ensuring convective transport of nutrients and oxygen throughout tissues. Angiogenesis, the formation of these capillaries, occurs naturally in the body in response to biochemical signals. From [estrellamountain.edu].

venous vasculature to ensure nutrient and oxygen transport via convection (Figure 1-4, Figure 1-5). Endothelial cells respond to biochemical angiogenic signals such as vascular endothelial growth factor (VEGF) to form endothelial tubes, which are later stabilized by mural cells (Figure 1-6).

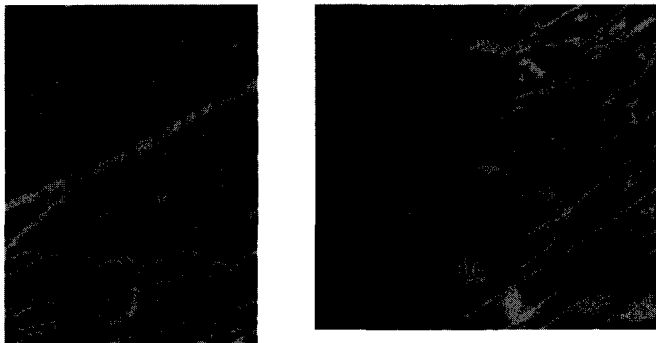


Figure 1-5 Capillary networks formed under normal conditions are “patterned” by the body to optimize transport. From [Jain 2005].

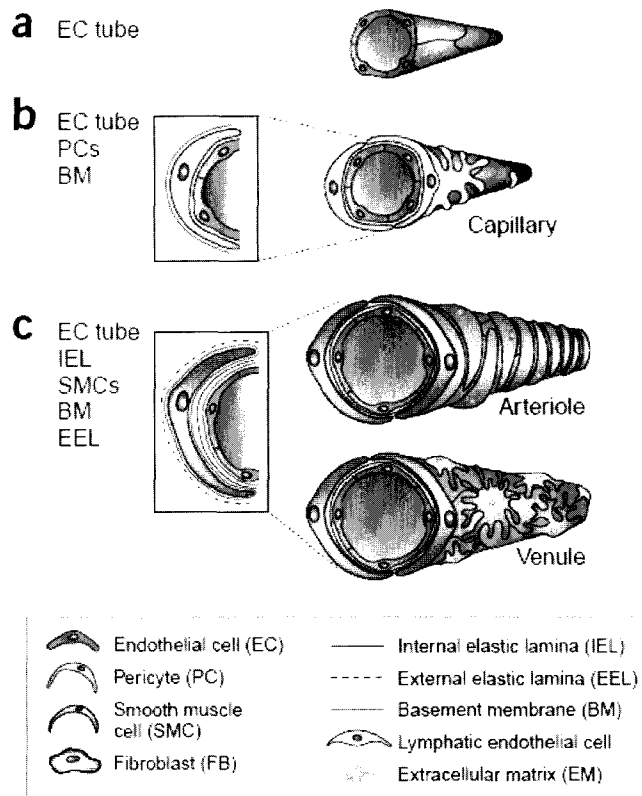


Figure 1-6 Blood vessel types originate from (a) endothelial tubes, which are stabilized by pericytes and basement membrane to form (b) capillaries. Capillaries can remodel into (c) larger vessels, which require more strength, derived from smooth muscle cells and fibrous tissue. From [Jain 2003].

Initiation

New capillary formation does not frequently occur in adults, unless under conditions of wound healing, tumor growth, or inflammation [Ausprunk 1977]. Capillary growth occurs due to endothelial cell proliferation

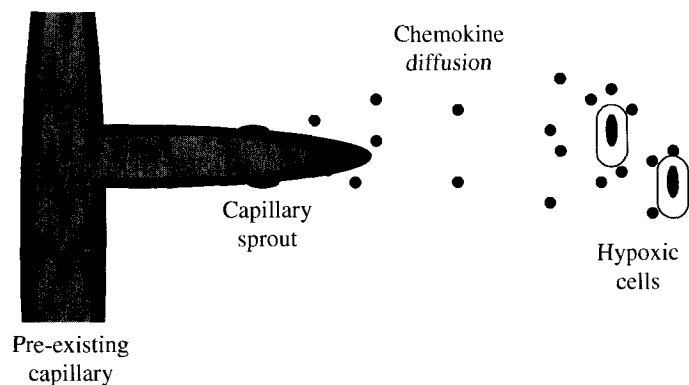


Figure 1-7 New capillaries form when pre-existing capillary endothelial cells sprout in response to chemokines secreted by hypoxic cells (adapted from [Gerhart 2005]).

and migration [Cliff 1963]. In pioneering studies of angiogenesis, Ausprunk and Folkman found that, in response to implanted tumor tissue in rabbit cornea, quiescent endothelial cells would alter to mitosis-indicative morphology at one day after implantation and begin extending processes and migrating towards the tumor tissue by Day 2 (Figure 1-7). They discovered that pre-existing endothelial cells would begin migrating before proliferating. Between Days 2 and 3, leakage of blood vessels was observed. Capillary buds formed by Day 4, and many new capillaries were observed by Day 6. Once small capillary buds are formed, migration of cells is found primarily in the pioneering tips of the capillaries, while cells behind these, in the walls of the capillary, proliferate to compensate for gaps leading to leakiness [Ausprunk 1977].

Several angiogenic signals are involved in initiating the cellular response of migration and proliferation to form endothelial tubes. Additionally, cell-secreted proteases release ECM-bound biochemical signals and cleave ECM proteins to allow gaps for cell migration. Initiation of angiogenesis occurs via soluble mitogens [Folkman 1987]. Tissue regions receiving low nutrients and oxygen signal to existing capillaries to “bud” and extend to reach the hypoxic region. Gene expression of VEGF is induced by low oxygen tension, as mediated through hypoxia-inducible factor (HIF)-1 [Ferrara 2003]. Secreted VEGF diffuses to existing capillary endothelial cells [Gerhart 2005], where it promotes endothelial permeability, mitosis, and angiogenesis [Keck 1989]. Increased permeability leads to leakiness of vasculature, which allows a provisional fibrin matrix for migrating endothelial cells [Roy 2006]. Once endothelial cells in the capillary bud begin migrating, the remaining cells must proliferate to ensure that the forming tube maintains integrity. Several growth factors support VEGF expression and are thus

implicated in angiogenesis as well. Angiogenic growth factors are often secreted by nearby pericytes and lymphocytes [Robinson 2001]. VEGF mRNA expression is upregulated by transforming growth factor (TGF)- α , TGF- β , insulin-like growth factor-1, fibroblast growth factor (FGF), platelet derived growth factor (PDGF), epidermal growth factor, and keratinocyte growth factor [Ferrara 2003]. Brogi et al. determined that treatment of vascular smooth muscle cells with PDGF-BB or TGF- β increases VEGF and bFGF gene expression. This explains the *in vivo* proangiogenic effect of these growth factors whereas, *in vitro*, PDGF-BB is not mitogenic for endothelial cells, and TGF- β actually inhibits endothelial cell proliferation [Brogi 1994]. Pertovaara et al. showed that TGF- β induces VEGF gene and protein expression in fibroblast and epithelial cells [Pertovaara 1994], further showing the *in vivo* interplay of several growth factors and cell types involved in angiogenesis. These other angiogenic growth factors are not triggered by hypoxia; VEGF is likely the only signal in hypoxia-induced angiogenesis [Brogi 1994, Enholm 1997]. Additionally, only VEGF is found at all sites of angiogenesis, and the spatial and temporal events of angiogenesis are closely tied only to VEGF levels [Robinson 2001].

For the initial steps of angiogenesis, endothelial cells must remodel the basement membrane between the endothelium and mural cells, the fibrin-composed matrix resulting from fibrinogen leaked from the vasculature, and the target tissue ECM. Indeed, local degradation of the ECM occurs before proliferation and migration of capillary EC [Robinson 2001]. The major ECM components of the vascular basement membrane include type IV collagen, type XV collagen, type XVIII collagen, laminins, nidogen/enactin, heparin-sulfate proteoglycans, perlecan, and secreted protein acidic and

rich in cysteine (SPARC). These ECM components are cleavable by matrix metalloproteinase (MMP)-2, -3, and -9 activity. During fibronolysis, plasmin, MMP-3, -7, -8, -12, -13, and membrane type (MT)1-MMP are active. MT1-MMP also cleaves interstitial collagens, and when overexpressed in endothelial cells (EC), stimulates migration, invasion, and tubulogenesis. MMP activity is one of earliest and most sustained events in angiogenesis; indeed, MMP and gelatinase (MMP-2 and -9) activity is necessary to initiate angiogenesis [Roy 2006].

VEGF promotes endothelial secretion of interstitial collagenase and urokinase- and tissue plasminogen activators [Pepper 1991]. The plasminogen activator – plasmin system is composed of tissue plasminogen activator (tPA) and urokinase plasminogen activator (uPA), which act on the substrate plasminogen, and plasminogen activator inhibitors (PAIs) [Roy 2006]. VEGF, bFGF [Pepper 1991], and TGF- β [van Hinsbergh 2005] promote expression of ECM proteases including u-PA and PAI-1. tPA, located in the ECM, and uPA, located on the cell surface due to its interaction with its cell surface receptor, uPAR, activate plasminogen to form plasmin, which can then cleave fibrin, laminin, collagen, fibronectin, and proteoglycans. Plasmin can also proteolytically cleave and activate MMPs (Figure 1-8). uPAR and MMP-9 have been implicated in the migration of capillary cells and the formation of capillary-like structures [Roy 2006].

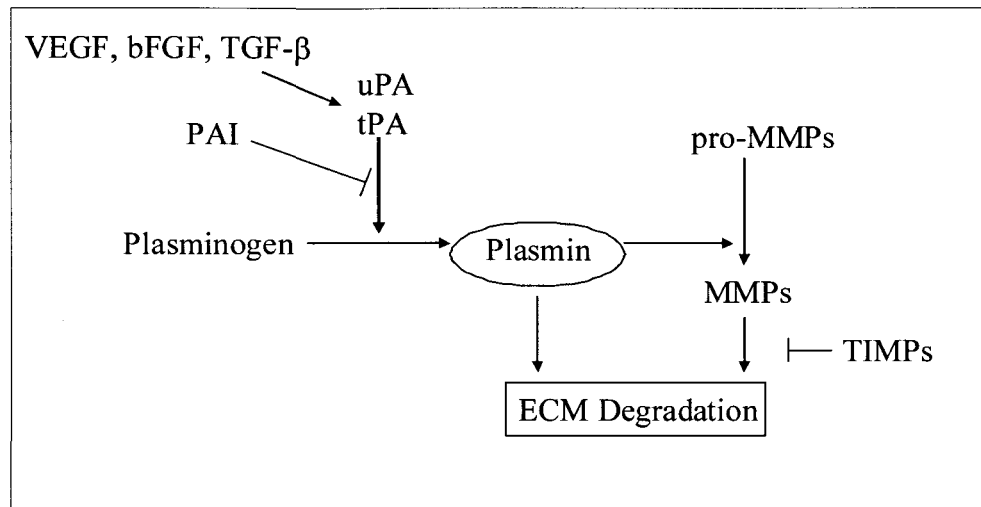


Figure 1-8 The plasminogen activator-plasmin system leads to controlled cell-mediated degradation of ECM proteins.

MMPs are produced by endothelial cells, and MMP expression can be regulated by VEGF and bFGF; however, MMPs can also regulate growth factor availability, function, and ligand-receptor interactions. Cytokines are synthesized as biologically inactive pro-forms, which must be cleaved by proteases to be converted to biologically active forms. VEGF and basic FGF (bFGF or FGF-2) bind to ECM through heparin binding sites, and MMPs can release these matrix-bound growth factors from the ECM. VEGF₁₆₅ binds to connective tissue growth factor (CTGF), which can be cleaved by MMP-1, -3, and -13 [Roy 2006]. Plasmin may also release bound VEGF₁₆₅, VEGF₁₈₉, and bFGF from the ECM [Houck 1992].

The localization of growth factors in the ECM has been shown to guide vessel formation [Jain 2003, Houck 1992]. FGF-2 accumulates at areas of capillary branching [Fernandez 2005], and so may play a role in patterning capillary geometry. Indeed, location of VEGF seems to affect cell function, as cleaved, soluble VEGF₁₆₅ induces EC

proliferation, while matrix-bound VEGF₁₆₅ promotes vascular sprouting and branching [Roy 2006]. Therefore, VEGF localization in tissue engineered matrices is a potential approach for inducing microvascularization.

Protease activity also affects other angiogenic molecules; perlecan-bound bFGF is released by MMP-1 and -3, while MT1-MMP degrades betaglycan to release TGF β , a strong mediator of fibrogenesis. MMP-1, -2, -3, and -11 can release insulin-like growth factor (IGF) from IGF binding proteins. Vascular endothelial (VE) cadherin regulates vascular integrity, EC migration, capillary tube formation, and VEGFR-2 activity. The alteration of VE-cadherin during angiogenesis may be MMP-dependent [Roy 2006].

As in most physiological processes, angiogenesis must be regulated to avoid pathophysiologies. MMPs also play a role in regulation, as they can downregulate angiogenesis by cleaving plasminogen and collagen XVIII into angiostatin and endostatin, which inhibit angiogenesis. Additionally, the biological activity of cytokines can also be downregulated by MMPs. MMP-2 can cleave the extracellular domain of FGF receptor-1, negatively regulating angiogenesis [Roy 2006]. TGF- β has also been shown to be anti-angiogenic, as it can control the bioavailability of proteases, their inhibitors, and matrix proteins to resist angiogenesis [van Hinsbergh 2005]. The initiation of angiogenesis clearly is driven by many, sometimes competing factors. Once endothelial tubes are formed, however, they must be stabilized by supporting cells to prevent regression of the new network.

Stabilization of Capillaries

Mural cells, which include vascular smooth muscle cells (vSMC) in large vessels and pericytes in capillaries, are suggested to be important in stabilizing primitive endothelial tubes [Betsholtz 2005]. Proposed functions of pericytes include sensing mechanical forces from blood flow and regulating blood flow through contraction. They may signal to endothelial cells to control EC proliferation and differentiation, as well as deposit ECM [Betsholtz 2005].

Mural cells originate in mesodermal tissue throughout the body, with the exception of the head, where their origin is ectodermal [Betsholtz 2005]. Mesenchymal perivascular cells secrete angiopoietin-1, which signals endothelial cells through Tie-2 receptor binding [Fernandez 2005]. TGF- β promotes differentiation of embryonic mural progenitor cells from the mesenchyme to a vSMC [Betsholtz 2005] or pericyte phenotype *in vitro* [van Hinsbergh 2005]. This mode of activation occurs *in vivo* during vasculogenesis [Betsholtz 2005], during which formation of capillaries occurs from the recruitment of progenitor capillary cells.

Pre-existing mural cells can also proliferate and migrate to the location of capillary formation through signaling of platelet derived growth factor B (PDGF-B), which is transduced through platelet derived growth factor receptor β (PDGFR β). The recruitment occurs through a paracrine signaling system, where EC secrete PDGF-B, and pericytes express PDGFR β . Angiogenesis promotes this co-recruitment [Betsholtz 2005]. Pericytes then form a single-cell layer around the endothelial tube [Jain 2003], stabilizing the immature endothelial tubes and preventing regression.

Pericytes are not required for endothelial tube sprouting; however, studies of angiogenesis in the central nervous system (CNS) show that vessels lacking pericytes are unstable, experiencing abnormalities such as endothelial hyperplasia, abnormal endothelial cell junctions, increases in vesicle transport, increased leakage of plasma and erythrocytes, and increases in variability of diameter and tortuosity of developing endothelial tubes. Endothelial tubes lacking pericytes also exhibit excess luminal membrane. VEGF upregulation occurs to compensate for lack of PDGF-B, and may cause some of these events; however, endothelial hyperplasia and abnormal capillary diameter occur before VEGF is upregulated. In retinal angiogenesis, when PDGF-B is not locally retained, the capillary network contains fewer sprouts and branching points [Betsholtz 2005]. While it is clear that the formation of endothelial tubes is a vital first step in forming functional microvasculature, the maturation of these vessels is equally critical.

Vascular Endothelial Growth Factor

To incorporate angiogenic signaling factors into a functional tissue-engineered product, their structures and functions must be understood. While many signaling factors are involved in this complex process, vascular endothelial growth factor (VEGF) plays the most vital role in promoting initiation of microvasculature. VEGF (Figure 1-9) was isolated by its role in promoting proliferation of endothelial cells and permeability in vascular endothelium [Keck 1989, Conn 1972, Leung 1989, Lobb 1985, Plouet 1989, Senger 1990]. Initially named vascular permeability factor (VPF), VEGF was found to

induce permeability in the vasculature within minutes. Lobb et al. suggested that it acted directly on endothelial cells [Lobb 1985]. Keck et al. found similarities between VPF₁₈₉ and the B chain of platelet-derived growth factor (PDGF-B). It was suggested that VPF₁₈₉ had a similar tertiary structure to PDGF-B. The gene for human VEGF is found on chromosome 6p21.3 [Vincenti 1996]. Human VPF₁₈₉, composed of 189 amino acids, shared “low but significant” similarity in DNA sequence with PDGF-B, PDGF-A, and



Figure 1-9 Protein structure of VEGF₁₆₅. From [Muller 1997]. VEGF₁₆₅ is a homodimer with MW ~40 kDa. Alternative gene splicing of the VEGF gene yields several isotopes, which all form homodimers of varying bioactivity levels.

other proteins related to the PDGF/*v-sis*

oncogene family, but was not similar in

genetic code to aFGF, bFGF, TGF- β ,

epidermal growth factor (EGF), or platelet-

derived endothelial cell growth factor.

VPF₁₈₉ and PDGF's polypeptide similarities

include several arginine- and lysine- rich

regions in the COOH-terminal areas, which

could be acted on by serine proteases [Keck

1989]. As such, proteolysis of hVPF₁₈₉ near

the COOH-terminal could allow variations

in VPF₁₈₉.

VEGF is secreted by cells as a homodimer composed of covalently linked monomers [Robinson 2001], linked by a disulphide bond between Cys51 of one monomer and Cys61 of the other [Pötgens 1994]. Houck et al. showed that alternative splicing of mRNA and subsequent proteolysis yield several lengths of VEGF: VEGF₁₂₁, VEGF₁₆₅, VEGF₁₈₉, and VEGF₂₀₆. Compared to VEGF₁₆₅, VEGF₁₂₁ lacks amino acids

116-159, and VEGF₁₈₉ has an insertion of 24 amino acids at amino acid #116. VEGF₁₂₁, VEGF₁₆₅, and VEGF₁₈₉ share identical N-terminal hydrophobic signals comprised of 26 amino acids. VEGF₁₂₁ was determined to be secreted and soluble in the extracellular fluid while VEGF₁₈₉ was secreted but remained bound to the cell surface or the extracellular matrix. VEGF₁₆₅ was found to be secreted and showed both solubility and binding, with ~50-70% bound. VEGF₁₆₅ and VEGF₁₈₉ can bind to heparin-containing proteoglycans. Plasmin treatment frees VEGF₁₆₅ and VEGF₁₈₉ from a bound form to a soluble 34 kDa bioactive dimer. VEGF₁₂₁ is weakly acidic, while VEGF₁₆₅ and VEGF₁₈₉ are increasingly more basic, which may affect their ability to bind heparin [Houck 1992]. Most VEGF-expressing cells secrete only VEGF₁₂₁, VEGF₁₆₅, and VEGF₁₈₉ [Robinson 2001].

Human VEGF₁₈₉ promotes permeability, mitosis, and angiogenesis, and thus was hypothesized to act during wound healing [Keck 1989]. VEGF has been shown to promote angiogenesis in the chick chorioallantoic membrane (CAM) model [Ferrara 1989]. Promotion of angiogenesis or vasculogenesis by VEGF may depend on the dose of VEGF administered [Springer 1998]. Elcin et al. found that at three weeks after implantation in rats, PLGA sponges containing 2 µg VEGF contained fewer capillaries than those containing 4 µg VEGF [Elcin 2006]. Springer et al. found that constant high VEGF serum levels *in vivo* via gene delivery promoted processes resembling embryonic vasculogenesis, the formation of blood pools and hemangiomas, in non-ischemic tissue, while lower serum levels had no effect on vessel number or size in adjacent non-ischemic tissue [Springer 1998]. These results suggest that the amount of VEGF incorporated into a therapy must be precisely determined, controlled, and preferentially localized. VEGF

has specificity for endothelial cells, which are the only cells with receptors responsive to this ligand [Ferrara 1989]. *In vitro*, VEGF promotes vasodilation due to nitric oxide production by endothelial cells [Ferrara 2003]. The effects of VEGF are due to VEGF interactions with cell surface receptors, which start a signaling cascade.

VEGF Receptors

Signaling by VEGF is considered a rate-limiting step in the initiation of angiogenesis [Ferrara 2003]. VEGF binds to two receptors, kinase domain receptor (KDR or VEGFR-2) and Fms-like tyrosine kinase (Flt-1 or VEGFR-1) [Ferrara 1997] (Figure 1-10). VEGF receptors are found nearly exclusively on vascular endothelial cells [Robinson 2001]. VEGFR-1 and VEGFR-2 both have seven immunoglobulin-type extracellular domains, a transmembrane segment, and a tyrosine kinase sequence which is interrupted by a kinase-insert domain. Upon VEGF binding, receptors dimerize, undergo tyrosine phosphorylation [Ferrara 2003], and signal EC mitogenesis [Ferrara 1997]. Ideally, VEGF incorporated into synthetic matrices would promote similar cell receptor responses, in order to initiate angiogenesis.

VEGFR-1 has been suggested to act as a “decoy” receptor, which would remove VEGF as a ligand for VEGFR-2 [Ferrara 2003]. VEGFR-1 has a high affinity for VEGF [de Vries 1992]. A HIF-1 dependent mechanism upregulates VEGFR-1 expression. Placenta growth factor (PlGF) and VEGF-B also bind to VEGFR-1, but not to VEGFR-2. VEGF or PlGF binding to VEGFR-1 occurs at the second immunoglobulin-like domain, causing weak tyrosine autophosphorylation. VEGFR-1 signaling results in growth factor

release and may have some mitogenic effect, as evidenced by the synergism that PlGF and VEGF show *in vivo* [Ferrara 2003].

VEGFR-2 is the main receptor for VEGF, and signal initiation for mitogenesis, angiogenesis, and EC enhancement of permeability occurs via this receptor (Figure 1-11). VEGFR-2 signaling also cues chemotaxis and survival (anti-apoptosis). EC proliferation occurs via activation of the Raf-Mek-Erk pathway (Figure 1-12). The survival signal occurs through the PI-3 kinase-Akt pathway. VEGF mutants which can bind VEGFR-2 can activate mitogenesis and increase permeability in endothelial cells [Ferrara 2003].

Coreceptors, called neuropilins (NRP), also interact with VEGF. NRP1 enhances VEGF₁₆₅ binding to VEGFR-2. NRP1 and NRP2 are not known to signal when bound to VEGF [Ferrara 2003]. Heparin-like molecules associated with the cell surface may help VEGF bind to VEGF receptors [Gitay-Goren 1992].

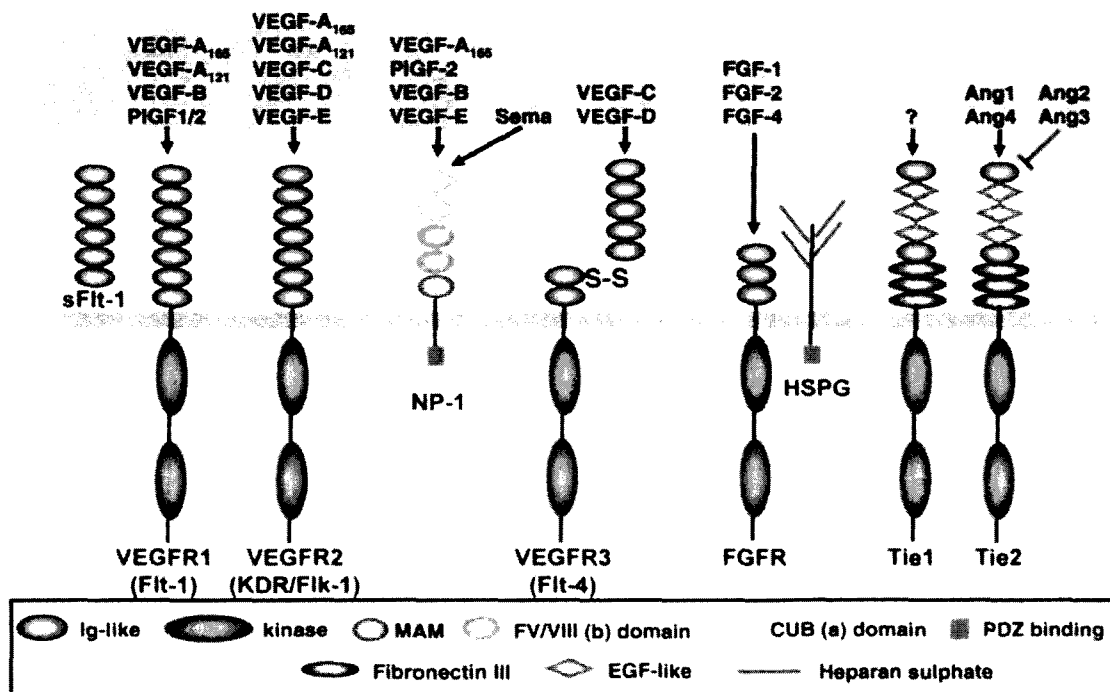


Figure 1-10 Ligand-receptor interactions within the VEGF family are part of a complex regulatory system. From [Zachary 2005].

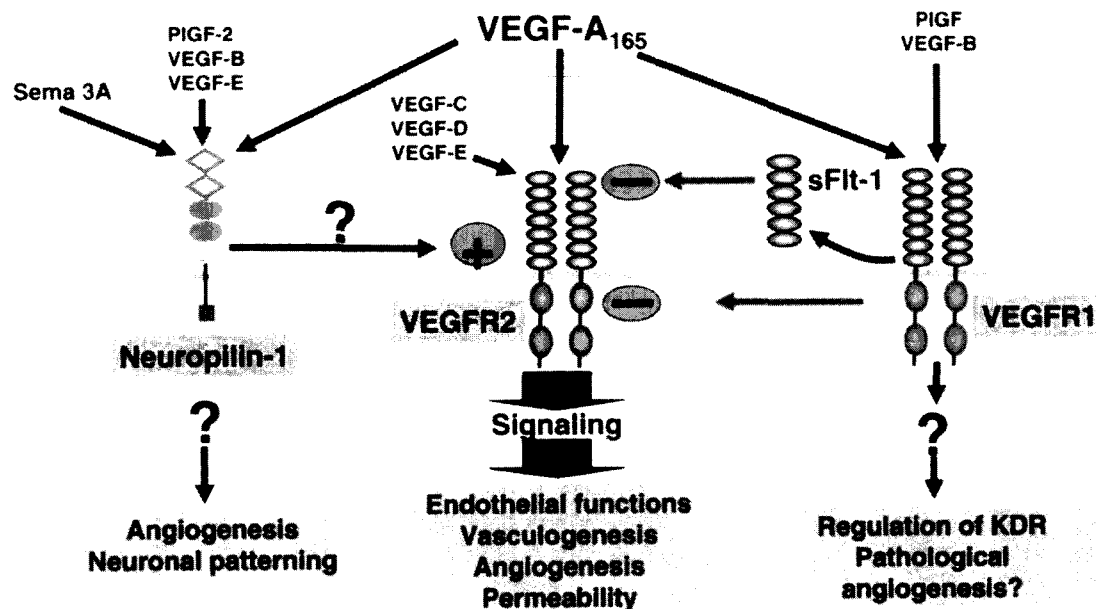


Figure 1-11 VEGFR-2, VEGFR-1, and Neuropilin-1 bind VEGF₁₆₅, leading to initiation and regulation of angiogenesis. From [Zachary 2005].

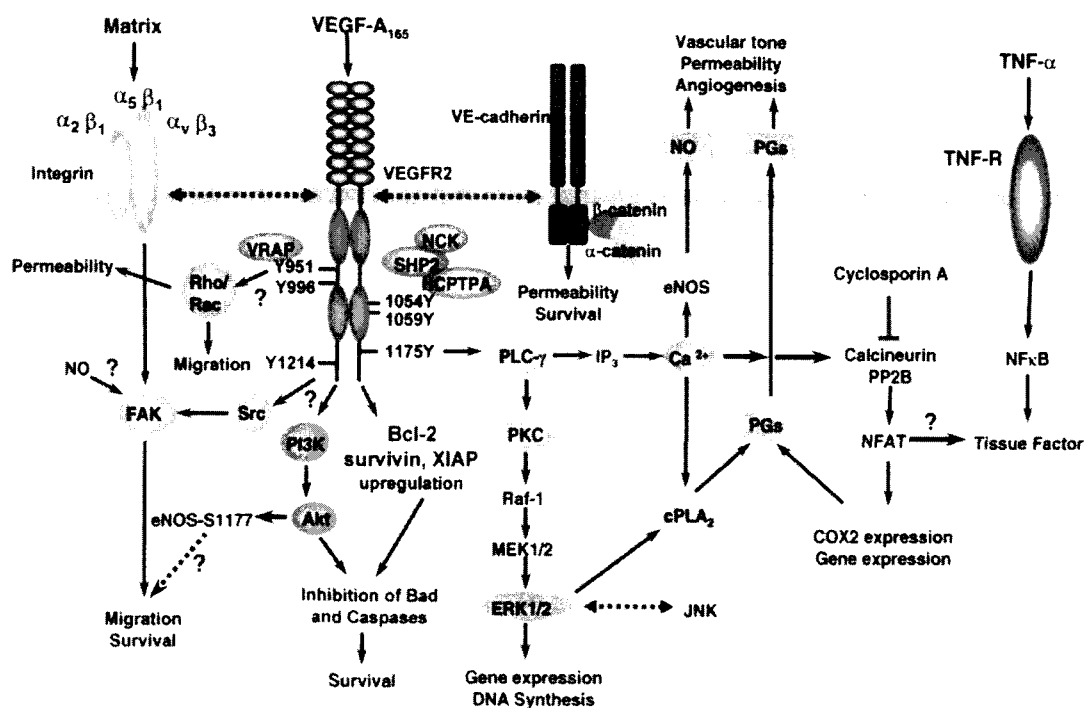


Figure 1-12 Integrins, VEGFR-2, and VE-cadherin binding initiate intracellular signaling pathways during angiogenesis. From [Zachary 2005].

VEGF Mimicking Peptide

The incorporation of a short peptide sequence instead of a large growth factor

protein in an engineered matrix would be a more

elegant approach to promoting microvascularization.

A short peptide is hypothesized to be less

immunogenic than a protein. D'Andrea et al. showed

that a synthetic 15-amino-acid peptide, based on a

region of the VEGF binding interface, possesses

similar biological activity to that of the VEGF

protein. D'Andrea et al. analyzed the x-ray structure

of VEGF bound to Flt-1 domain 2 (VEGFR-1). In

the VEGF/Flt-1_{D2} complex, there are three binding

regions. The VEGF binding region, Phe-17-Tyr-25, was synthesized with some

alterations to stabilize the α -helix conformation; this designed peptide was called QK.

The α -helix of the sequence was considered a necessity for bioactivity, as the tertiary

structure of the sequence determined ligand-receptor binding (Figure 1-13). The

physiological VEGF15 peptide, although an exact match in sequence, did not form an α -

helix in solution, presumably because it lacked the surrounding structures that stabilize it

in its effective conformation. The unstructured VEGF15 peptide did not display

bioactivity [D'Andrea 2005]. The sequences of the investigated physiological VEGF

binding region and the QK peptide are compared in Table 1-1.

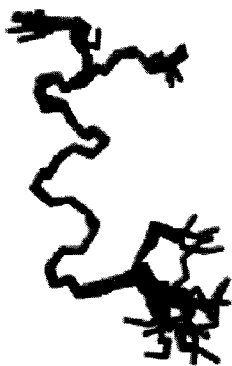


Figure 1-13 Conformation of QK. Superposition of 20 QK peptides [D'Andrea 2005]. QK was designed to assume an α -helix conformation in solution.

Table 1-1 Amino acid sequences of VEGF-VEGFR1 binding site and QK synthetic peptide. From [D'Andrea 2005].

VEGF15	Ac-KVKFMDVYQRSYCHP-amide
QK	Ac-KLTWQELYQLKYKGI-amide

QK was able to bind and activate both KDR (VEGFR-2) and Flt-1 (VEGFR-1)

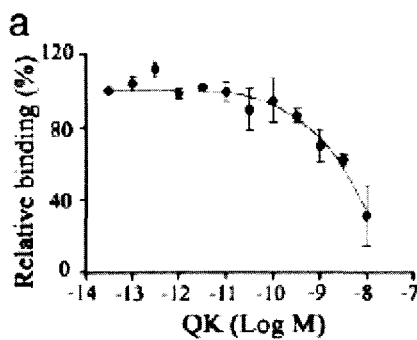
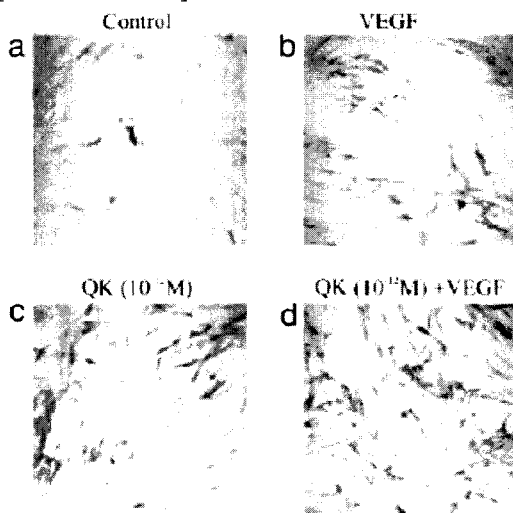


Figure 1-14 Binding of iodinated VEGF with cell membrane extract when in competition with QK. Increasing amounts of QK decrease VEGF binding, indicating competitive binding.

Figure 1-15 PECAM staining of endothelial tubes formed on Matrigel with QK or VEGF (100 ng/ml) in medium. Both figures from [D'Andrea 2005].



receptors *in vitro*. QK competed with iodinated VEGF for ligand-receptor binding on endothelial cell membranes (Figure 1-14). QK activated ERK1/2, which is a required step in VEGF-modulated angiogenesis. ERK1/2 was activated to different levels depending on dosage of QK, and QK and VEGF activation was additive. QK induced tubulogenesis on Matrigel, as assessed by CD31/PECAM-1 staining (Figure 1-15). QK also increased the tubulogenic response to VEGF. QK independently induced bovine aortic endothelial cell proliferation as well as enhanced VEGF-induced proliferation. D'Andrea et al. showed that QK could cause VEGF receptor dimerization and

subsequent activation despite its small molecular weight [D'Andrea 2005]. This novel, bioactive VEGF-mimicking peptide is another promising option to promote and control angiogenesis in tissue engineering matrices.

Summary: Angiogenesis

The natural process of angiogenesis relies on a complex system of signals and cell-cell/cell-matrix interactions. Tissue engineered matrix environments may be able to mimic such bioactive signaling to promote angiogenesis in an engineered tissue. Initiation of angiogenesis occurs by endothelial cell response to signaling factors such as VEGF. During angiogenesis, the patterned placement of growth factors in the matrix helps capillaries to form organized branching networks. Alternatively, a novel bioactive peptide which mimics VEGF could promote angiogenesis. Indeed, this thesis shows that these signaling factors are able to promote and control capillary formation when incorporated in suitable matrix material.

TISSUE ENGINEERING MATRIX MODIFICATIONS TO PROMOTE ANGIOGENESIS

Growth factor-incorporated matrices

Several groups have studied the angiogenic effects of released or attached growth factors in different matrix materials. These studies range from incorporating growth factors into naturally-derived matrices to highly engineering the time release of angiogenic signals from synthetic materials. This collection of previous work acts as a strong foundation and a direction-motivating framework for the current studies in this thesis.

Helm et al. studied the requirements for *in vitro* blood and lymphatic capillary formation in collagen and fibrin gels incorporating matrix-bound VEGF and interstitial flow. They found that lymphatic capillaries organized themselves most readily in fibrin matrices with high hydraulic resistance while blood vessel endothelial cells organized themselves preferably in collagen-fibrin matrices with high fluid permeability. Both cell types preferred highly compliant matrices, presumably for remodeling and migrating. MMP levels were examined and were found to correspond with the compliance of the matrix – where cells were required to remodel the most, MMP levels were the highest. They noted that since natural scaffolds were used in this study, there were several uncharacterized properties such as mechanical properties, proteolytic sensitivity, cytokine retention, and integrin ligand availability that could alter the capillary formation processes studied [Helm 2007].

Peters et al. engineered a poly(lactide-co-glycolide) (PLG)-Matrigel matrix to control the local release of VEGF. They noted that too much growth factor can be toxic and nonlocal growth factor could cause tumor growth. Pores were created in the PLG matrix to allow endothelial cell vessel formation. The efficiency of VEGF incorporation, kinetics of release, and biological activity of the released VEGF were determined. Human microvascular endothelial cells formed capillaries within the matrix *in vivo* in SCID mice [Peters 2002]. Matrix bound growth factors, such as those presented in this thesis, drastically reduce the pathologies associated with growth factor release.

Zisch et al. used biodegradable PEG hydrogels with covalently attached VEGF₁₂₁ or VEGF₁₆₅ to induce angiogenesis of the scaffold in CAM and rat models. VEGF was bound to PEG in a manner so that cell-secreted MMPs could cleave and release the protein from the matrix. The PEG hydrogel also contained proteolytically-degradable peptide sequences to allow cell invasion. Results showed that these matrices support host tissue regeneration *in vivo* [Zisch 2003].

Nilleson et al. induced *in vivo* capillary formation and maturation in collagen scaffolds by incorporating heparin-bound FGF2 and VEGF. Scaffolds were implanted in rats and removed for characterization after 3, 7, and 21 days. Samples were stained for smooth muscle actin (SMA) to determine the maturity of the vessels and for hypoxia inducible factor 1- α (HIF1- α) to determine the amount of hypoxic cells in the scaffold. At day 3, 97-98% of the cells in the scaffolds were hypoxic. Hypoxia decreased dramatically to 2% by Day 7 and 0.2% by Day 21 in scaffolds containing VEGF and FGF2 while it remained at 37% (Day 7) and 21% (Day 21) in collagen scaffolds without

growth factors. They hypothesized that the copresentation of VEGF and FGF2 promoted cell expression of PDGF for vessel maturation [Nillesen 2007].

Chen et al. incorporated VEGF and PDGF into scaffolds formed from compressed poly(lactide-co-glycolide) microspheres. The scaffolds consisted of two distinct regions, in which different amounts of each growth factor were incorporated. Growth factors were not covalently bound to the scaffold, and followed release profiles such that PDGF, which was encapsulated in the microspheres, diffused more slowly than VEGF, which was mixed with the final microsphere solution before compressing. The acellular scaffolds were implanted in a mouse model of hindlimb ischemia. Vessels in scaffolds containing only VEGF remained immature, as shown by a low amount of α -SMA staining indicative of mural cells. PDGF delivery induced vessel maturation, as evidenced by larger vessel diameters and more vessels containing smooth muscle cells [Chen 2007].

This work supports the hypothesis that vessel maturation can be controlled by the components, such as growth factors and peptides, added to the system. To improve upon general incorporation of these signaling factors, several strategies, including patterning and incorporating a smaller angiogenic peptide, may be instrumental.

Scaffold Material

In choosing a tissue engineering scaffold material, one must consider several factors of biocompatibility, including toxicity, hydrophilicity, degradation properties, and immunogenicity. Biomaterial surfaces resistant to protein adsorption are imperative in

some biomaterial applications, as protein adsorption on the surface of an implant leads to an immune response as well as undesired cell attachment; however, desired anchorage-dependent cells must be able to attach and spread on a substrate to survive [Kane 1999]. Additionally, the material might be required to provide an ECM-like niche for cells by providing a physical support containing biochemical, mechanical, and electrical cues to cells. While natural ECM materials may offer this environment, synthetic polymer matrices are often mechanically stronger and more easily characterized than natural materials.

Poly(ethylene glycol) (PEG) is a biocompatible, hydrophilic polymer that has been used in FDA-approved applications including as a coating for drug delivery of pharmaceuticals, which renders them stealthy to the immune system [Harris 1997]. PEG chains are biocompatible when their molecular weights fall within the range of 1 – 20 kDa. PEG chains shorter than 1 kDa are toxic, can result in blindness, and do not display the bioinert properties of longer chains. Size limitations of renal glomerular filtration constrains the length of chains used to be less than ~ 20 kDa, but slower clearance of longer chains through urine and feces is possible [Roberts 2002].

PEG chains can be modified with cross-linkable acrylate groups, with one acrylate group on each end of the PEG polymer chain, yielding PEG diacrylate (PEGDA, Figure 1-16). PEGDA chains then can be crosslinked to form hydrogels with tunable mechanical properties [Hahn 2007] (Figure 1-17). These hydrogels are a promising choice for soft tissue scaffolds. PEGDA resists protein adsorption and subsequent nonspecific cell adhesion, and thus acts as a “blank slate” for designing complex tissue organization [Hahn 2007]. Crosslinking of polymer chains can be initiated by light, by

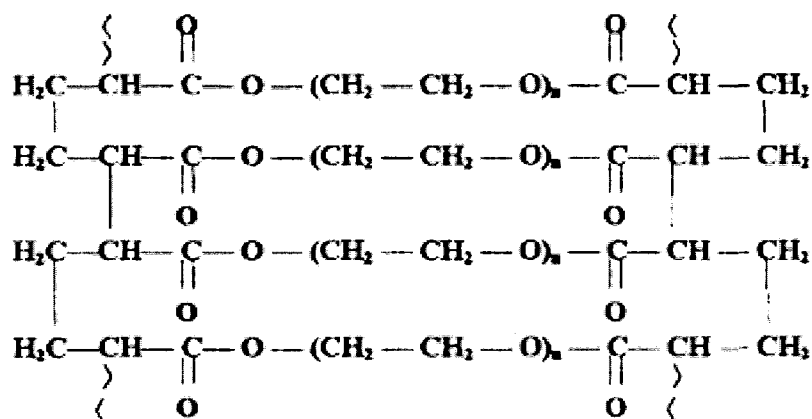


Figure 1-17 Idealized network crosslinking of PEGDA chains. Crosslinking occurs between the carbons in the acrylate groups at the end of each polymer chain. From [Padmavathi 1996].

One of the most widely used cell-adhesive ligands is the amino-acid chain Arginine-Glycine-Aspartic Acid, or RGD. The tetrapeptide, RGDS, was first isolated from fibronectin by Ruoslahti et al. in 1983 by testing libraries of peptide chains found in fibronectin, starting by testing cell attachment to fibronectin fragments, continuing to ~30 amino acid chains, then sequentially shortening bioactive chains to pinpoint the exact sequence. Ruoslahti et al. quickly found that the RGDS sequence also existed in the databases for five other proteins, including fibrinogen and collagen, and that the RGD sequence exists in more than 500 proteins [Ruoslahti 2003]. RGDS acts as a cell-adhesive ligand for most mammalian cells and is a biomimetic ligand which can easily be incorporated into PEG hydrogels by linking via the free amine at the N terminal of the peptide.

The peptide GPQGIAGQ is an MMP-sensitive linear oligopeptide found in the $\alpha 1(I)$ collagen chain and can be cleaved between glycine and isoleucine by several MMPs [Aimes 1995]. GGGPQGIWGQGK is a mutated version of the native

oligopeptide with increased degradation kinetics [Barrett 1998, Aimes 1995, Lutolf 2003]. The MMP-sensitive linear oligopeptide can be incorporated into the backbone of the polymer by reacting both peptide termini with acrylated PEG linkers, creating a linear PEG-peptide-PEG sequence that can be crosslinked into a hydrogel network that can then be remodeled by cells [West 1999].

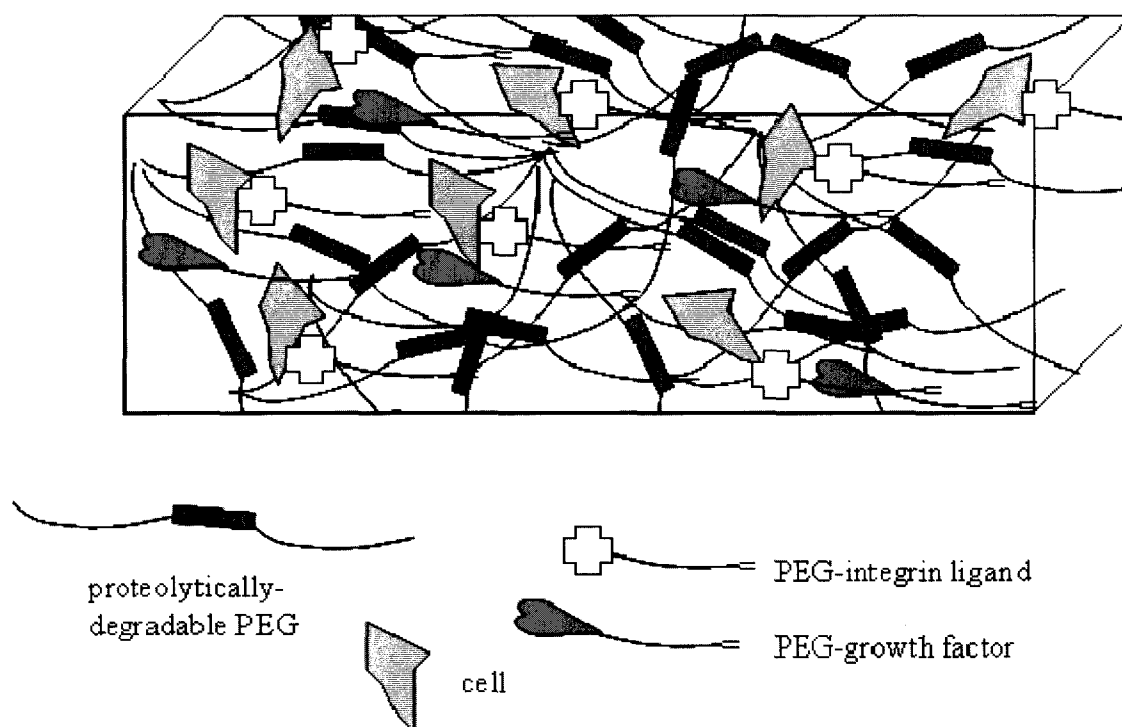


Figure 1-18 Biomimetic PEG hydrogels can contain proteolytically-degradable sequences and covalently linked cell integrin ligands and growth factors. Cells can be encapsulated at the time of hydrogel formation due to the biocompatible photopolymerization process.

In vivo, proteoglycans containing heparan sulfate act to bind and concentrate certain growth factors, such as bFGF, in the ECM as well as near cell surfaces [Houck 1992]. Localization of growth factors and cell-adhesive ligands can similarly be

achieved in PEG-based hydrogels, by covalently crosslinking these substrates to the hydrogel [DeLong, Gobin, et al. 2005; DeLong, Moon, et al. 2005]. A short (3.4 kDa) PEG chain containing an N-hydroxy-succinimide (NHS) end group can be reacted with free amine groups on a peptide or protein to yield a pegylated protein or peptide. This biomolecule can then be crosslinked on the surface or into the bulk of a PEGDA hydrogel. DeLong et al. showed that covalently attached integrin ligand RGDS on PEGDA hydrogels remained bioactive, affecting fibroblast migration and alignment [DeLong, Gobin, et al. 2005] and covalently attached bFGF's bioactivity could similarly promote vascular smooth muscle cell proliferation and migration [DeLong, Moon, et al. 2005].

Patterned Ligand Presentation to Control Cell and Tissue Functionality

Patterning the presentation of cell adhesive ligands and signaling factors may allow the geometric restriction of cell location and function in a tissue engineered construct. Tight control over cell behavior can potentially allow creation of highly organized and intricate tissues and organs. One of the most widely used methods for patterning materials is photolithography (Figure 1-19). Photolithography relies on the requirement for excitation via light for chemical bonding. By masking areas exposed to the light, regions of chemical bonding can be controlled. Light passes only through the pattern to photopolymerize the substrate below. The type of mask used determines the resolution of patterning. The use of photolithography allows feature sizes to be less than 1 μm , if desired. Rapid prototype masks, using transparency film printed with the design,

usually limit features to larger than 20 μm [Kane 1999]. In order to create smaller features, a chrome photomask is created by a laser writer in a clean room. Once masks are produced, photolithography allows fast, repeatable patterning.

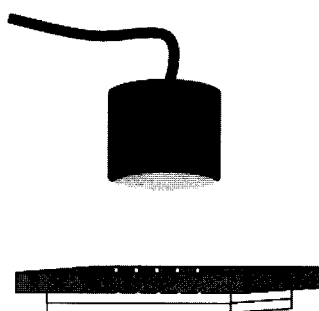


Figure 1-19 Photolithographic patterning requires a mask to control exposure of light to the photo-sensitive substrate below.

While photolithography offers a rapid patterning process once a mask is made, there are several disadvantages to this system. First, an iterative process is nearly impossible when working with patterns on a scale of microns, the order of capillaries, as the sample must be precisely aligned. Further, many pieces of the set-up must work precisely for wavelengths of light to successfully pass through a micron-sized pattern and project that pattern onto the hydrogel to be patterned. A recent advancement, Laser Scanning Lithography (LSL), overcomes these challenges [Hahn 2005]. By using the precision of confocal microscopy, in which a laser is tightly focused onto a specimen and scanned across the specimen with sub-micron precision, the exposure to light and subsequent photopolymerization can be controlled spatially (Figure 1-20). Miller and Hahn added Laser Scanning Lithography as an additional tool to the arsenal of

photopatterning techniques and successfully showed its utility in several applications, including PEG hydrogels [Hahn 2005].

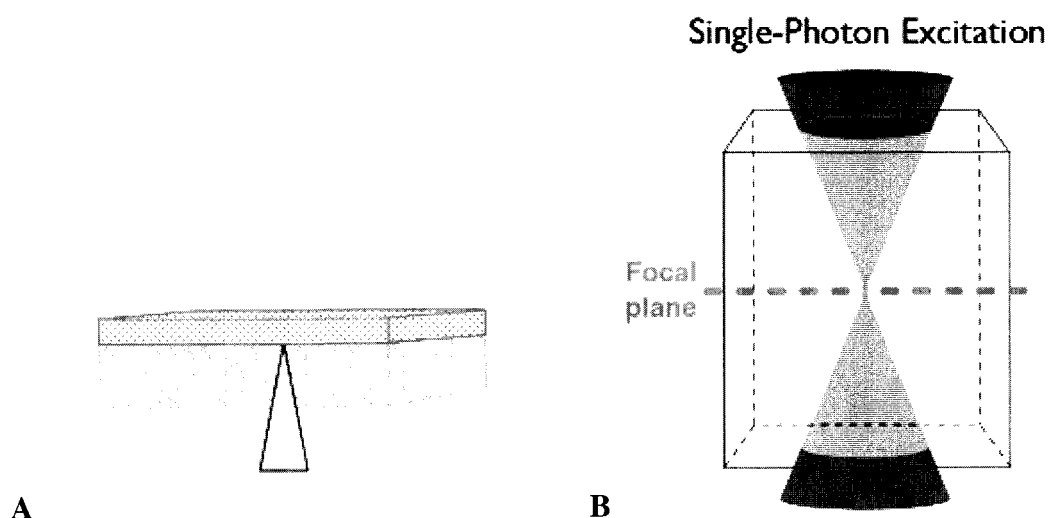


Figure 1-20 a) Photopolymerization of surface-immobilized ligands via single-photon excitation provided by confocal microscopy. b) Excitation is most precise at the focal plane (from Jordan Miller).

Ligand presentation plays a vital role in angiogenesis. Extracellular matrix plays a major role in this process, since ECM regulates cell spreading, which has been shown to determine the fate of the cell. Additionally the density of available surface-immobilized ECM molecules, such as fibronectin, determines growth or differentiation [Ingber 1990]. Indeed, ECM density has been shown to affect activation of integrins, binding efficiency, prompting of intracellular signaling pathways, and alterations in gene expression [Ingber 1990, Dike 1996].

Dike et al. elucidated the importance of spatially restricting presentation of adhesion molecules in promoting angiogenesis. Gold-coated glass coverslips were

coated with a saturated density of fibronectin via microcontact printing and self-assembling monolayer (SAM) formation. Bovine capillary endothelial cells attached to patterned lines of either 10 μm or 30 μm in width and were cultured in medium saturated with FGF. Cells on both 10 and 30 μm -wide lines aligned along the long axis of the patterned lines between 48-72 h. Cells on the 30 μm -wide lines remained spread and flattened while cells on the 10 μm -wide lines switched to a differentiation route, with little proliferation or apoptosis (Figure 1-21). Linear cellular cords formed on the 10 μm -wide lines and appeared to possess a centralized hollow space, as visualized by confocal microscopy. A single, continuous, central lumen extended over several cell lengths, and single cell bodies stretched around a negatively labeled lumen. Cells were observed to be partially retracted from the surface, and cells appeared to increase in height. PECAM staining showed strong cell-cell attachment and continuous linear presence including at cell junctions [Dike 1999].

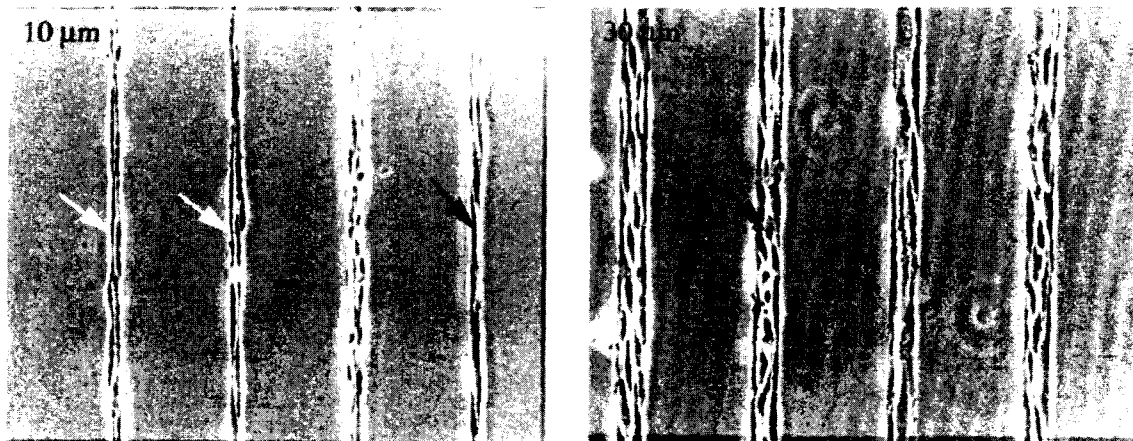


Figure 1-21 Endothelial cells formed tube-like structures with lumens (arrows) on lines of patterned surface-adsorbed fibronectin with line width of 10 μm but not 30 μm . From [Dike 1999].

Since geometric restriction of ligand presentation affects cell function, this phenomenon has been used in this thesis to improve microvascularization of tissue constructs. The ability to pattern PEG hydrogels allows control of tissue organization while the patterned presentation of ligands contributes to activation of angiogenic pathways.

Summary

Clinical need for tissues and organs for transplantation outweighs supply through donation. The field of tissue engineering strives to provide functional tissues and organs grown in the laboratory; however, the current roadblock in attaining this goal is the incorporation of microvasculature in engineered tissues. Biocompatible, bioinert poly(ethylene glycol) hydrogels act as “blank slates” into which bioactivity can be tailored and photolithographically patterned. This otherwise “stealthy” material can support and promote desired biological activity when modified with bioactive moieties. This thesis provides several novel techniques and improvements to promote microvascularization in poly(ethylene glycol) diacrylate hydrogels. Microvascularization of native tissue is highly regulated by biochemical signaling, matrix interactions and remodeling, and cooperation of several cell types. The requirements for vascularizing engineered tissues are similarly complex. The enabling knowledge base and technological base are solid to support investigation into the best processes for successfully vascularizing engineered tissue. Previous research contributions are used in combination in this work to determine the signals, cells, and matrix material needed to

promote, control, and stabilize microvasculature to contribute to the field of tissue engineering and its clinical promise.

Chapter 2 Covalently immobilized PEG-VEGF promotes endothelial tubulogenesis in PEGDA hydrogels

A large amount of content in Chapter II is taken from Leslie-Barbick, J.E., J.J. Moon, and J.L. West. (2009). "Covalently-immobilized vascular endothelial growth factor promotes endothelial cell tubulogenesis in poly(ethylene glycol) diacrylate hydrogels." *Journal of Biomaterials Science: Polymer Edition* 20: 1763-79.

INTRODUCTION

The induction of microvasculature into engineered tissues is currently a roadblock to successfully engineering functional tissues of significant thicknesses (see Chapter 1 for full discussion). Because most engineered tissues cannot depend solely on diffusion for transport, microvascularization before implantation should be considered a requirement for three-dimensional engineered tissues. One possible method to achieve *in vitro* microvascularization of engineered tissues may be mimicking the natural *in vivo* process of capillary formation, angiogenesis. In this process, capillary endothelial cells respond to biochemical angiogenic signals such as vascular endothelial growth factor (VEGF) to form endothelial tubes, which are later stabilized by mural cells. Signaling by VEGF, a protein dimer, is considered a rate-limiting step in the initiation of angiogenesis [Ferrara 2003]. This work investigates whether by sequestering and presenting VEGF in an extracellular matrix-like environment, endothelial cell tubulogenesis can be promoted.

Previous studies explored the angiogenic effects of released or attached growth factors in different matrix materials. Helm et al. used matrix-sequestered, cleavable VEGF for *in vitro* blood and lymphatic capillary formation in collagen and fibrin gels [Helm 2007]. Peters et al. used a poly(lactide-co-glycolide) (PLG)-matrigel matrix to

control the local release of VEGF. Human microvascular endothelial cells formed capillaries within the matrix *in vivo* in SCID mice [Peters 2002]. Zisch et al. used biodegradable PEG hydrogels with covalently attached but proteolytically detachable VEGF₁₂₁ or VEGF₁₆₅ to induce angiogenesis of the scaffold in CAM and rat models. VEGF was bound to PEG in a manner so that cell-secreted MMPs could cleave and release the protein from the matrix [Zisch 2003]. Nillesen et al. induced *in vivo* capillary formation and maturation in collagen scaffolds by incorporating heparin-bound FGF2 and VEGF. They hypothesized that the copresentation of VEGF and FGF2 promoted cell expression of PDGF for vessel maturation [Nillesen 2007]. Chen et al. incorporated VEGF and PDGF into scaffolds formed from compressed poly(lactide-co-glycolide) microspheres. The matrices promoted release profiles which released first VEGF, followed by PDGF [Chen 2007].

In working to create functional microvasculature, there is a need for a method to characterize the host angiogenic response to presented stimuli with respect to the progress of capillary formation and the resulting ability of the microvasculature to transport blood cells. The process of angiogenesis can be transparently studied using a chorioallantoic membrane (CAM) model. In this model, the chorioallantoic membrane surrounding a chick embryo in the egg is responsive to angiogenic stimuli. The CAM's main purpose is to provide gas exchange in the egg, and so also contains a network of capillaries. Development of the embryo begins upon incubation of the egg. On Day 4 of incubation, the CAM forms when the ectoderm epithelium (chorion) fuses to the endoderm epithelium (allantois). In this preliminary stage, the CAM contains undifferentiated blood vessels. On Day 8, capillaries form from the differentiation of the preliminary

blood vessels. The egg shell can be opened without disturbing the CAM or embryo. The angiogenic stimulus, transplanted tissue, or tissue engineering matrix can then be placed on the CAM. The CAM is best used for tissue engineering vascularization studies between Days 9 and 12, as then it is at its maximum potential [Borges 2003]. The CAM model provides a responsive system to determine the effects of a particular matrix on the pre-existing CAM vasculature, as well as the ability of tissue engineered capillary networks to connect to the host and functionally transport blood. In preliminary studies in attracting host microvasculature to the hydrogel, release of VEGF from hydrogels was quantified over time and VEGF-releasing hydrogels were introduced into a CAM chicken embryo model to show an angiogenic response, in which the hydrogel can direct host microvasculature to approach the hydrogel, creating an environment in which microvessels could anastomose to those in the hydrogel.

Sequestering growth factors in a matrix, rather than local release, however, provides a more engineered and controllable environment and consequent biological response (Figure 2-1). Release of VEGF has the potential to yield unwanted, nonlocal activity. Mazue et al. showed that too much growth factor can be toxic to red blood cell production and kidneys, and nonlocal growth factor could support tumor growth [Mazue 1991, 1992, 1993]. Additionally, when administered in bolus injections, VEGF is eliminated quickly, with a half-life of less than 1 h [Lazarous 1996]. Because of the often unwanted responses due to released growth factors and the biological need for signaling duration not met by bolus release, an approach has been chosen which covalently binds VEGF to a matrix that supports cell adhesion and angiogenic activity.

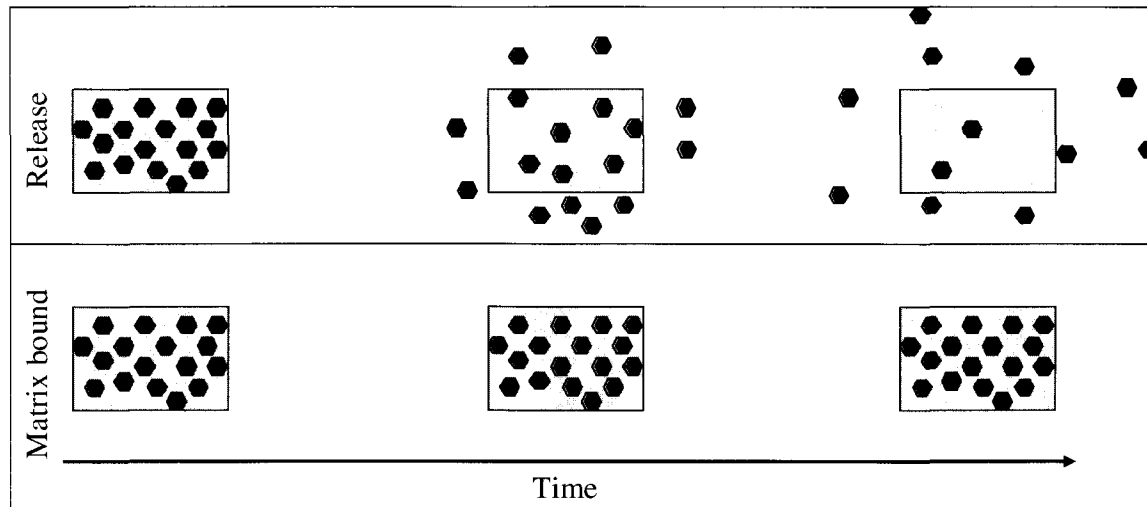


Figure 2-1 Release of growth factors compared to matrix-bound sequestering. Release leads to a sink effect in which growth factor concentration is quickly decreased within the matrix, and growth factors continue to diffuse to other, unwanted areas in the body. In contrast, matrix bound growth factors remain localized, at engineered concentrations to yield desired effects.

In the current studies, PEG-based hydrogels were modified to incorporate local, controlled biochemical signaling to cells. VEGF was covalently coupled to the PEGDA hydrogel matrix, and the endothelial cell responses to the sequestered growth factor were analyzed. A synthetic matrix was developed which can support and promote *in vitro* tubulogenesis, the first step in creating a functional microvasculature in engineered tissues.

MATERIALS AND METHODS

Cell Culture

Human umbilical vein endothelial cells (HUVEC, Cambrex/Lonza, Walkersville, MD) were used between passages 2 and 6. Cells were maintained in VEGF-free endothelial cell growth medium (EGM-2 medium, Cambrex/Lonza) that contained hydrocortisone, fibroblast growth factor (hFGF-B), insulin-like growth factor (R³-IGF-1), ascorbic acid, epidermal growth factor (hEGF), GA-1000 (gentamicin, amphotericin-B), heparin, 2% fetal bovine serum (FBS) (Bulletkit, Lonza), 2 mM L-glutamine, 1 U/mL penicillin, and 1 µg/mL streptomycin (GPS, Sigma, St. Louis, MO). Cells were maintained at 37°C in a 5% CO₂ environment. Before 3D encapsulation, HUVECS were labeled with Celltracker Green CMFDA (Molecular Probes). 50 µg Celltracker Green was dissolved in 5 µl DMSO and diluted in cell medium for a final concentration of 2 µg/ml. HUVECs were incubated in the prepared medium for 1 h. Labeling was visually confirmed, and labeling medium was replaced with normal EGM-2 medium (without VEGF). Cells were washed repeatedly with phosphate buffered saline (PBS) before enzymatic lifting using trypsin and subsequent encapsulation.

Preparation and Purification of Poly(ethylene glycol) Diacrylate (PEGDA)

Poly(ethylene glycol) (PEG; Fluka/Sigma, MW = 6000 Da) was reacted with acryloyl chloride (Sigma) at a 1:4 molar ratio in anhydrous dichloromethane (DCM; Sigma) with triethyl amine (TEA; Sigma) at a 1:2 (PEG:TEA) molar ratio under argon

overnight at 25°C (Figure 2-2). PEGDA was purified via phase separation using 2 M K_2CO_3 . The organic phase containing PEGDA was dried using anhydrous $MgSO_4$ and filtered. PEGDA was precipitated in diethyl ether, filtered, and dried overnight and under vacuum, then characterized by 1H -NMR, and stored at -20°C under argon until use.

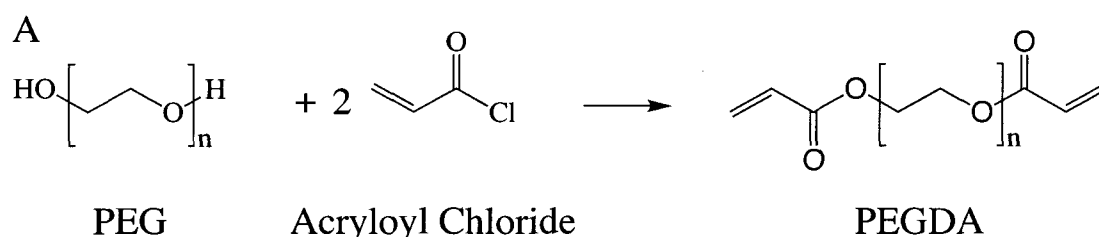


Figure 2-2 PEGDA synthesis occurs through a reaction of poly(ethylene glycol) and acryloyl chloride. The product is a PEG chain with reactive end groups that allow crosslinking of chains into networks.

Preparation and Purification of PEG-succinimidyl carbonate (PEG-SMC)

Due to a discontinuation of Acryloyl-PEG-NHS (Nektar) to the research community, PEG-SMC, which has similar chemical functionality to PEG-NHS, was synthesized. Monoacrylated PEG was prepared by reacting PEG (Fluka/Sigma, MW = 3400 Da) with 1.5 molar excess Ag_2O (Sigma), 1.1 molar excess acryloyl chloride (Sigma), and 0.3 molar ratio KI (Sigma) in anhydrous dichloromethane (DCM; Sigma) overnight at 0-4°C. The resulting solution was filtered using Celite 521 (Spectrum Chemical Manufacturing Corp, Gardena, CA) to remove silver. The filtered solution was dried using a Rotovap, and then dissolved in DI H_2O and the pH was altered to pH=3

using HCl. The solution was then heated to 35°C for 1 h. Activated charcoal (Fisher) was added to the mixture to remove iodine. The solution was subsequently filtered using Celite 521. NaCl was added with DCM, followed by DCM extraction. Chloride ions and acid were removed via phase separation using 2 M K₂CO₃. Monoacrylated PEG was dried using sodium sulfate (Fisher), concentrated using a Rotovap, precipitated in ethyl ether, and vacuum filtered. PEG-monoacrylate was then reacted with 4 molar excess disuccinimidyl carbonate (Sigma) in anhydrous acetonitrile (Sigma) and pyridine (Sigma) under argon overnight. The product was dried using a Rotovap, dissolved in anhydrous DCM, and filtered. PEG-SMC was isolated via phase separation in acetate buffer (0.1 M, pH 4.5, 15% NaCl), dried using anhydrous MgSO₄, filtered, precipitated in ethyl ether, filtered, and dried overnight and under vacuum. PEG-SMC was characterized by ¹H-NMR and MALDI-TOF and stored at -80°C under argon until use.

Preparation and Purification of PEG-RGDS

The cell-adhesive peptide RGDS (American Peptide, Sunnyvale, CA) was dissolved in 50 mM sodium bicarbonate buffer (pH 8.5) at a concentration of 25 mM. Acryloyl-PEG-N-hydroxysuccinimide (PEG-NHS, Nektar, Huntsville, AL, MW=3400) or PEG-SMC was similarly dissolved at a concentration of 50 mM. PEG-NHS or PEG-SMC was added dropwise to RGDS in a 1:1.2 molar ratio with slow mixing and allowed to react for 2 h at 25°C or 4 d at 4°C, respectively. The product was dialyzed against DI H₂O for 8 h using a membrane with a 1 kDa molecular weight cutoff (Spectrum Laboratories, Rancho Dominguez, CA). PEG-RGDS (Figure 2-3) was then

lyophilized and stored at -80°C under argon until use. Conjugation was characterized by gel permeation chromatography (GPC) using a PLgel column ($5\text{ }\mu\text{m}$, $500\text{ }\text{\AA}$, Polymer Laboratories, Amherst, MA), 0.1% ammonium acetate in DMF solvent, and evaporative light scattering (ELS) detector (Polymer Laboratories), run against an unreacted PEG-NHS standard.

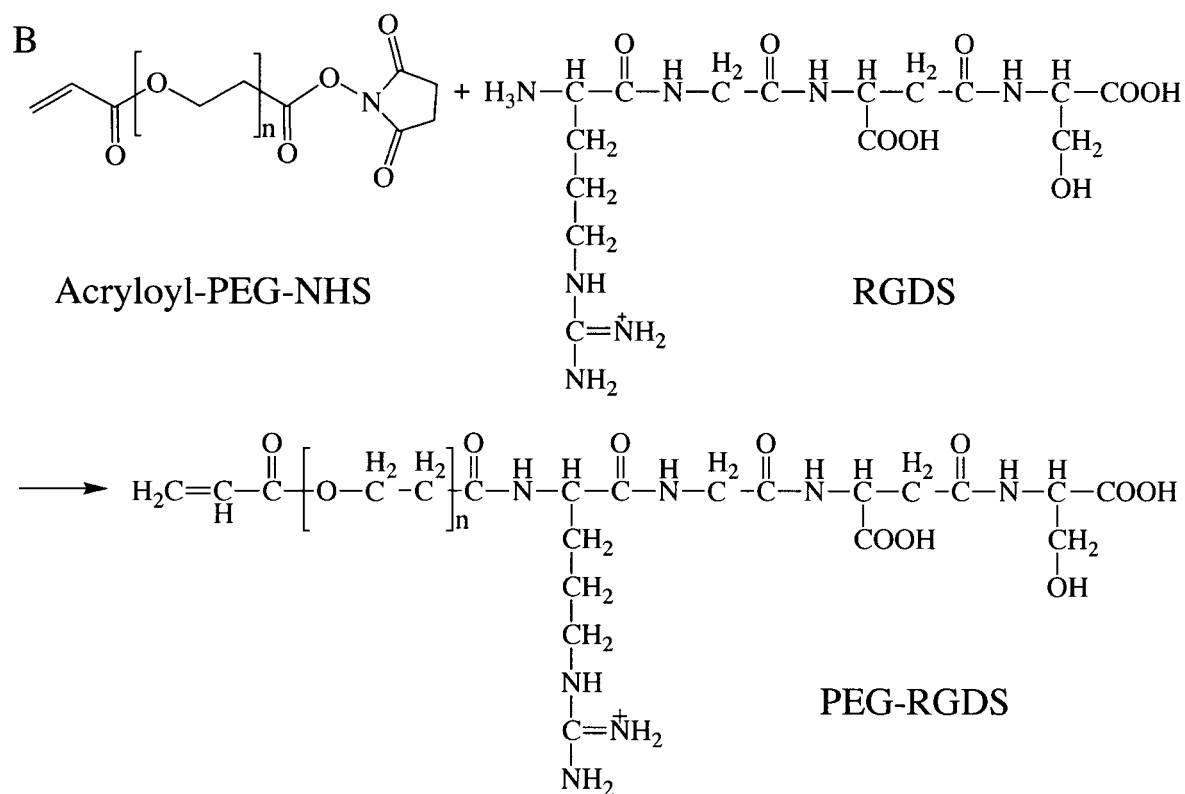


Figure 2-3 PEG-NHS reaction with peptide RGDS. The NHS end group on the PEG chain leaves, allowing covalent binding to a free amine in the peptide, yielding a PEG-peptide molecule.

Synthesis of Collagenase-Degradable PEG-PQ-PEG

A collagenase-sensitive peptide (PQ) GGGPQGIWGQGK was prepared on a peptide synthesizer (Aapptec, Louisville, KY) using standard Fmoc chemistry. The peptide was cleaved from the resin using 95% trifluoroacetic acid (TFA), 2.5% triisopropylsilane (TIPS) in water and precipitated in ether. The peptide was reacted with acryloyl-PEG-NHS (Nektar) or PEG-SMC in sodium bicarbonate buffer (pH 8.5, 50 mM) to generate a PEG-diacrylate derivative with PQ in the polymer backbone, and conjugation was confirmed via GPC with ELS detection as described above.

Synthesis of PEG-VEGF

VEGF₁₆₅ (Sigma) was dissolved in sterile 50 mM sodium bicarbonate buffer (pH 8.5, 0°C). Acryloyl-PEG-SMC was similarly dissolved and sterilized via filtration (0.2 µm). PEG-SMC was added to VEGF in a 200:1 molar ratio with slow mixing under sterile conditions and allowed to react for 4 d at 4°C yielding PEG-VEGF. PEG-VEGF (Figure 2-4) was then lyophilized under sterile conditions and stored in HEPES buffered saline (HBS; 100 mM NaCl, 10 mM HEPES in deionized water; pH 7.4) with 0.1% bovine serum albumin (BSA) at 4°C until use. Conjugation was confirmed via Western blot using reducing conditions on a Tris-HCL precast polyacrylamide gel (Biorad, Hercules, CA), rabbit polyclonal anti-VEGF primary antibody (Santa Cruz Biotechnology, Santa Cruz, CA), HRP-conjugated goat anti-rabbit IgG (MP Biomedicals, Aurora, OH), and ECLTM chemiluminescent Western Blotting analysis system (GE Healthcare, Buckinghamshire, UK). Film (Kodak, Rochester, NY) was exposed to

Western Blot membrane for 5 s and then developed using a Micromax Developer (Hope, Warminster, PA) with T₂ developer and T₂ fixer (White Mountain Imaging, Salisbury, NY).

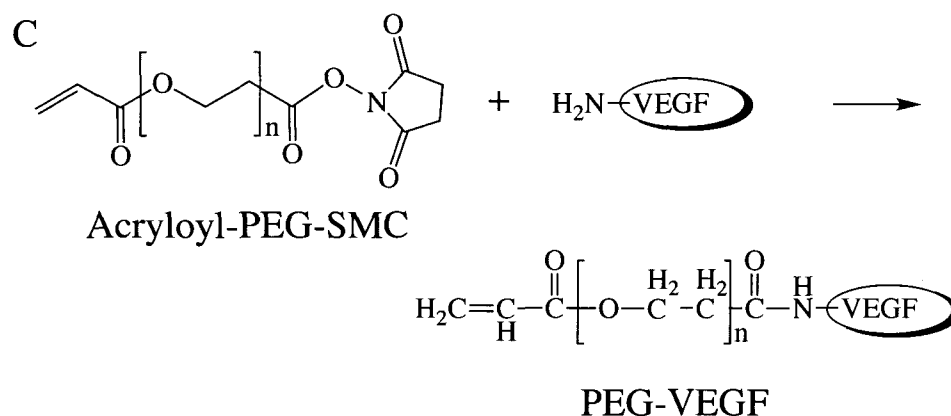


Figure 2-4 PEG-SMC reaction with VEGF protein. The reaction yields a PEG-protein molecule.

Bioactivity Assay

Bioactivity of PEG-VEGF was determined by measuring its pro-mitotic effect on endothelial cells. HUVECs were seeded at 1.05×10^3 cells/cm² in EGM-2 medium without VEGF on Day 1. On Day 3, medium was replaced with EGM-2 medium without VEGF and FGF, with an addition of either 5 ng/ml VEGF (positive control), 5 ng/ml PEG-VEGF, or no VEGF (negative control). This medium was replaced after 4 h with EGM-2 without VEGF and FGF. On Day 5, cells were trypsinized and counted using a Coulter Counter. Statistical differences between groups was analyzed using ANOVA,

followed by Tukey's Least Significant Difference post hoc analysis, with $p < 0.05$ considered statistically significant.

Formation of PEGDA Hydrogels

6 kDa PEGDA was dissolved in HEPES buffered saline (HBS) in a 10% w/v solution and sterilized via filtration (0.2 μm). 10 $\mu\text{L/mL}$ of 300 mg/mL 2,2-dimethoxy-2-phenylacetophenone in N-vinylpyrrolidone (NVP) was added to the solution. Molds were constructed by placing poly(tetra fluoroethylene) (PTFE, 0.5 mm thickness) spacers between two glass slides on three sides and securing with clips. The polymer solution was pipetted into molds and crosslinked through exposure to long wavelength ultraviolet light (B-200SP UV lamp, UVP, 365 nm, 10 mW/cm²) for 30 s. After crosslinking, the mold was removed, and the PEGDA hydrogel slab was placed in sterile PBS with 0.1% sodium azide until further use.

Surface Modification of PEGDA Hydrogels

Hydrogel slabs were soaked for 1 h in sterile PBS to remove sodium azide. 5 mm diameter circles were punched from PEGDA hydrogel slabs. A polymer solution consisting of 420 pmol/mL PEG-VEGF, 30 $\mu\text{mol/mL}$ PEG-RGDS, 15 $\mu\text{L/mL}$ triethanolamine (TEOA), 1 $\mu\text{mol/mL}$ eosin Y, and 3.95 $\mu\text{L/mL}$ NVP was prepared. From this solution, 10 μL was pipetted onto the top surface of the gel, completely covering the surface. The gel and polymer solution were exposed to a 532 nm laser at

30 mW/cm² for 30 s. The surface-modified gel was then soaked in sterile PBS for 1 d to allow non-reacted polymer and excess photoinitiator to diffuse from the gel.

Quantification of Surface-Immobilized VEGF and RGDS

An ELISA assay was used to determine the amount of VEGF that was covalently immobilized on hydrogel surfaces. Hydrogels were modified with PEG-VEGF and PEG-RGDS, then allowed to soak in HBS with 0.1% BSA for 3 d, with collection and replacement of the saline solution on the second day. The amount of PEG-VEGF in the saline samples from both days was quantified using a VEGF ELISA kit (R&D Systems, Minneapolis, MN) with PEG-VEGF standards. The amount of PEG-VEGF released from the gels after two and three days was then used to calculate surface conjugation.

To quantify the amount of covalently-linked PEG-RGDS on the surface of the gels, a ninhydrin assay was used following degradation of the hydrogels and peptides in acid. The ninhydrin assay measures amine content, which results from the presence of the grafted peptide [Landua 1949]. A chemical reaction occurs between ninhydrin molecules and free amines, which results in the formation of a colorimetric dye. The concentration, and thus intensity, of the dye is linearly related to the concentration of available reactive amine. Samples were soaked after conjugation to allow unbound RGDS to diffuse from the hydrogel before analysis. Standards were created by adding known amounts of PEG-RGDS to PEGDA hydrogels. Standards and hydrogels modified with PEG-RGDS were lyophilized, then degraded using 6 N HCl for 3 h at 100°C. HCl was removed using a Rotovap, and samples, RGDS standards, and glycine standards

were dissolved in 0.1 M sodium citrate buffer (pH = 5). Ninhydrin reagent (Sigma) was added, and the samples were boiled for 15 min, centrifuged, and the resulting colored product was read at 570 nm to determine the amount of RGDS on hydrogels.

Endothelial Tubule Formation

HUVECs were seeded (8.5×10^4 cells/cm²) onto gels with either PEG-RGDS only or PEG-RGDS and PEG-VEGF covalently attached to the surface. HUVEC tubulogenic response on the gels was monitored and EGM-2 medium changed every other day. Three experimental groups were observed: VEGF- and RGDS-modified hydrogels cultured in EGM-2 medium (without soluble VEGF, 1% serum), RGDS-modified hydrogels cultured in EGM-2 medium (without soluble VEGF, 1% serum), and RGDS-modified hydrogels cultured in EGM-2 medium (with soluble VEGF, 1% serum). Images were taken of each entire gel and merged using Photoshop Elements software. Tubules were traced using Adobe Illustrator software, and length of each tubule was calculated in ImageJ software (NIH, Bethesda, Maryland). The total sum of tubule length per area was calculated for each sample. Data from separate experiments was pooled, and ANOVA followed by Tukey's Least Significant Difference post hoc analysis was performed to determine significant differences between groups, with $p < 0.05$ considered significant. All data are presented as mean \pm standard deviation.

Formation of Three-dimensional Proteolytically Degradable PEG Hydrogels

Collagenase-degradable hydrogels with encapsulated HUVEC cells (3×10^7 cells/mL, labeled with Celltracker Green) were prepared. PEG-PQ-PEG (0.1 g/mL), acryloyl-PEG-RGDS (3.5 μ mol/mL), and acryloyl-PEG-VEGF (400 pmol/mL or 2 nmol/mL) were mixed with a cell suspension and photocrosslinked by exposing to long wavelength UV (365 nm, 10 mW/cm²) for 9 min, using Irgacure 2959 as the photoinitiator (0.3% w/v). Control hydrogels were crosslinked without incorporation of PEG-VEGF.

Timelapse Study of Endothelial Tubulogenesis in Three-dimensional Degradable PEG Hydrogels

Constructs were cultured for 5 h in EGM-2 medium without VEGF at 37°C in a 5% CO₂ environment and then transferred to a confocal microscope (Zeiss Live5, Thornwood, NY) with a stage chamber providing a regulated environment (37°C and 5% CO₂). No additional proteolytic enzymes or protease inhibitors were added to the culture. Z-stack images were collected every hour for 60 h using the Multi Time Series macro (Zeiss), Plan-Apochromat 20x objective with 0.8 numerical aperture, and excitation wavelength = 489 nm, emission bandpass (BP) filter = 500-525 nm, and pinhole = 55 μ m. Timelapse movies were analyzed for cell migration and cell-cell contact formation. For cell migration quantification, the movement of 3 cells randomly selected from each sample was tracked using Zeiss LSM5 Image Browser software, which allows

the tracing and quantification of cell paths through timeframe progression. For cell-cell contact formation quantification, the number of all cell-cell contacts formed within the viewing field was counted by timeframe progression using the same software. Data from separate experiments was pooled, and Student's two-tailed, unpaired T-tests were performed to determine significant differences between groups, with $p < 0.05$ considered statistically significant. Representative samples were fixed with 4% formaldehyde in PBS at 27 h, permeabilized with 0.5% Triton X-100 for 30 min, blocked with BSA for 30 min, and stained with Alexa Fluor 568-conjugated phalloidin (10 U/mL, Molecular Probes) for 2 h and DAPI (2 μ M, Invitrogen, Carlsbad, California) for 30 min to label cell actin filaments and nuclei. Samples were visualized using confocal microscopy (Zeiss Live5, Plan-Neofluar oil-immersion 40x objective with 1.3 numerical aperture, for phalloidin: excitation = 532 nm, emission BP filter = 560-675 nm, for DAPI: excitation = 405 nm, emission BP filter = 415-480 nm, pinhole = 10 μ m) to obtain z-stack images which were then processed into 3D projections using ImageJ software.

VEGF Release Study

5% w/v PEGDA hydrogels (PEGDA MW=6 kDa) were made in volumes of 5 μ l containing 2 μ g VEGF (Peprotech) using Irgacure 2959 (Ciba Specialty Chemicals) photoinitiator (0.27 ng/ μ l hydrogel) and exposed to UV for 10 min. Hydrogels were placed in 30 μ l PBS at 37° C and transferred to fresh PBS at 2, 4, 6, 8, and 24 h. Released VEGF was quantified using the bicinchoninic acid (BCA) assay (Pierce), using bovine serum albumin (BSA) standards ranging from 0 to 70 μ g/ml.

Chorioallantoic Membrane Assay

White Leghorn chicken embryos were acquired from Utah State University. On Day 0, eggs were transferred from 16°C to a humidified incubator (37.8°C, 65% humidity). On Day 8, eggs were opened, and 5 µl hydrogels containing 1.8 µg unbound VEGF₁₆₅ were polymerized on the chorioallantoic membrane (CAM) using acetophenone and long wavelength UV (365 nm, 6 min). On Day 12, effects of hydrogels on the embryonic vasculature were observed *in ovo* via light microscopy.

RESULTS

Polymer Characterization

Conjugation of RGDS to acryloyl-PEG-NHS or acryloyl-PEG-SMC was confirmed via GPC, which showed the product PEG-RGDS to have an increase in molecular weight compared to PEG-NHS (Figure 2-5). Conjugation of PEG-PQ-PEG was similarly confirmed via GPC (Figure 2-6). Conjugation of VEGF to acryloyl-PEG-SMC was confirmed via Western blot (Figure 2-7). Native VEGF appears in two bands, at 38 and 19 kDa, indicating dimer and monomer species, respectively. The marked increase in molecular weight of PEG-VEGF indicates successful pegylation of the protein [DeLong, Moon, et al. 2005], and the larger breadth of the PEG-VEGF band indicates the presence of several species of PEG-VEGF due to a distribution of the number of PEG chains per VEGF.

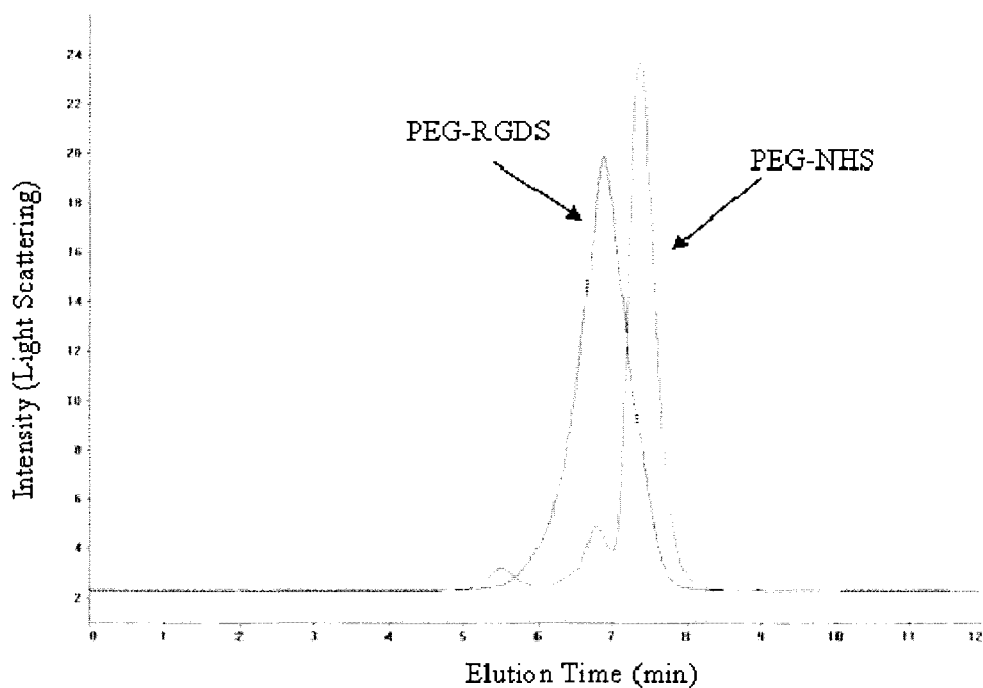


Figure 2-5 Gel Permeation Chromatography Analysis of PEG-RGDS conjugation. Black line, with peak at 7 shows molecular weight distribution of conjugated PEG-RGDS. Red line with main peak at 7.5 shows molecular weight distribution of PEG-NHS. Successful conjugation is shown by a shift in the peak, indicating increase in molecular weight, and lack of PEG-NHS peak in PEG-RGDS sample.

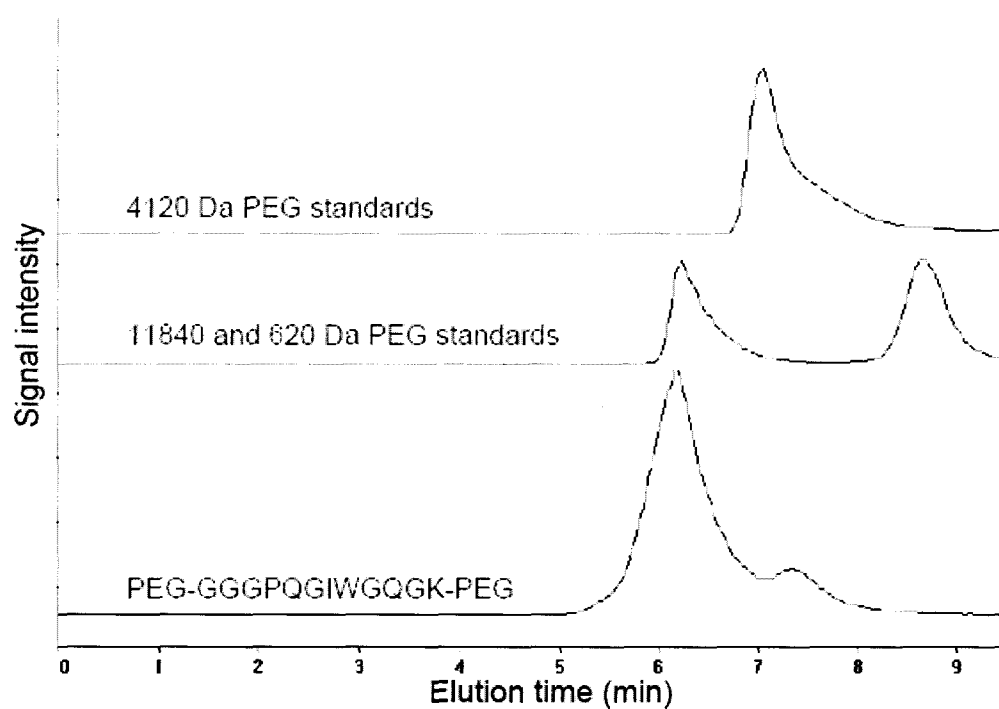


Figure 2-6 Gel Permeation Chromatography Analysis of PEG-PQ-PEG. Shift of peak to left indicates increase of molecular weight and hydrodynamic size of polymer with peptide.

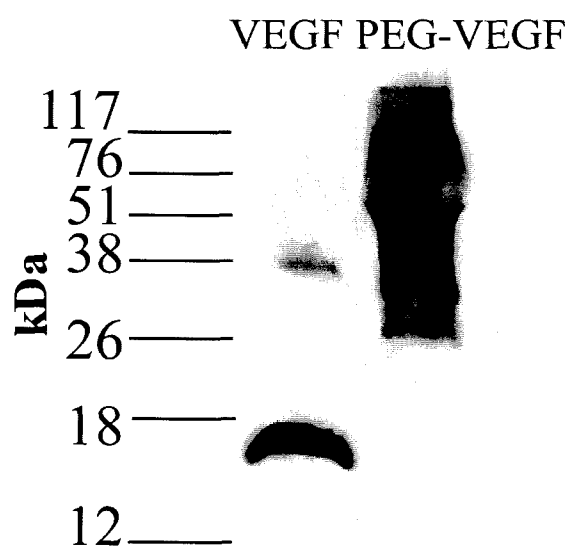


Figure 2-7 Western blot of pegylated VEGF compared to native VEGF shows a substantial increase in molecular weight, indicating pegylation of the protein.

Bioactivity of PEG-VEGF

Bioactivity of PEG-VEGF was measured by its pro-mitotic effects on endothelial cells. Proliferation was measured by counting cell number after treatment with bioactive media containing VEGF, PEG-VEGF, or No VEGF. PEG-VEGF increased endothelial cell number 1.35 ± 0.25 fold, compared to a 1.43 ± 0.09 fold increase in response to nonpegylated VEGF. These results were not statistically different from each other and are in range with VEGF proliferation expected results [Zisch 2003]. Both VEGF, as the positive control, and PEG-VEGF promoted a proliferation response that was statistically higher than the No VEGF control, with ** $p < 0.05$ between PEG-VEGF and No VEGF and * $p < 0.01$ between VEGF and No VEGF (Figure 2-8).

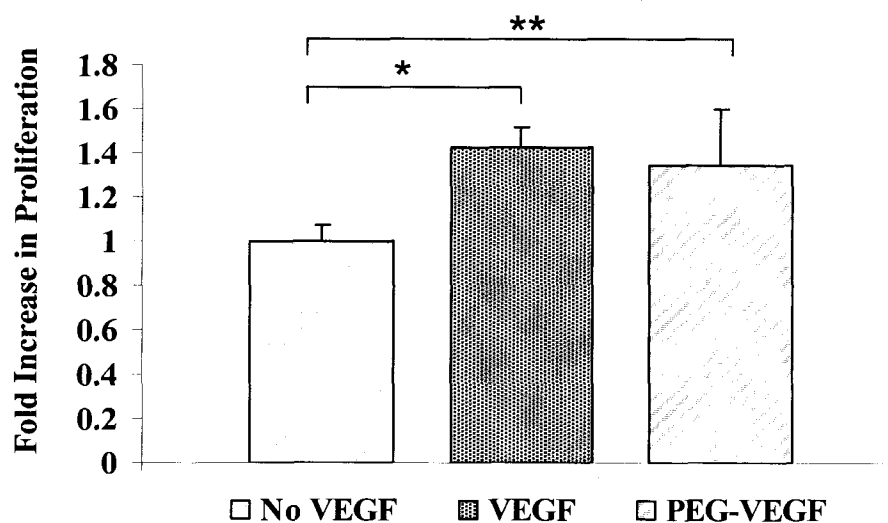


Figure 2-8 Proliferation of HUVEC cells in response to soluble PEG-VEGF. Medium containing soluble PEG-VEGF promoted an increase in cell number as compared to the No VEGF control. PEG-VEGF showed statistically similar results to unpegylated VEGF. * $p < 0.01$, ** $p < 0.05$

Quantification of PEG-VEGF and PEG-RGDS on the Surface of Hydrogels

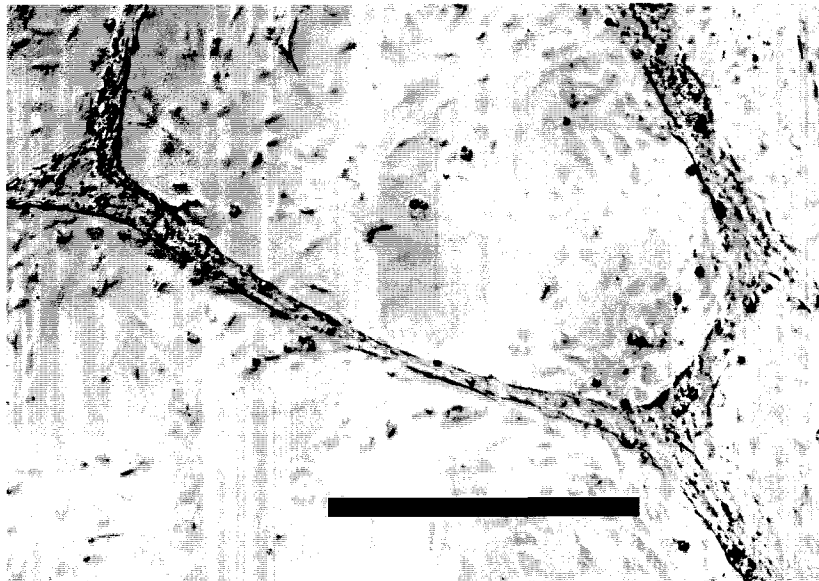
Hydrogels had an average of 19 ± 0.75 pmol/cm² PEG-VEGF on the surface, which corresponds to a conjugation of approximately 82% of the PEG-VEGF in the polymer solution. After an additional 24 h incubation in buffer, 98-99% of the initial PEG-VEGF remained attached to the surface. Hydrogels had an average of 5.4 ± 3.2 nmol/cm² PEG-RGDS on the surface. The concentration of PEG-VEGF in the prepolymer solution was matched to that used by Zisch et al. in three-dimensional hydrogels [Zisch 2003]. A higher level of PEG-VEGF (5x) in the prepolymer solution reduced cell attachment and thus did not promote extended endothelial cell tubulogenesis. The level of RGDS was optimized to support long term (30+ d) endothelial cell attachment.

Surface-immobilized VEGF Promotes Tubulogenesis

Within 30 d in culture, endothelial cells exhibited extensive branching networks of endothelial tubes on hydrogels modified with PEG-VEGF and PEG-RGDS. Control hydrogel surfaces modified with PEG-RGDS allowed HUVEC attachment and growth, but did not promote tubulogenesis (Figure 2-9). Endothelial tubes formed on the surface of hydrogels modified with RGDS and VEGF were stained for visualization of actin filaments and cell nuclei. Visualization via confocal microscopy confirmed tubule-like structures on the surface of the hydrogel (Figure 2-10), and a cross-sectional image of the tubule shows the tubule above surrounding spread cells and suggests a patent lumen (Figure 2-11). Hydrogels modified with PEG-RGDS and PEG-VEGF promoted

significantly more tubulogenesis than those modified with PEG-RGDS alone (Figure 2-12; $p < 0.05$). Endothelial cells grown on hydrogels modified with PEG-VEGF and PEG-RGDS, cultured without VEGF in the medium, formed tubules totaling $1127 \pm 974 \mu\text{m}/\text{mm}^2$, while cells on hydrogels modified with PEG-RGDS only, cultured without VEGF in the medium, formed tubules totaling $234 \pm 310 \mu\text{m}/\text{mm}^2$, and cells on hydrogels modified with PEG-RGDS only, cultured with VEGF in the medium, formed tubules totaling $217 \pm 591 \mu\text{m}/\text{mm}^2$. Additionally, tubules formed on RGDS- and VEGF-modified hydrogels were stable for at least 60 d, suggesting that PEG-VEGF promotes a controlled angiogenic response on surfaces of hydrogels. Lower levels of PEG-RGDS on the surface (0.5 and $0.05 \text{ nmol}/\text{cm}^2$) did not support extended endothelial cell attachment.

A



B

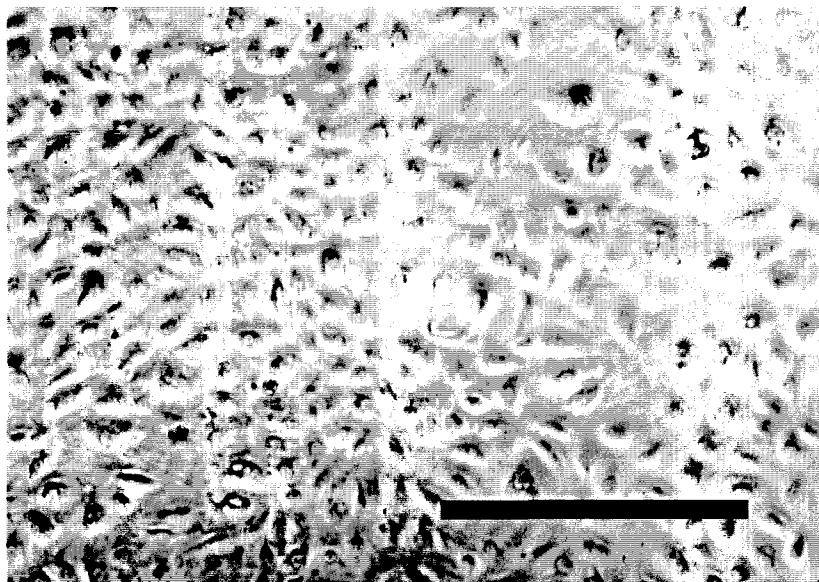


Figure 2-9 A) Branching endothelial tubule networks formed on the surface of hydrogels modified with RGDS and VEGF at 19 d. B) Fewer tubules formed on hydrogels modified with RGDS only at 19 d. Scale bar = 500 μ m.

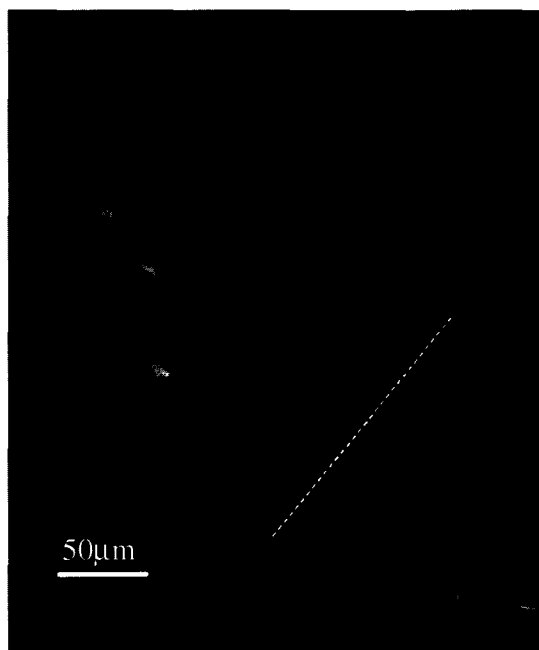


Figure 2-10 Endothelial tube on hydrogel surface stained with phalloidin (red) and DAPI (blue). White line indicates cross-sectional view in Figure 2-11.

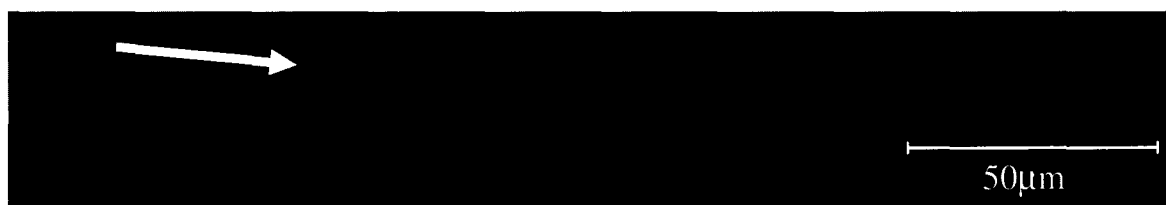


Figure 2-11 Cross-section of tube structure on the surface of hydrogel. Arrow points to tube structure rising above plane of surrounding spread cells.

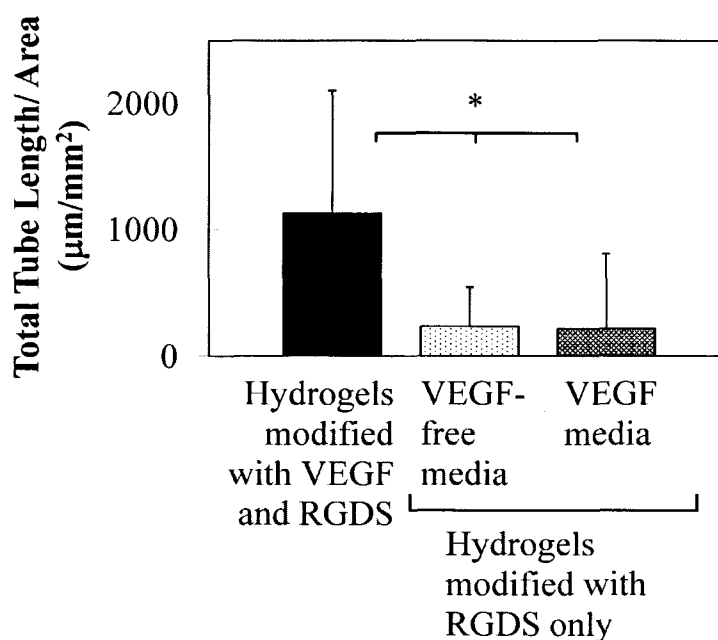


Figure 2-12 Quantification of tubulogenesis shows a significant endothelial cell response to immobilized VEGF on the surface of PEGDA hydrogels. Hydrogels modified with VEGF and RGDS were cultured in VEGF-free media. Error bars show standard deviation. (ANOVA $p < 0.01$, Tukey's Least Significant Difference between VEGF group and both RGDS groups $p < 0.05$).

Immobilized VEGF in 3D Degradable Hydrogels Promotes Cell Motility, Cell-Cell Contact Formation, and Tubulogenesis

In three dimensional PEG hydrogels with immobilized VEGF, endothelial cells exhibited extensive angiogenic behavior, as observed by timelapse confocal microscopy. Between 21-42 h after encapsulation, HUVECs formed elongated multiple-cell structures in hydrogels with RGDS and VEGF homogeneously and covalently bound to the matrix

but less so in hydrogels with RGDS only (Figure 2-13, Figure 2-14, Figure 2-15, and Figure 2-16).

Figure 2-13 Time series of confocal images illustrating cell behavior in 3D collagenase-degradable PEG hydrogels. White arrows point to cell migration and cell-cell contact formation. Yellow arrows show paths of cell migration and tubule formation. Cellular migration, cell-cell contact formation, and branching tube formation inside collagenase-degradable PEGDA hydrogels modified with PEG-VEGF and RGDS. Scale bar = 100 μm .

RGDS and VEGF (400 pmol/mL)

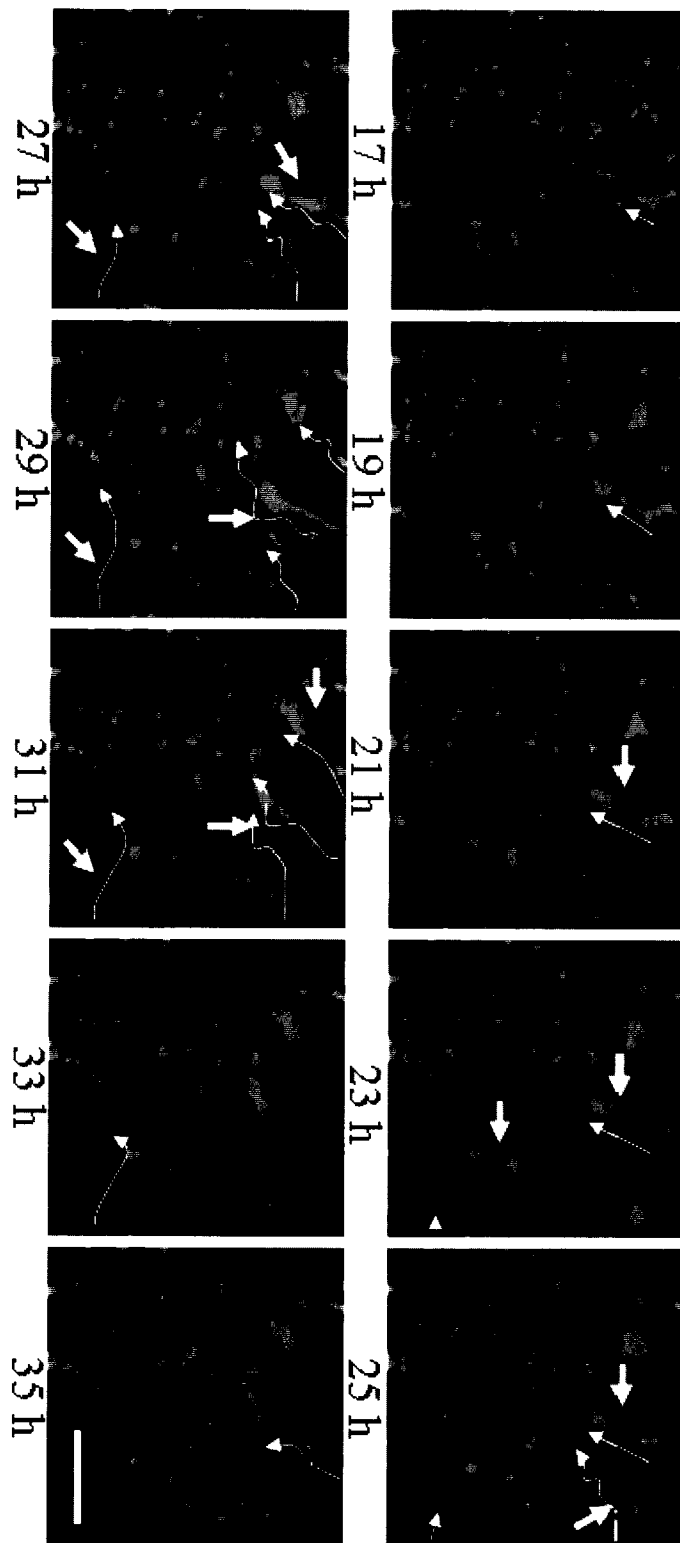


Figure 2-14 Time series of confocal images illustrating cell behavior in 3D collagenase-degradable PEG hydrogels. White arrows point to cell migration and cell-cell contact formation. Yellow arrows and lines show paths of cell migration and tubule formation. Accelerated angiogenic activity and hydrogel degradation in response to a 5-fold increase in attached PEG-VEGF. Scale bar = 100 μm .

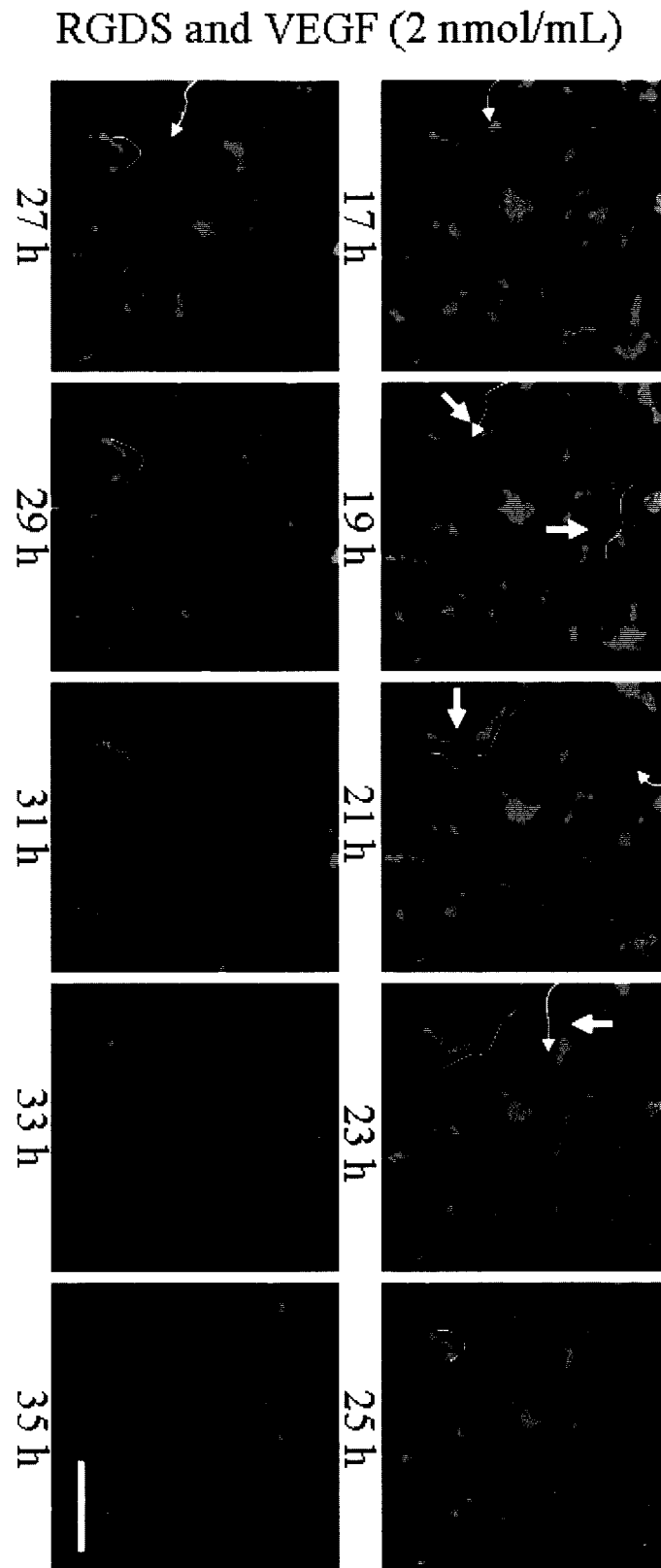
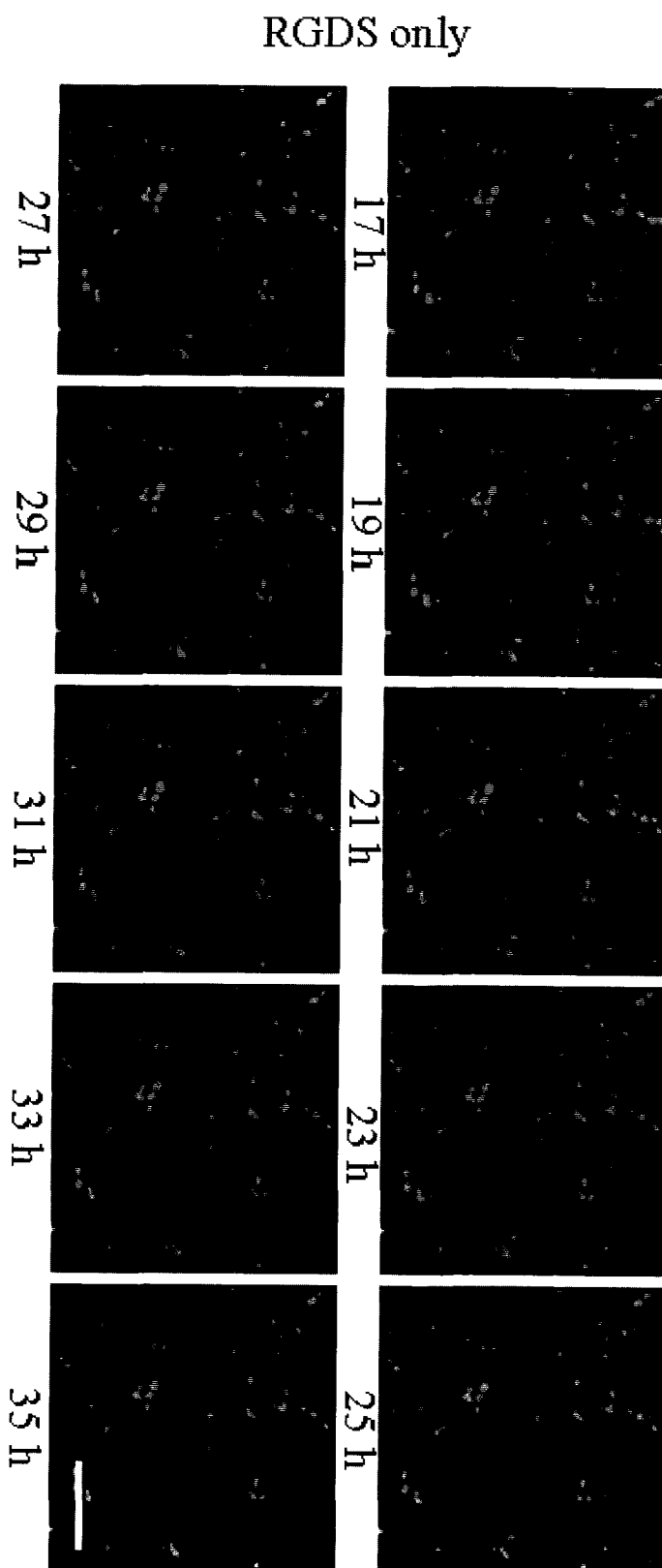


Figure 2-15 Time series of confocal images illustrating cell behavior in 3D collagenase-degradable PEG hydrogels. Less cellular activity in hydrogels modified with RGDS only. Scale bar = 100 μm .



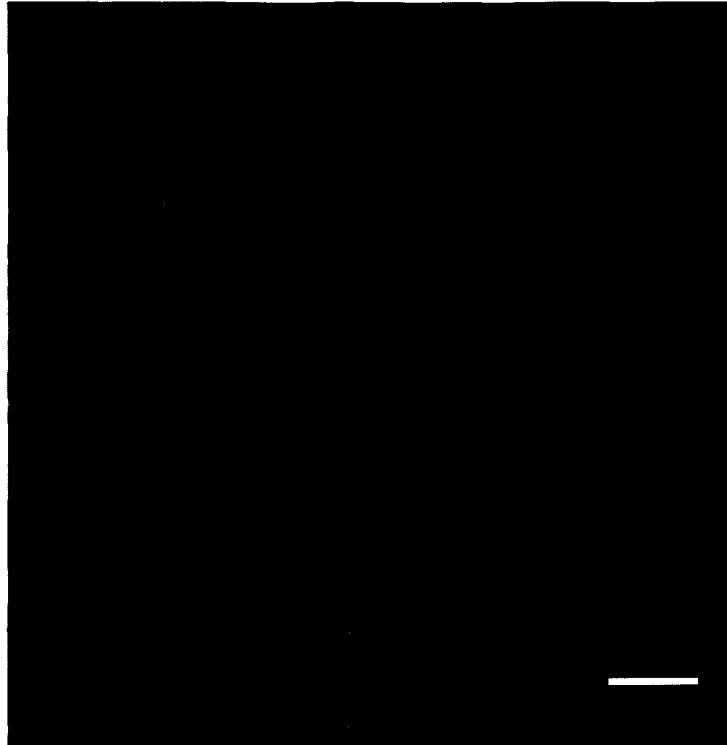


Figure 2-16 Three-dimensional confocal image of endothelial tube structures formed at 27 h in 3D collagenase-degradable PEG hydrogels modified with VEGF and RGDS. Cellular structures were stained with DAPI (blue) and phalloidin (red) to visualize cell nuclei and actin filaments, respectively. Scale bar = 20 μm .

Cells in VEGF-modified hydrogels with 400 pmol/ml (VEGF/volume of hydrogel) had significantly more migratory behavior, traveling 14 times farther, and formed 3 times more cell-cell contacts than cells in hydrogels without VEGF (Figure 2-17, Migration Distance: $p < 5.45 \times 10^{-7}$, Cell-cell Contacts: $p < 0.006$). Both migration and cell-cell contact formation through surface projections are fundamental behaviors during angiogenesis [Ausprunk 1977].

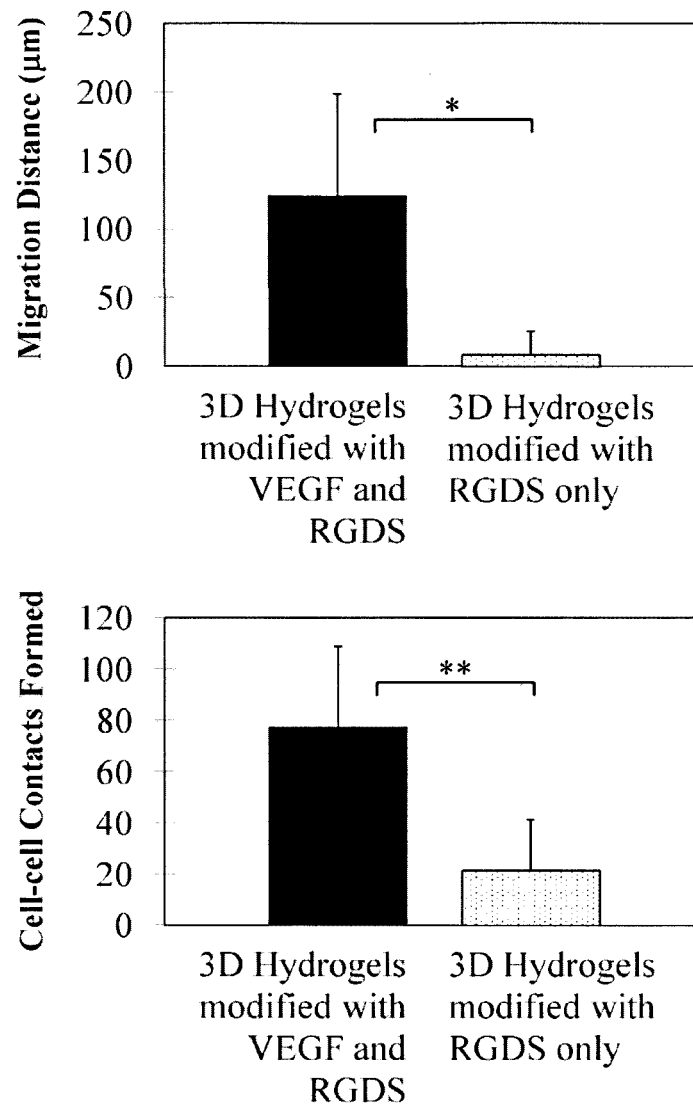


Figure 2-17 Quantification of angiogenic activity in 3D collagenase-degradable PEG hydrogels shows a significant endothelial cell migration and cell-cell contact response to immobilized VEGF (400 pmol/ml) bound within the hydrogel. Hydrogels were cultured in VEGF-free media. Error bars show standard deviation. (* $p < 5.45 \times 10^{-7}$, ** $p < 0.006$).

Time lapse confocal microscopy showed endothelial tubes in 400 pmol/ml VEGF hydrogels regressing after 51 h, most likely due to the absence of mural cells, such as pericytes, that stabilize forming capillaries. Endothelial cells cultured in hydrogels with

2 nmol/ml immobilized VEGF exhibited faster migration and caused the accelerated degradation of the hydrogel within hours (Figure 2-13). The accelerated migration and degradation is hypothesized to be due to an increase in secreted MMPs in response to higher VEGF signaling. These results suggest that dosing of immobilized VEGF in collagenase-degradable hydrogels must be highly regulated to achieve the desired tubulogenic and hydrogel degradation temporal response. Ideally, cells should lay down new matrix proteins at a comparable rate to PEG degradation to ensure integrity of the tissue construct. This study shows that incorporating growth factors which affect MMP expression and secretion will drastically affect the tissue remodeling behavior of encapsulated cells. HUVEC migratory behavior in VEGF hydrogels continued until the study ended, suggesting that the covalently-bound VEGF retained bioactivity throughout the study and was able to induce the first steps of angiogenesis: endothelial cell migration, cell-cell contact formation, and endothelial tubule formation.

VEGF Release

Diffusion of soluble, nonpegylated VEGF out of hydrogel materials was assessed *in vitro* in PBS at 37°C. After 8 hours, 60% of the incorporated VEGF had been released by the hydrogel. The total amount of VEGF released did not increase substantially after 8 hours (Figure 2-18). This modified burst effect is hypothesized to allow VEGF signaling to be delivered to the host over a short amount of time, after which the effects of the released VEGF would be expected to be silenced by angiogenesis control mechanisms inherent in the body.

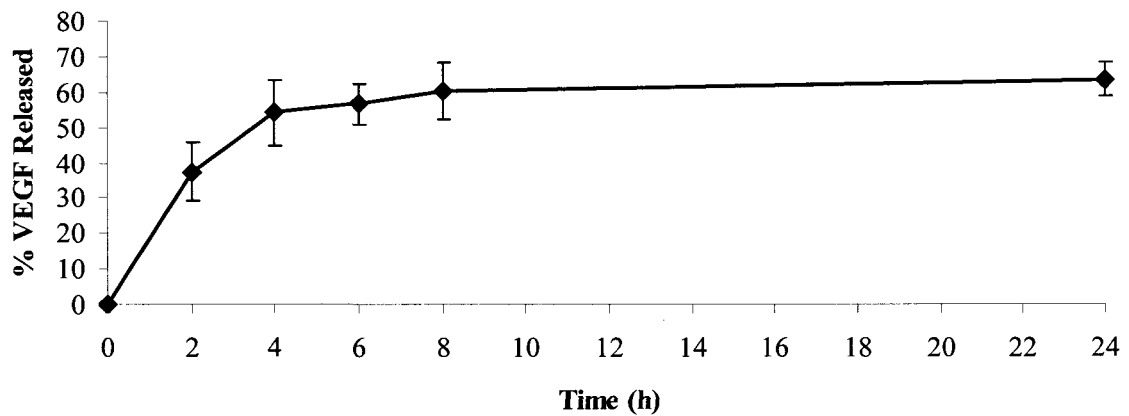


Figure 2-18 VEGF release profile of PEGDA hydrogels initially containing 2 μ g VEGF shows an initial burst within the first 8 hours. This release profile allows the hydrogel to provide an initial larger dose of growth factor signaling, followed by a slow, long lasting release of signaling to surrounding tissue.

CAM Assay

VEGF released from hydrogels promoted an angiogenic response from CAM microvasculature at Day 12, four days after the hydrogel was introduced to the system (

Figure 2-19). Control microvasculature exhibited a normal branching structure, while microvasculature near VEGF-releasing hydrogels remodeled its geometry to approach the hydrogel and was more tortuous, indicative of newly formed microvasculature. This approach of releasing VEGF from the hydrogel can be used to attract host microvasculature, thus facilitating anastomosis of hydrogel pre-existing microvascular networks to the host vasculature.

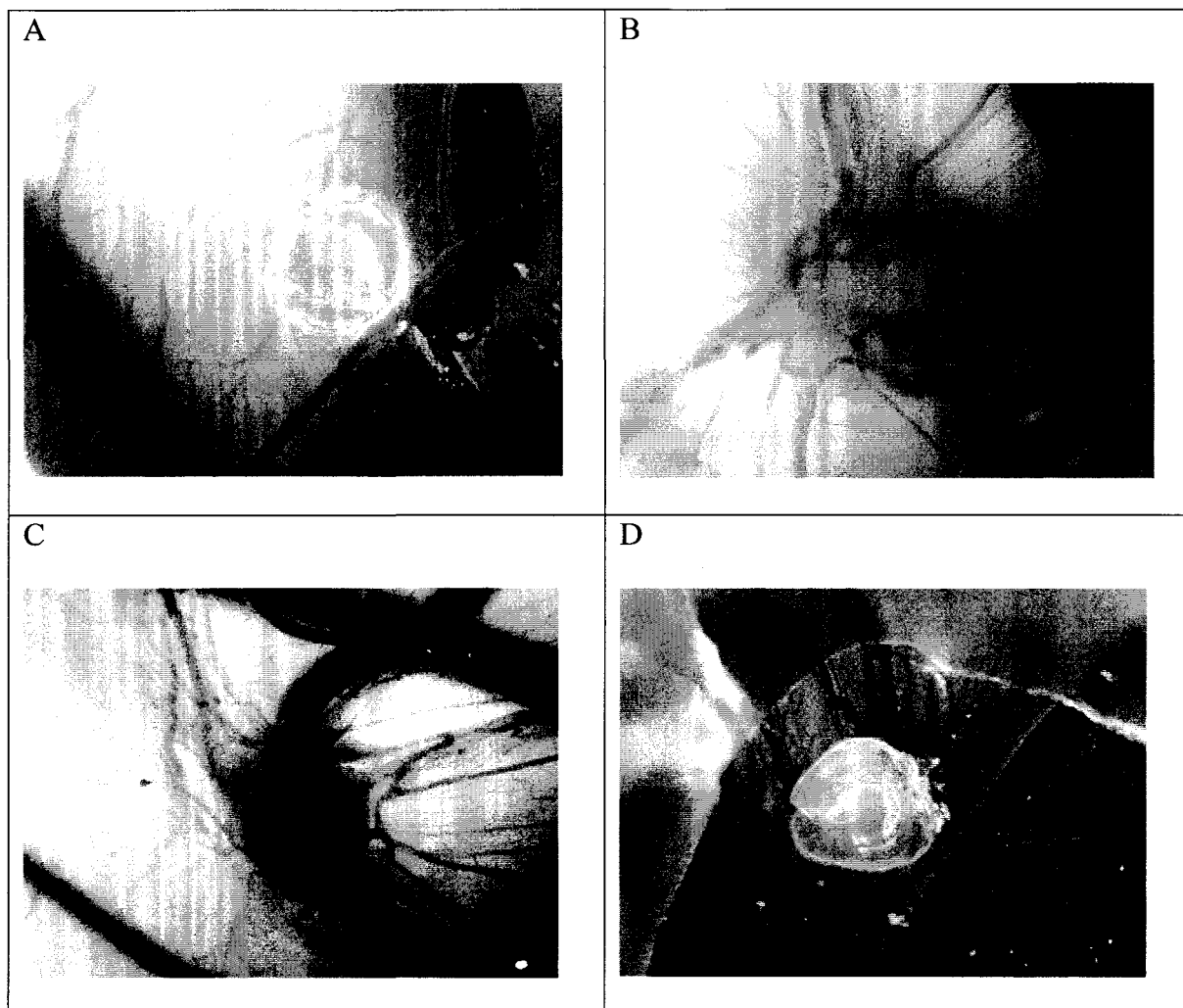


Figure 2-19 Micrographs of CAM microvasculature response to hydrogels. A) Control gel, no VEGF. B, C, D) VEGF-loaded hydrogels. The CAM angiogenic response to released VEGF from PEGDA hydrogels promotes growth of native capillaries towards the hydrogel. 6.4X magnification.

DISCUSSION

Several studies have examined releasing or sequestering growth factors in tissue engineering matrices. Nillesen et al. induced *in vivo* capillary formation and maturation in collagen scaffolds by incorporating heparin-bound VEGF and FGF2. Hypoxia decreased dramatically from 97-98% at day 3 to 2% by day 7 and 0.2% by day 21 in scaffolds containing VEGF and FGF2 while it remained at 37% (day 7) and 21% (day 21) in collagen scaffolds without growth factors [Nillesen 2007]. This study confirms the extended state of hypoxia in nonvascularized tissues and also points to the longevity of signaling and biological response to matrix-bound growth factors. Collagen scaffolds with incorporated heparin, however, allow continual release and rebinding of growth factors, and can interact not only with the desired growth factors, but also with other proteins supplied by the host at the area of the implant. Thus, the environment is not regulated, and the results cannot be shown to be directly related to the influence of the matrix design.

Peters et al. engineered a poly(lactide-co-glycolide) (PLG)-Matrigel matrix to control the local release of VEGF. Pores were created in the VEGF-releasing PLG matrix to allow endothelial cell vessel formation. Human microvascular endothelial cells were suspended in Matrigel, which was then absorbed into the polymer scaffold. Human microvascular endothelial cells formed capillaries within the PLG-Matrigel matrix *in vivo* in SCID mice in 5 days [Peters 2002]. This study relied on released VEGF and Matrigel to promote angiogenesis within a synthetic matrix. The release kinetic profile of VEGF was engineered into the synthetic matrix design; however, the matrix was not used to

support cell adhesion on its own. Further engineering and refinement of synthetic matrices incorporating growth factors could improve control of angiogenic cellular behavior both *in vitro* and *in vivo*.

Helm et al. studied the requirements for *in vitro* capillary formation in collagen and fibrin gels incorporating matrix-bound VEGF and interstitial flow. After 10 days, blood vessel endothelial cells organized themselves preferably in collagen-fibrin matrices with high fluid permeability and preferred highly compliant matrices, presumably for remodeling and migrating. The researchers noted that because natural scaffolds were used in this study, there were several uncharacterized properties such as mechanical properties, proteolytic sensitivity, cytokine retention, and integrin ligand availability that could alter the capillary formation processes studied [Helm 2007]. Complications arise when attempting to understand the results seen in combination natural matrices with uncontrolled signal and integrin ligand densities.

The results presented in this thesis show that covalently immobilized, pegylated VEGF retains its ability to induce angiogenic behaviors by HUVECs on PEG hydrogels, and thus may be useful for spatially controlled angiogenesis in engineered tissues. Furthermore, the tubulogenic process was quantified *in vitro*, as a step to assure quality before implantation. Such quality assurance is vital when implanting tissue into compromised patients whose bodies may not be able to vascularize implanted tissues at expected rates.

The time course of tubulogenesis on 2D PEG hydrogels differs from those studies using natural matrix materials, where tubulogenesis was reported between 5-10 d. The main reasons for the differences are hypothesized to be due to the microenvironment

presented to the cells. Matrigel, a largely uncharacterized reconstituted basement membrane material, and fibrin/collagen gels present numerous integrin ligands and sequester many growth factors and other extracellular matrix molecules which can interact with cells. Additionally, these matrices are much softer than the PEGDA hydrogels used in this study, and material stiffness can play a major role in the kinetics of tubulogenesis [Helm 2007]. The materials used in the present studies were specifically designed to limit integrin and receptor interactions to intentionally immobilized peptides and proteins. Thus, the results observed in the present *in vitro* studies are due solely to the scaffold-bound factors and soluble factors in the controlled medium. The low level of tubulogenesis seen on RGDS-only gels cultured in VEGF-free EGM-2 is most likely due to bFGF in the medium. The presented data shows that pegylated, covalently-immobilized VEGF has a greater angiogenic effect than repeated doses of soluble VEGF and other soluble angiogenic factors, as presented in the medium for control groups. An additional advantage of immobilization of VEGF is that it should allow local and controlled angiogenic therapy without unwanted activity elsewhere in the body.

While it took on the order of weeks to observe branching networks of endothelial tubes on the surface of the hydrogels in 2D culture, initial angiogenic activity, including extensive cell migration and cell-cell contact formation, was observed within days for the 3D matrix. This phenomenon could be due to the nature of the matrix. Previous work on RGDS concentrations has shown that a higher level of RGDS in the matrix, which allows more integrin-ligand binding required for extended culture of cells, also reduces cell migration, due to the requirement of cells to detach from the substratum to move forward. In the 2D experiments, PEG-RGDS levels were optimized for long-term attachment;

while in the 3D experiments, PEG-RGDS levels were optimized for migration [Gobin 2002]. Therefore, while migration and tube formation were observed earlier in 3D matrices, formed tubules on 2D matrices were stable for at least 60 d. Furthermore, cells in the 3D matrices received VEGF signaling from all directions, whereas those on the surface of gels received VEGF signaling and integrin attachment ligands only from the basal side of the cell. Thus, the amount of signaling available to cells might have been dissimilar between microenvironments and could have affected the kinetics of tubulogenesis.

Three-dimensional hydrogels allowed extracellular matrix cleavage through the activity of cell-secreted proteases. VEGF has been shown to increase the expression of collagenase by endothelial cells [Unemori 1992]. In matrices with covalently-linked VEGF, cell migration and cell-cell contact formation were significantly higher than in matrices with RGDS only, and cellular spreading and elongation showed similar trends. Because no exogenous collagenase was added to these cultures, the cellular activity suggests that cells in VEGF-matrices produced and secreted more collagenase than those in matrices without VEGF, possibly due to the increased VEGF signaling. Increasing the amount of covalently-bound VEGF to 2 nmol/mL in 3D collagenase-degradable hydrogels accelerated matrix degradation, further supporting the specific activity of covalently bound VEGF on endothelial behavior.

Proteolytically degradable PEG hydrogels provide a controllable system for engineering tissue formation. Degradation kinetics can be modified by varying the concentration of proteolytically degradable PEG in the hydrogel or by utilizing any combination of proteolytically degradable PEG with conventional nondegradable

PEGDA. Hydrogels consisting of only proteolytically degradable PEG have been studied *in vivo* for 14 days [Zisch 2003], while combination degradable/nondegradable hydrogels can be cultured for weeks to months in bioreactor conditions [Hahn 2007]. Zisch et al. used biodegradable PEG hydrogels with cleavable, covalently attached VEGF₁₂₁ or VEGF₁₆₅ to induce post-implantation angiogenesis in the scaffold in chorioallantoic membrane and rat models. VEGF was bound to PEG in a manner so that cell-secreted collagenase could cleave and release the protein from the matrix. Their material also contained proteolytically degradable peptide sequences to allow cell invasion. Results showed that these matrices support host tissue generation *in vivo* after 14 d [Zisch 2003]. In the current reported studies, a similar technology was used to further study and enhance the angiogenic potential of PEGDA hydrogels as tissue engineering scaffolds. This work shows that covalently binding the growth factor directly to the matrix also promotes angiogenic activity in PEG-based hydrogels and that release of growth factor is not needed for this response. The attachment of VEGF to the matrix provides longevity of signaling (shown up to 30 d in this study) and works towards the prevention of undesired angiogenesis in other locations. In these studies, promotion of microvascularization was achieved *ex vivo*, under non-invasive observation. VEGF release from hydrogels was characterized *in vitro*, and *in ovo*, was shown to promote a host microvascular response in which capillary networks approached the hydrogel, a method which could be used to allow anastomosis of prevascularized hydrogels with host microvasculature.

CONCLUSIONS

PEGDA hydrogels have the potential to act as tissue engineering scaffolds due to their biocompatibility and ability to be tailored for specific applications by incorporating relevant integrin ligands and growth factors to promote desired cell behavior. In this work, PEGDA hydrogels were modified to contain the cell-adhesive peptide RGDS and the angiogenic growth factor VEGF to promote endothelial tubulogenesis, the first step in creating a functional microvasculature in tissue engineered constructs. PEG-VEGF was shown to retain bioactivity as evidenced by its ability to promote proliferation of endothelial cells. Surface immobilization of VEGF significantly enhanced endothelial tubulogenesis, resulting in branching networks of capillary-like tubules on the surface of the hydrogel. Three-dimensional collagenase-degradable PEGDA hydrogels with covalently attached RGDS and VEGF promoted endothelial angiogenic activity by encapsulated HUVEC cells. The incorporation of a collagenase-sensitive peptide sequence within the framework of the hydrogel allowed cells to remodel the matrix during migration and cell-cell contact formation. Covalently immobilized VEGF is a promising avenue for promoting tubulogenesis in engineered tissues. PEG-VEGF covalently attached to the hydrogel retained bioactivity, as evidenced by the continued migratory and contact-forming behavior of cells in VEGF-modified hydrogels. The covalent immobilization of VEGF within the matrix ensures a predicted, local, and engineered response. The modification of PEGDA hydrogels with angiogenic signals appears to be a promising method for the generation of microvasculature in tissue engineered products. The clinical application of this technique may provide

prevascularized engineered tissues for implantation. Further studies will determine if the incorporation of additional signaling molecules and cell types would provide optimal microvascular formation and stability.

Chapter 3 Micron-scale Spatially Patterned, Covalently Immobilized VEGF on Hydrogels Accelerates Endothelial Tubulogenesis and Increases Cellular Angiogenic Responses

INTRODUCTION

The natural process of angiogenesis relies on a complex system of biochemical signals and cell-cell/cell-matrix interactions. *In vivo*, capillaries form “self-patterned” networks to allow transport of nutrients, oxygen, and waste throughout tissue, connecting arterial and venous vasculature to ensure nutrient and oxygen transport via convection (Figure 3-1). Patterning occurs when endothelial cells respond to sequestered growth factors to form preliminary endothelial tubes, which are later reorganized via tubule regression and stabilization in order to meet the nutrient and oxygen requirements of the tissue. Initiation of angiogenesis occurs through an endothelial cell response to signaling factors such as vascular endothelial growth factor (VEGF). *In vivo*, endothelial cells respond to VEGF by forming preliminary endothelial tubules, which are later stabilized by supportive mural cells to form capillaries [Jain 2003]. In the body, expression of VEGF is induced by low oxygen tension, as mediated through hypoxia-inducible factor (HIF)-1 [Ferrara 2003]. Secreted VEGF diffuses from hypoxic cells to existing capillaries [Gerhart 2005], where it promotes endothelial permeability, mitosis, and angiogenesis (Figure 3-2) [Keck 1989].



Figure 3-1 Capillary networks formed under normal conditions are “patterned” by the body to optimize transport. From [Jain 2005].

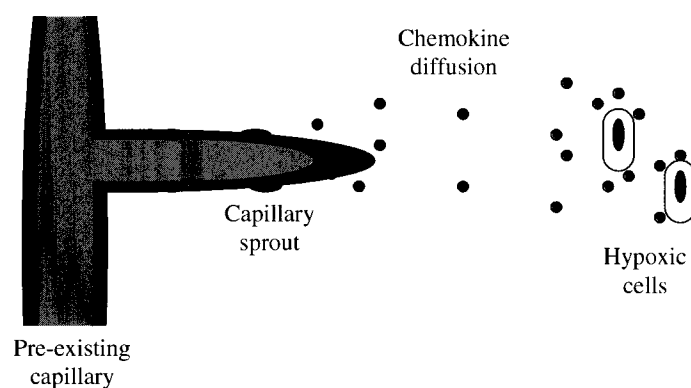


Figure 3-2 New capillaries form when pre-existing capillary endothelial cells sprout in response to chemokines secreted by hypoxic cells (adapted from [Gerhart 2005]).

As in most physiological processes, angiogenesis must be tightly regulated to avoid pathophysiologies. In the current study, angiogenic signaling is controlled and limited to distinct regions by covalently binding a growth factor to the matrix. Zisch et al. showed an angiogenic response due to signaling from pegylated VEGF which was cleaved by cellular enzymes from a PEG matrix [Zisch 2003]. Further work has shown that covalently-bound VEGF elicits an angiogenic response from endothelial cells cultured on poly(ethylene glycol) diacrylate hydrogels and that PEG-matrix dissociation is not necessary for this response (Chapter 2).

In addition to improving safety, localization of growth factors in the extracellular matrix may guide vessel formation [Jain 2003, Houck 1992]. For example, *in vivo*,

fibroblast growth factor-2 (FGF-2) accumulates at areas of capillary branching [Fernandez 2005] and may play a role in patterning capillary geometry. In addition, localization of VEGF has been shown to affect cell function, as cleaved, soluble VEGF₁₆₅ induces endothelial cell proliferation, while matrix-bound VEGF₁₆₅ promotes vascular sprouting and branching [Roy 2006]. Recent research has elucidated the role of cell-surface Eph receptors and their cell-surface ephrin ligands in patterning the localization of arterial and venous vasculature [Wang 1998]. Because the Eph/ephrin system is instrumental in capillary remodeling, expression of these cell-surface receptors is also of interest when working towards a functional microvasculature.

Dike et al. elucidated the importance of spatially restricting presentation of adhesion molecules in promoting angiogenesis. In Dike's work, gold-coated glass coverslips were coated with a saturated density of fibronectin via microcontact printing of hexadecanethiol, followed by self-assembling monolayer (SAM) formation of tri(ethylene glycol)-terminated alkanethiol and then fibronectin. Bovine capillary endothelial cells attached to patterned fibronectin lines of either 10 μm or 30 μm width and were cultured in medium saturated with FGF. Cells on 30 μm -wide lines remained spread and flattened while cells on 10 μm -wide lines organized into linear cellular cords which appeared to possess a centralized hollow space, as visualized by confocal microscopy [Dike 1999]. Underlying tendrils of laminin and fibronectin were observed. After several days, a single, continuous, central lumen extended over several cell lengths, and single cell bodies stretched around a negatively labeled lumen. Cells were observed to be partially retracted from the surface, and cells appeared to increase in height.

PECAM staining showed strong cell-cell attachment and continuous linear presence including at cell junctions [Dike 1999].

Dike et al. suggested that since binding of integrins stimulates chemical signaling in angiogenesis, cytoskeletal tension-dependent changes in cell shape may have a role in determining cell fate. Substrate-immobilized fibronectin promotes integrin clustering and activates integrin signaling pathways in capillary cells. They suggested that by restricting spreading, spatial restriction of extracellular matrix ligands promoted cell-to-cell contact, and thus promoted tube formation. Additionally, they hypothesized that both cell-generated traction forces causing partial retraction of the tendril away from the surface and matrix remodeling into thread-like configuration could be required in tube development [Dike 1999]. Since geometric restriction of ligand presentation affects tubulogenesis, this phenomenon could be used to improve microvascularization of tissue engineered constructs by tightly controlling ligand presentation in tissue engineering scaffold materials. The current studies explore the response of endothelial cells to patterned ligand and growth factor protein on the surface of biocompatible poly(ethylene glycol) (PEG) hydrogels. While restriction of cell-material interactions could be used to direct microvascular formation and anastomosis on the surface of biomaterials, two-dimensional patterning also acts as a foundation for future studies in three dimensions.

A promising biomaterial is poly(ethylene glycol) diacrylate (PEGDA), a biocompatible hydrophilic polymer that can be crosslinked to form hydrogels used for soft tissue scaffolds [Hahn 2007; DeLong, Moon, et al. 2005]. Crosslinking of polymer chains can be accomplished via photopolymerization [Hahn 2007, Mann 1999, Hahn 2005]. PEGDA hydrophilicity acts to resist protein adsorption, preventing nonspecific

cell adhesion, and thus acts as a “blank slate” which can be tailored to guide complex tissue organization [Hahn 2007].

In vivo, proteoglycans containing heparan sulfate act to bind and concentrate certain growth factors, such as bFGF, in the extracellular matrix as well as near cell surfaces [Houck 1992]. Localization of growth factors and cell-adhesive ligands can similarly be achieved in PEG-based hydrogels by covalently crosslinking these substrates to the hydrogel via photopolymerization [DeLong, Gobin, et al. 2005; DeLong, Moon, et al. 2005]. Because PEG hydrogels can be crosslinked and modified via chemical reactions initiated by light, localization of hydrogel components can be precisely patterned. Moon et al. showed that spatial restriction of PEG-RGDS in 50- μm -width lines on PEGDA guided endothelial tubule formation by 18 d as compared to 200- μm -width lines, which supported cell spreading but not tubulogenesis [Moon 2008].

Micron-scale Patterning Techniques

One of the most widely used methods for patterning materials is photolithography (Figure 3-3). The major requirement for photolithography is the ability to control chemical reactions by excitation via light. By restricting areas of light exposure, location of chemical reaction is controlled. A light-impermeable mask is created with transparent patterned areas. Light passes only through the pattern to the substrate below, thereby activating a desired chemical reaction. Rapid prototype masks, using transparency film printed with the design, usually limit features to larger than 20 μm [Kane 1999]. For

smaller features, a chrome photomask created by a laser writer in a clean room is required.

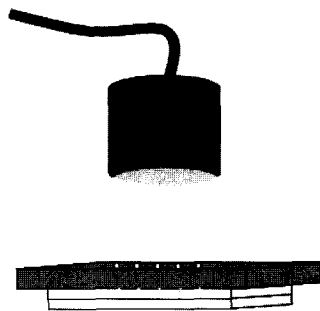


Figure 3-3 Photolithographic patterning requires a mask to control exposure of light to the photo-sensitive substrate below.

Photolithography has been optimized for substrates involved in microprocessor chip fabrication [Whitesides 2001]. These materials are hard, stiff, and unchanging substrates. Often, the materials are pressed together tightly to ensure high integrity of patterns. The pressing is required to reduce light scattering. For very small patterns, highly aligned light must pass directly through the pattern perpendicularly to achieve the same dimensions on the substrate to be patterned. Preliminary studies of using chrome photomasks and a columnated laser showed that small patterns were not reproducible when working with compliant hydrogel substrates and liquid prepolymer solution which could not be tightly pressed together. Furthermore, usual methods of photolithography require the use of clean room facility instrumentation, and wet hydrogel substrates were not compatible with such instrumentation designed for hard, dry substrates.

Another commonly used method for micron-scale patterning is soft lithography. This method uses a simple “stamp and ink” method to transfer surface-modifying

moieties as an ink, which is pressed in contact with a desired surface. These moieties then attach to the surface via chemical bonding (Figure 3-4) [Whitesides 2001].

Although soft lithography utilizes a “stamp” method, photolithography is used in making a silicone stamp, and therefore, this method also requires the use of chrome photomasks, photoresists, and cleanrooms. The success of accurate pattern transfer during the stamping procedure is highly dependent on operator ability. The method of microcontact printing is also difficult on wet, compliant surfaces such as hydrogels, as resulting patterns are not precise.

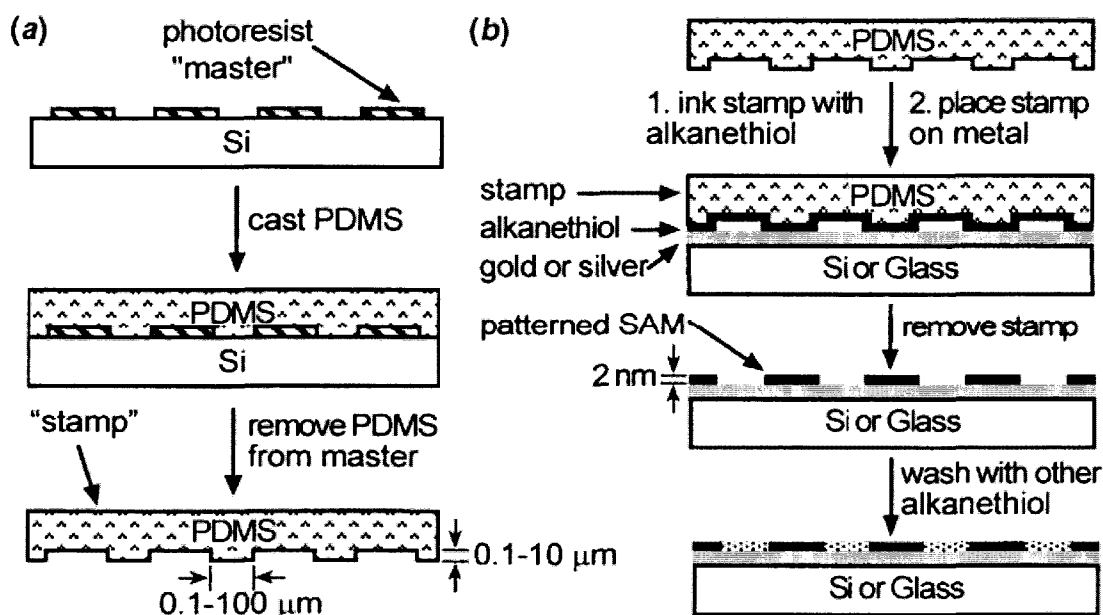


Figure 3-4 Process of microcontact printing [from Whitesides 2001]. “Stamp and ink” method of creating micron-scale pattern on silicon or glass surfaces. This process is most successful on hard surfaces, which do not mimic elastic properties of natural extracellular matrix.

A recent advancement, Laser Scanning Lithography (LSL), overcomes scale and reproducibility challenges often encountered in photolithography and soft lithography [Hahn 2005]. By using the precision of a confocal microscope, in which a laser is tightly focused onto a specimen and scanned with sub-micron precision, exposure to light and subsequent photopolymerization can be controlled spatially (Figure 3-5). Because the scanning laser is under the control of computer software, it is facile to restrict the laser excitation to particular areas of the specimen, as is frequently used in fluorescence-bleaching experiments. The user-defined Region of Interest (ROI) is drawn with exact coordinates using the software, allowing precisely calculated areas of excitation. The spatial area of laser scanning, power of the laser, laser scan speed, and number of iterations of scanning can be controlled via software which runs the microscope assembly. Additionally, since this method does not require the production of photomasks, patterns can be easily varied.

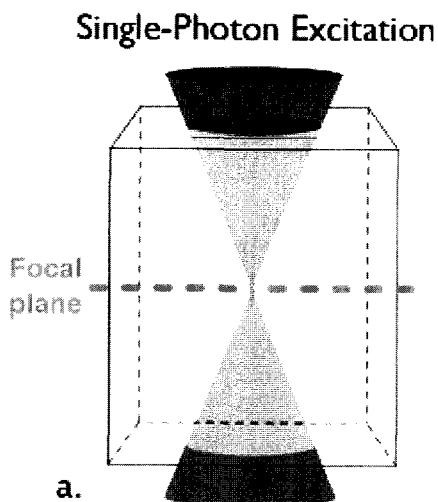


Figure 3-5 Excitation provided by single-photon laser. The excitation and subsequent photopolymerization is controlled by aligning the focal plane of the laser beam with the interface of the hydrogel and polymer solution. No mask or stamp is used, thereby allowing facile adjustment of patterns via software (from Jordan Miller).

Patterning the presentation of biochemical signals to be highly localized allows control of the geometry of the capillary bed and also should discourage uncontrolled angiogenesis in undesired locations. The presented use of matrix-bound VEGF₁₆₅ in patterned locations within biocompatible polymer hydrogels is hypothesized to promote endothelial tubulogenesis, thereby leading to highly organized vessel formation. This work introduces a system that stimulates and spatially controls the formation of endothelial tubules by patterning the localization of integrin ligands and growth factors on the surface of PEG hydrogels.

MATERIALS AND METHODS

Cell Culture

Human umbilical vein endothelial cells (HUVEC, Cambrex/Lonza, Walkersville, MD) were maintained in VEGF-free endothelial cell growth medium (EGM-2 media, Cambrex/Lonza) containing fibroblast growth factor (hFGF-B), epidermal growth factor (hEGF), insulin-like growth factor (R^3 -IGF-1), heparin, hydrocortisone, ascorbic acid, GA-1000 (gentamicin, amphotericin-B), 2% fetal bovine serum (FBS) (Bulletkit, Lonza), 1 U/mL penicillin, 1 μ g/mL streptomycin, and 2 mM L-glutamine, (GPS, Sigma, St. Louis, MO). Cells were maintained at 37°C in a 5% CO₂ environment and used between passages 3 and 6.

Preparation and Purification of Poly(ethylene glycol) Diacrylate (PEGDA)

PEGDA was prepared by reacting poly(ethylene glycol) (PEG; Fluka/Sigma, MW = 6000 Da) with acryloyl chloride (Sigma) in a 1:4 molar ratio in anhydrous dichloromethane (DCM; Sigma) containing triethyl amine (TEA; Sigma) at a 1:2 (PEG:TEA) molar ratio at 25°C under argon overnight. PEGDA underwent purification by phase separation using 2 M K₂CO₃. The organic phase, which contained PEGDA, was dried using anhydrous MgSO₄ and filtered. PEGDA was first precipitated in diethyl ether, then filtered and dried overnight and under vacuum. ¹H-NMR characterization of PEGDA was used to confirm acrylation (Avance 400 Hz; Bruker) with D₂O as a solvent. PEGDA was stored under argon at -20°C.

Preparation and Purification of Acryl-PEG-Succinimidyl Carbonate

Acryl-PEG-succinimidyl carbonate (PEG-SMC) was synthesized by reacting PEG (Fluka/Sigma, MW = 3400 Da) with 1.5 molar excess Ag₂O (Sigma), 1.1 molar excess acryloyl chloride (Sigma), and 0.3 molar ratio KI (Sigma) in anhydrous dichloromethane (DCM; Sigma) overnight at 0-4°C to produce monoacrylated PEG. Silver oxide was removed from the resulting solution via filtration using Celite 521 (Spectrum Chemical Manufacturing Corp, Gardena, CA). The product was dried via Rotovap, then dissolved in DI H₂O, and the pH was titrated to 3 with HCl. This solution was heated at 35°C for 1 h, and activated charcoal (Fisher) was added for iodine removal, followed by subsequent filtration using Celite 521. Sodium chloride (NaCl) in DCM was added, followed by DCM extraction. Hydrochloric acid and chloride ions were removed through phase separation utilizing 2 M K₂CO₃. PEG-monoacrylate was dried with sodium sulfate (Fisher), concentrated via Rotovap, precipitated in ethyl ether, and vacuum filtered. Acryl-PEG-SMC was produced by reaction of monoacrylated PEG with 4 molar excess disuccinimidyl carbonate (Sigma) in pyridine (Sigma) and anhydrous acetonitrile (Sigma) under argon overnight. Acryl-PEG-SMC was dried via Rotovap, dissolved in anhydrous DCM, and filtered. The product was recovered via phase separation in acetate buffer (0.1 M, pH 4.5, 15% NaCl), dried using anhydrous MgSO₄, filtered, precipitated in ethyl ether, filtered, and dried overnight and under vacuum. Acryl-PEG-SMC was characterized by MALDI-TOF (MS Autoflex, solvent: methanol) to determine molecular weight and ¹H-NMR and stored at -80°C under argon.

Preparation and Purification of PEG-RGDS

The cell-adhesive peptide RGDS (American Peptide, Sunnyvale, CA) was dissolved in dimethylsulfoxide (DMSO, Sigma) at a concentration of 35 mM and diisopropylethylamine (DIPEA, Sigma) was added in a 2:1 molar ratio (DIPEA:PEG-SCM). Acryloyl-PEG-SCM was added at a concentration of 30 mM in a 1:1.2 (PEG-SCM:RGDS) molar ratio and allowed to react for 24 h at 25°C under agitation. The product was dialyzed against DI H₂O for 8 h using a dialysis membrane with a 3500 Da molecular weight cutoff (Spectrum Laboratories, Rancho Dominguez, CA). PEG-RGDS was lyophilized and stored under argon at -80°C. Conjugation was determined by gel permeation chromatography (GPC) using 0.1% ammonium acetate in dimethylformamide (DMF), a PLgel column (5 µm, 500 Å, Polymer Laboratories, Amherst, MA), and evaporative light scattering (ELS) detector (Polymer Laboratories), run against a PEG-SCM standard.

Synthesis of PEG-VEGF

VEGF₁₆₅ (Sigma) was dissolved in sterile 50 mM sodium bicarbonate buffer (pH 8.5, on ice). Synthesized acryloyl-PEG-SMC was similarly dissolved and sterilized via filtration (0.2 µm). PEG-SMC was added to VEGF in a 200:1 molar ratio under sterile conditions and allowed to react with agitation for 4 d at 4°C. PEG-VEGF was then lyophilized under sterile conditions, dissolved in HEPES buffered saline (HBS; 100 mM NaCl, 10 mM HEPES in deionized water; pH 7.4) with 0.1% bovine serum albumin (BSA) and stored at 4°C. PEG conjugation was confirmed via Western blot on a

Tris-HCl precast polyacrylamide gel (Bio-rad, Hercules, CA), detected with rabbit polyclonal anti-VEGF primary antibody (Santa Cruz Biotechnology, Santa Cruz, CA), HRP-conjugated goat anti-rabbit IgG secondary antibody (MP Biomedicals, Aurora, OH), and ECLTM chemiluminescent Western blot analysis system (GE Healthcare, Buckinghamshire, UK). The membrane was exposed to film (Kodak, Rochester, NY), which was developed using a Micromax Developer (Hope, Warminster, PA) with T₂ developer and T₂ fixer (White Mountain Imaging, Salisbury, NY).

Synthesis of PEG-RGDS-Fluor

PEG-RGDS was dissolved in 50 mM sodium bicarbonate buffer (pH 8.5). Alexafluor 350 carboxylic acid, succinimidyl ester (Invitrogen) was dissolved in DMF (0.5 mg/ml). Alexafluor solution was added dropwise to PEG-RGDS in a 10:1 molar ratio with slow mixing, and allowed to react overnight at 25°C. The product was dialyzed for 8 hr using a dialysis membrane with a 3.5 kDa molecular weight cutoff (Spectra/Por). PEG-RGDS-Fluor350 was lyophilized and stored at -80°C under argon.

Formation of PEGDA Hydrogels

PEGDA (6 kDa) was dissolved at 10% w/v in HBS and sterilized via filtration (0.2 µm). 10 µL of 300 mg/mL 2,2-dimethoxy-2-phenylacetophenone in N-vinylpyrrolidone (NVP) was added to each mL of polymer solution. Molds were constructed by placing 0.75 mm poly(tetra fluoroethylene) (PTFE) spacers between glass

slides which were secured with binder clips, sealing the molds on three sides. Polymer solution was pipetted into the molds and crosslinked through exposure to long wavelength ultraviolet light (B-200SP UV lamp, UVP, 365 nm, 10 mW/cm²) for 30 s. After crosslinking, the PEGDA hydrogel slab was stored in sterile PBS with 0.1% sodium azide for 24 h to allow swelling.

Laser Scanning Lithography Patterning of Ligand Surface Immobilization

5-mm diameter disks were cut from PEGDA hydrogel slabs. Hydrogel disks were soaked for 1 h in sterile PBS to remove sodium azide. A polymer solution with 30 μ mol/ml PEG-RGDS, 420 pmol/ml PEG-VEGF, 1 μ mol/ml eosin Y, 1.5% triethanolamine, and 3.95 μ l/ml NVP was prepared. Control solutions were made by omitting PEG-VEGF. 10 μ l of this solution was pipetted, as a drop, onto a #1 cover slip with attached chamber slide, and a hydrogel was placed on top of the drop, allowing the entire bottom surface of the gel to be in contact with the polymer solution. The gel and polymer solution were exposed to 514 or 532 nm laser excitation in specific locations using Laser Scanning Lithography (LSL). The surface-modified gel was again soaked in sterile PBS for 1 d to allow non-reacted polymer, excess photoinitiator, and residual sodium azide to diffuse out of the hydrogel (Figure 3-6).

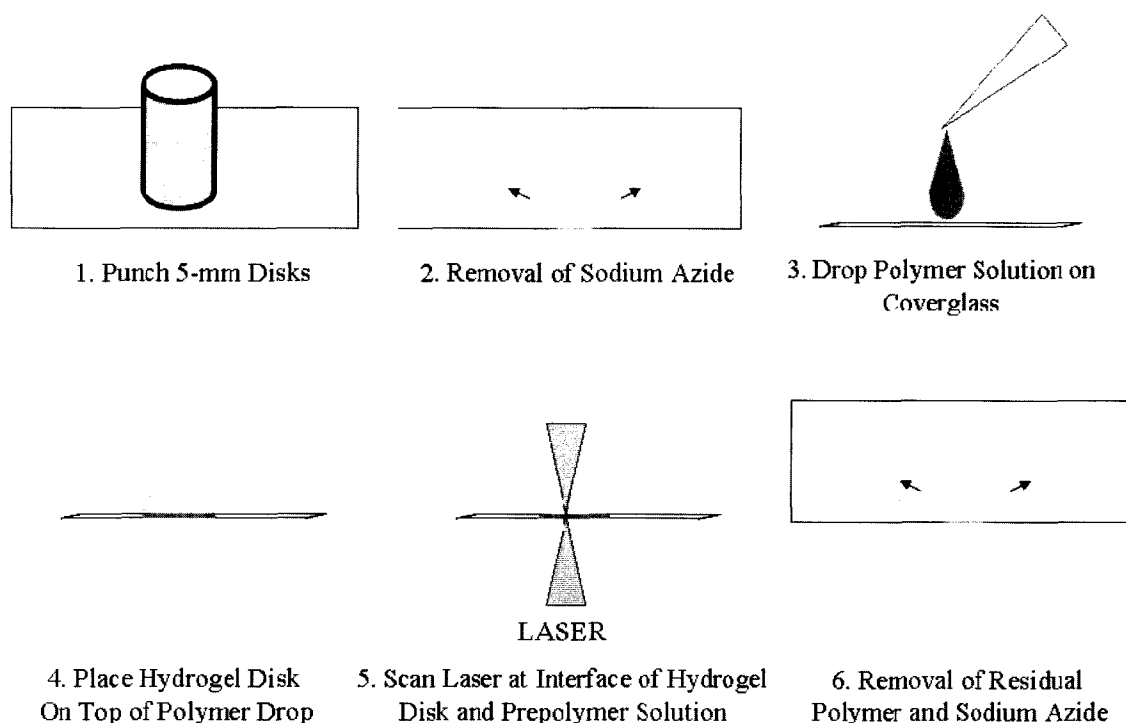


Figure 3-6 Schematic of patterned surface modification process of PEG hydrogels. Hydrogel disks were placed on top of surface-modifying polymer solution. A laser was focused onto the interface of the hydrogel disk and polymer solution by utilizing confocal microscopy. The laser was scanned across user-defined regions of interest to control photopolymerization and subsequent surface modification to restricted areas.

This method allows immobilization of the PEG-monoacrylate derivatives in the polymer/photoinitiator solution at defined sites on the hydrogel surface. Specifically, a Zeiss LSM 510 or 5Live confocal microscope (Plan-Apochromat objective 10x, 0.45 NA, area: 512 x 512 pixel, scan speed: 51.2 $\mu\text{sec/pixel}$, iterations: 10; zoom: 1, laser power: 0.26 $\text{mW}/\mu\text{m}^2$) was focused onto the hydrogel interface and liquid polymer solution. The laser was then raster scanned across the sample in a predetermined geometry, as programmed using Zeiss software region-of-interest choices. Several patterns of varying dimensions were patterned onto each sample, providing both experimental and control groups on the same hydrogel. To compare the effects of restricted cell spreading,

patterned lines of 10 μm width by 1000 μm length or 100 μm width by 1000 μm length were created side by side on the same hydrogel surface. This allows the experimental group (thin lines) and the control group (wide lines) to be on the same hydrogel sample (Figure 3-7). To determine feasibility of patterning capillary networks, patterns of branching 10 μm lines were created on the surface of hydrogels (Figure 3-7).

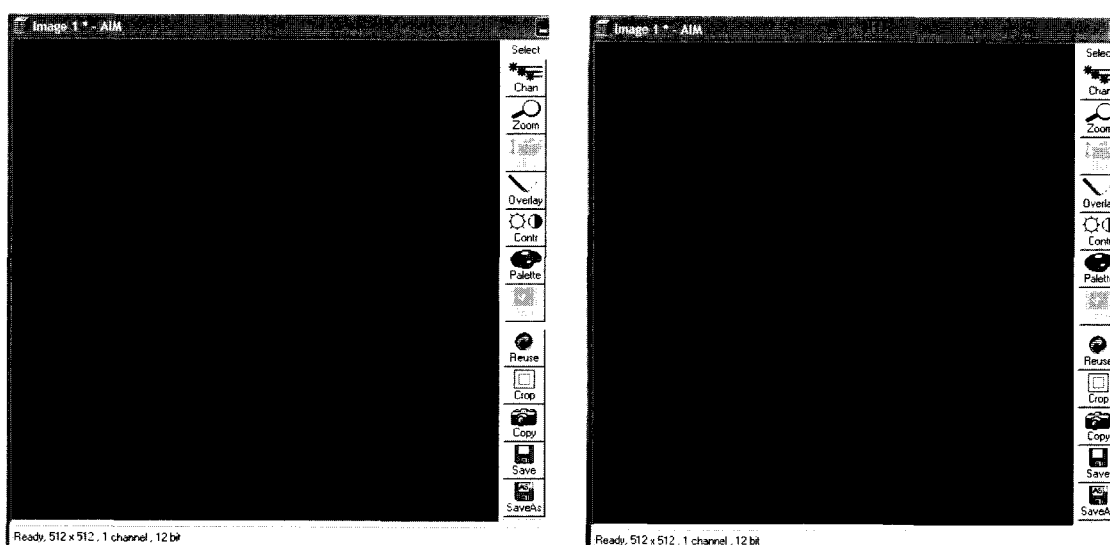


Figure 3-7 Patterned Regions of Interest used to command laser scanning software on Zeiss Live 5 or LSM 510 confocal microscopes. Photopolymerization was localized to these regions of interest, thus ensuring patterned areas of RGDS and VEGF on the surface of hydrogels.

Quantification of Surface-Immobilized VEGF and RGDS

PEG-VEGF and PEG-RGDS were immobilized via Laser Scanning Lithography to restricted 10 μm x 1mm or 100 μm x 1 mm areas on 6 kDa hydrogels as described above. An ELISA was used to determine the amount of covalently-attached VEGF. Briefly, gels were modified with PEG-VEGF and PEG-RGDS and allowed to soak in

saline with 0.1% BSA overnight. The amount of PEG-VEGF remaining in the saline was quantified using a VEGF ELISA kit (R&D) against dilutions of initial PEG-VEGF solution initially added to hydrogels. To quantify the amount of RGDS on the hydrogel surface, fluorescently-labeled PEG-RGDS-Fluor350 was patterned to the hydrogels. Hydrogels were soaked for two days, and the amount of unbound fluorescently-labeled PEG-RGDS was quantified using a fluorescent plate reader (Molecular Devices SpectraMax M2, excitation: 345 nm, emission: 446 nm) with fluorescently-labeled PEG-RGDS standards created from the PEG-RGDS solution initially added to the hydrogels. The amounts of PEG-VEGF and PEG-RGDS conjugated to patterned areas were then calculated.

Endothelial Tubule Formation and Quantification of Angiogenic Markers

HUVECs were seeded (8.5×10^4 cells/cm²) onto hydrogels with PEG-RGDS and PEG-VEGF covalently attached to the surface in restricted areas of 10 μ m x 1000 μ m or 100 μ m x 1000 μ m. On Day 2, images were taken of each patterned area and merged with Adobe Photoshop software. Each pattern was analyzed for tubule formation and measured for final dimensions of the area of cell attachment to the pattern. Due to inherent variability in focusing the confocal laser onto the interface of the hydrogel and polymer solution, some patterns were larger than designed, due to the increased laser beam width on specimen areas that were not in exact focus. An ANOVA was performed to determine significant differences between groups (RGDS, RGDS and VEGF, separated into bins depending on final dimension, with Tukey's Least Significant Difference post-

hoc analysis, $p < 0.05$ considered significant). After imaging on Day 2, cells cultured on top of hydrogels were fixed with 4% formaldehyde, washed with PBS, blocked with 10% normal donkey serum (Sigma) for 1 h, incubated for 1 h with primary antibodies (two groups: group A: mouse anti-VEGFR1 (Santa Cruz Biotechnology), goat anti-VEGFR2/Flt1 (Santa Cruz Biotechnology), and rabbit anti-ephA7 receptor (Santa Cruz Biotechnology); group B: mouse anti-fibronectin (Sigma), rabbit anti-laminin (Sigma), and goat anti-PECAM (Santa Cruz Biotechnology); diluted 1:50 in PBS with 1% BSA). Samples were washed several times with PBS, incubated for 1 h with the following secondary antibodies: Alexafluor 555 donkey anti-rabbit, Alexafluor 647 donkey anti-mouse, and Alexafluor 488 donkey anti-goat (dilution 1:200, Invitrogen, Molecular Probes), and then washed several times with PBS. Other samples were permeabilized with 0.1% Tween-20 for 30 min, blocked with BSA for 30 min, then treated with Alexafluor 568-conjugated phalloidin (10 U/mL, Molecular Probes) and DAPI (2 μ M, Invitrogen, Carlsbad, California) for 45 min to label cell actin filaments and nuclei, and visualized using confocal microscopy (Zeiss Live5, Plan-Apochromat 20x objective with 0.8 numerical aperture, Plan-Neofluar oil-immersion 40x objective with 1.3 numerical aperture, Plan-Apochromat oil-immersion 63x with 1.4 numerical aperture, for Alexafluor 488: excitation = 489 nm, emission BP filter = 500-525 nm; for Alexafluor 555: excitation = 532nm, emission BP filter = 560-675 nm, pinhole = 33 μ m; for Alexafluor 647, excitation = 635 nm, emission longpass filter = 650, pinhole = 100 μ m; for phalloidin: excitation = 532 nm, emission BP filter = 560-675 nm; for DAPI: excitation = 405 nm, emission BP filter = 415-480 nm, pinhole = 0.5 μ m). Images of tubules stained with phalloidin/DAPI were captured via z-stack images which were then

processed into 3D projections using ImageJ Volume Viewer software. Fluorescent immunocytochemistry images were processed with ImageJ to quantify expression of markers by measuring pixel intensity per cell. ImageJ returned intensity data in histogram format. Threshold levels were determined for each image by measuring the intensity of any background fluorescence. Data points were processed by weighting the number of pixels at each intensity level by the value of the intensity (range: 0-256). Data from each experiment was normalized to the average intensity measured in the control group (wide lines). Normalized data from several experiments was pooled into one data set per marker analyzed. Significance was determined using Student's T-test within each marker group, with $p < 0.05$ considered significant.

RESULTS

Polymer Characterization

Polymer products were determined to be successfully synthesized, as explained in full in Chapter 2. Briefly, GPC results confirmed that the PEG-RGDS product increased in molecular weight relative to the initial PEG-SCM reactant, showing successful conjugation. Western blot results showed successful pegylation of VEGF, as determined by comparing the molecular weight of the VEGF and PEG-VEGF bands.

Photolithographic Patterning of Ligand Surface Immobilization

PEG-RGDS and PEG-VEGF were patterned successfully on the surface of 6 kDa PEGDA hydrogels. Eosin Y, present in patterned areas, was visualized via confocal microscopy, which suggested that patterns from 10 to 100 μm in width and 1000 μm in length were produced (Figure 3-8). PEG-RGDS was covalently attached to patterned regions of the PEGDA hydrogels at a concentration of $74 \pm 21 \mu\text{mol}/\text{cm}^2$. PEG-VEGF was covalently attached to patterned regions at a surface concentration of $1.18 \pm 0.3 \text{ nmol}/\text{cm}^2$. Previous work showed that higher levels of RGDS, as compared to full-surface modification levels, are required for cells to successfully attach to thin lines [Moon 2007, Moon 2008]. Additionally, the initial amounts of PEG-RGDS and PEG-VEGF in the polymer solution were equal to those used in previous work (Chapter 2), and higher final concentrations are due to the different laser used for photopolymerization.

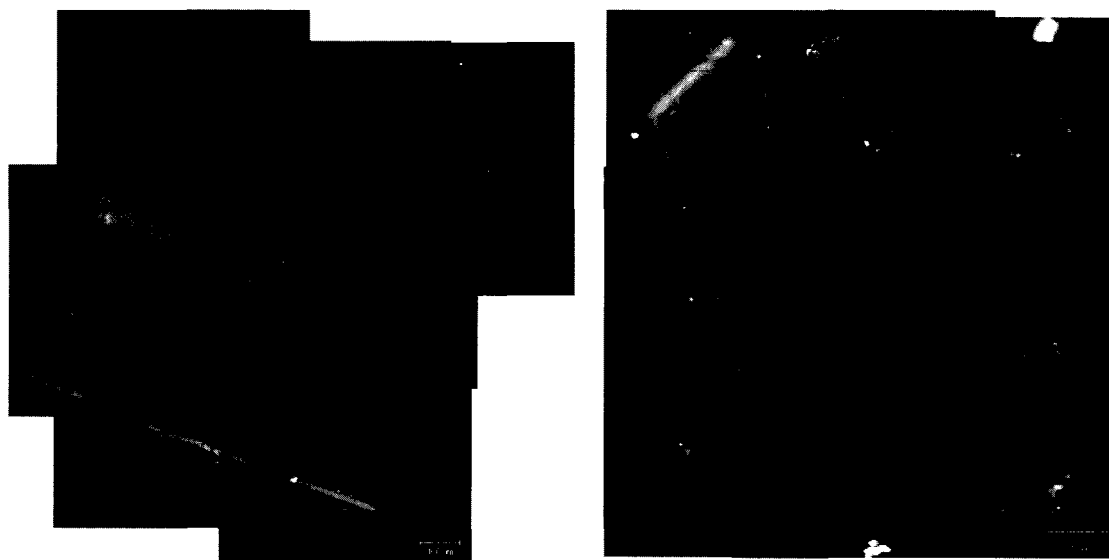


Figure 3-8 Confocal images of LSL patterns, with attached and fluorescently labeled cells. LSL patterns are fluorescent due to incorporation of fluorescent eosin Y, used as the photoinitiator for the polymerization crosslinking reaction between the PEGDA hydrogel base and the PEG-RGDS and PEG-VEGF modifying the surface. Scale bar = 100 μm .

Endothelial Response to Patterned PEG-RGDS and PEG-VEGF

In previous work, branching networks of endothelial tubes formed within 30 d on hydrogels modified with PEG-VEGF and PEG-RGDS when no spatial restriction of attachment and signaling was applied. Significantly less tubulogenesis occurred on hydrogels modified with PEG-RGDS only (Chapter 2). Patterning the presentation of cell adhesive ligands and signaling factors allows geometric restriction of cell location and function in a tissue engineered construct. Tight control over cell behavior can potentially allow creation of highly organized and intricate tissues and organs.

Presented results of patterning PEG-VEGF and PEG-RGDS on the surface of PEGDA hydrogels, suitable for tissue engineering matrices, are in agreement with work

performed on glass cover slips by Dike et al. [Dike 1999]. Using LSL, lines of $\sim 10\ \mu\text{m}$ and $\sim 100\ \mu\text{m}$ of covalently-bound PEG-RGDS and PEG-VEGF were patterned on the same hydrogel surface. Two days after seeding, HUVECs formed tube-like structures on thin lines of RGDS and VEGF but remained spread on wide lines (Figure 3-9). Additionally, tubule formation occurred on thin lines at a significantly higher proportion than on wide lines, where it was virtually nonexistent (Figure 3-10). Additionally, tubule formation occurred on RGDS & VEGF-thin lines at a significantly higher proportion than on RGDS-only thin lines (width of cell attachment $< 70\ \mu\text{m}$) (Figure 3-11). Endothelial cells cultured on branching patterns formed branching networks of tubules (Figure 3-12). Three-dimensional volume rendering of tubules formed on thin lines show areas of continuous tubules as well as locations in which tubules have begun to detach from the hydrogel, which correlates to Dike's findings of tubule retraction from the matrix surface (Figure 3-13, Figure 3-14). Cross-sectional images of DAPI and phalloidin labeled tubules on $10\text{-}\mu\text{m}$ -width patterned lines of RGDS and VEGF show negatively labeled lumens along these tubules, suggesting patent lumens (Figure 3-15). Patent lumens were not observed on the RGDS-only control patterns of $10\ \mu\text{m}$ lines (Figure 3-16).

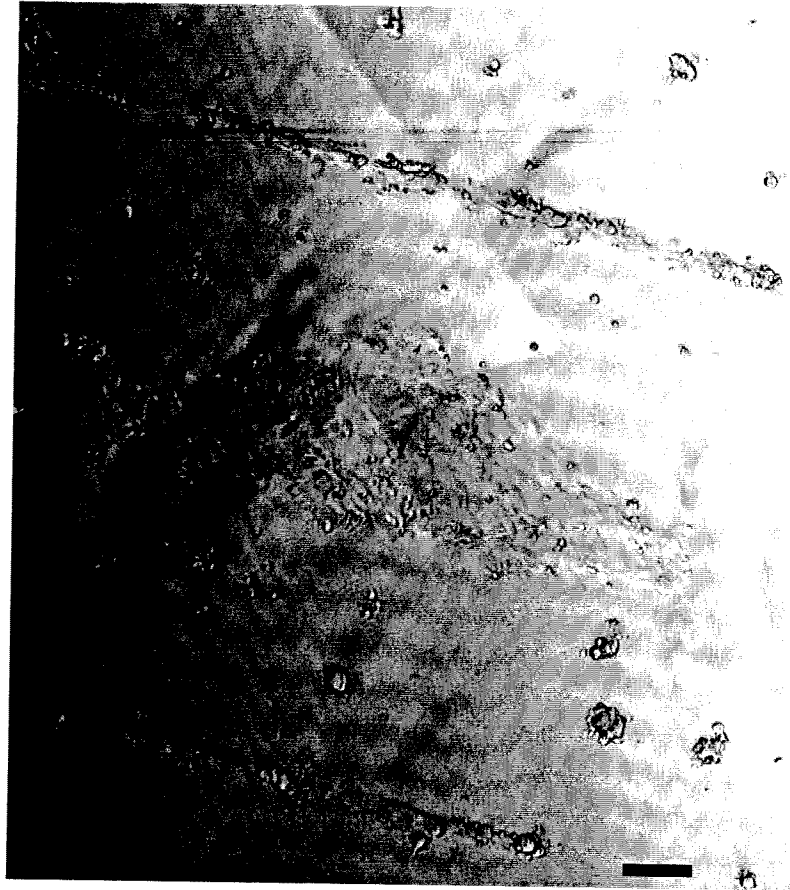


Figure 3-9 Phase contrast image of patterned endothelial cells. Cells patterned on ~10 µm lines of RGDS and VEGF formed capillary-like structures by day 2, while those allowed to spread to ~100 µm remained in a cobblestone morphology. Scale bar = 100 µm.

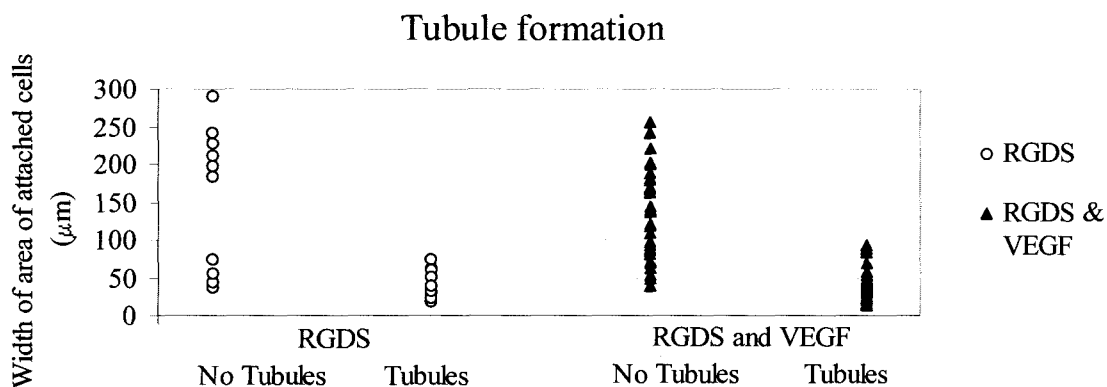


Figure 3-10 Quantification of tubule formation by Day 2 on patterned areas. Width of area of attached cells acts as a switch to promote tubule formation, with tubules forming only on areas less than 100 μm .

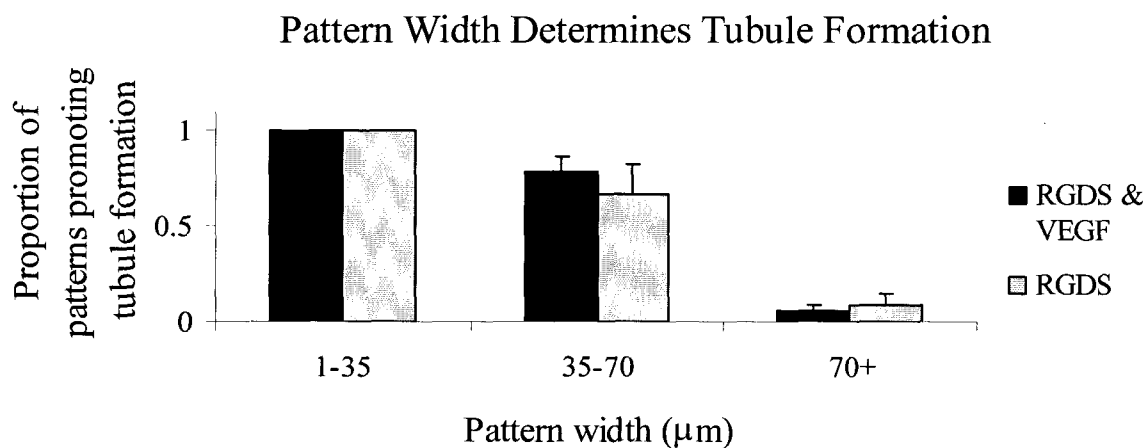


Figure 3-11 Quantification of the effect of pattern size on tubule formation. All patterned lines less than 35 μm promoted tubule formation. As the pattern size increases, the percentage of patterns that promote tubule formation decreases. For patterns between 35 and 70 μm , patterns with RGDS and VEGF promote more tubule formation than RGDS only. Error bars show standard deviation ($\text{SD} = \sqrt{pq/n}$, where p =proportion of success, q =proportion of failure, n =sample size). Statistical differences ($p < 0.01$) between all groups except groups showing 100% tubule formation (RGDS, RGDS & VEGF 1-35 μm).

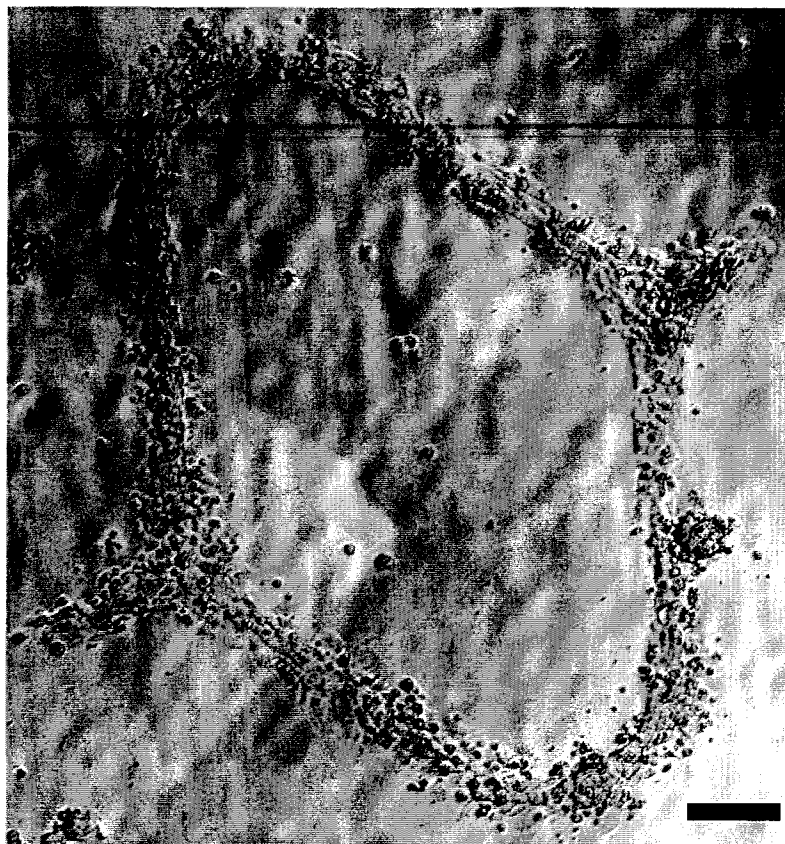


Figure 3-12 Endothelial cells patterned to form branching unit. Scale bar = 100 μm .

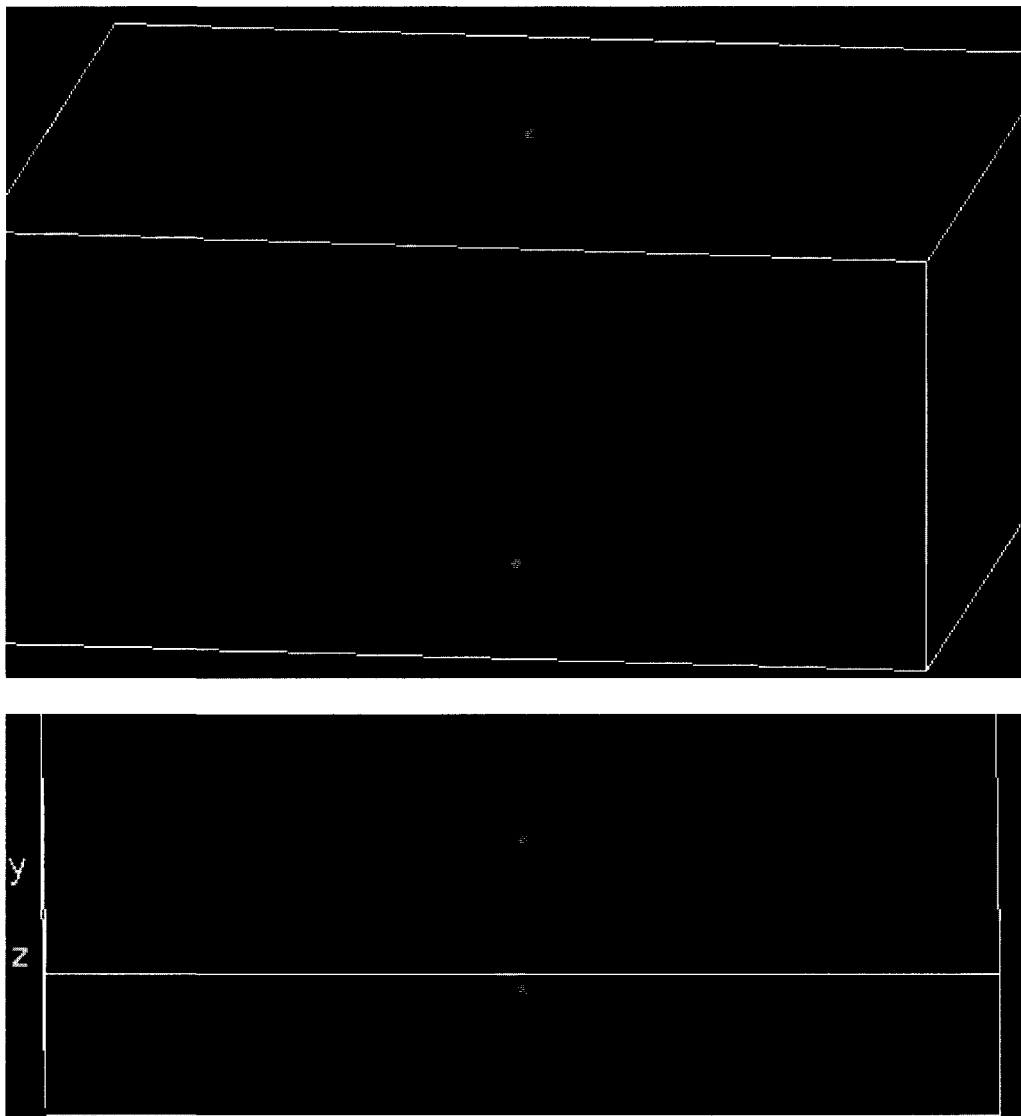


Figure 3-13 Volume renderings. Three dimensional images of endothelial tubules formed on thin patterned lines of RGDS and VEGF. These images suggest that the tubule has begun to detach from the hydrogel, which may be part of the tubulogenic process. Images also show vacuole formation in surrounding cells attached to thin lines, which is an earlier step before tubulogenesis.

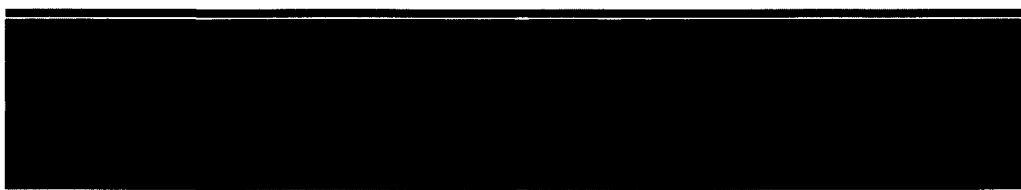


Figure 3-14 Volume rendering. Three dimensional image of endothelial tube formed on thin patterned line of RGDS only. Although some tubule-like structures formed by Day 2 on RGDS only lines, no patent lumens were observed.

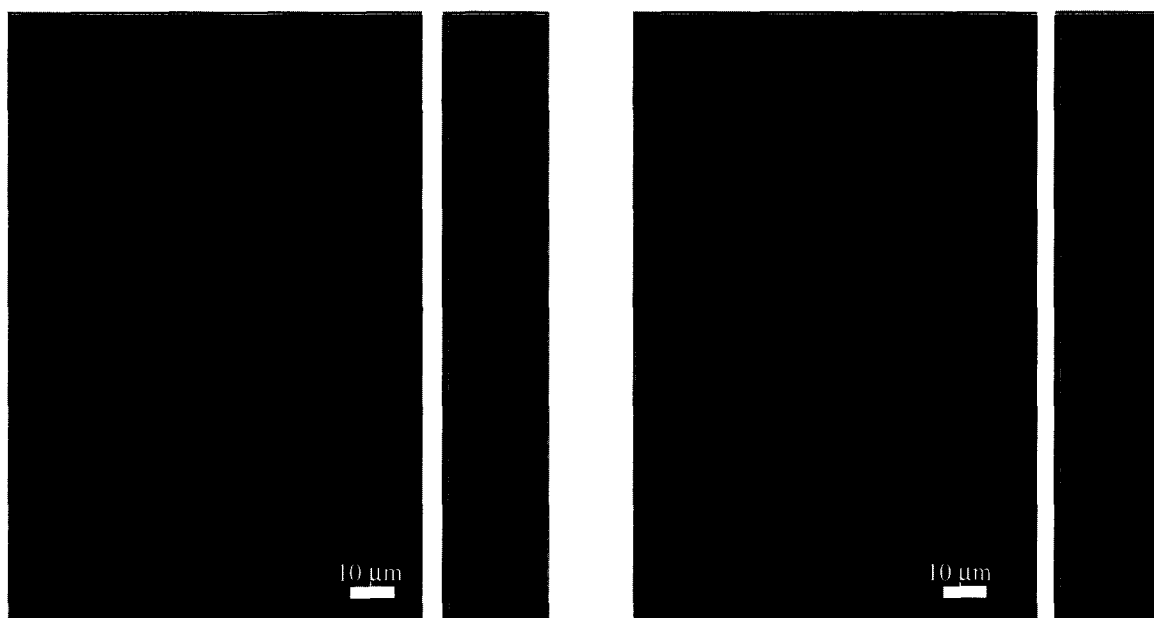


Figure 3-15 Visualization of actin filaments (red) in tubule formed on patterned RGDS and VEGF. A) Top view and cross-section of tubule shows lumen. B) Top view and cross-section of cell forming vacuole. Red line shows region of cross-section.

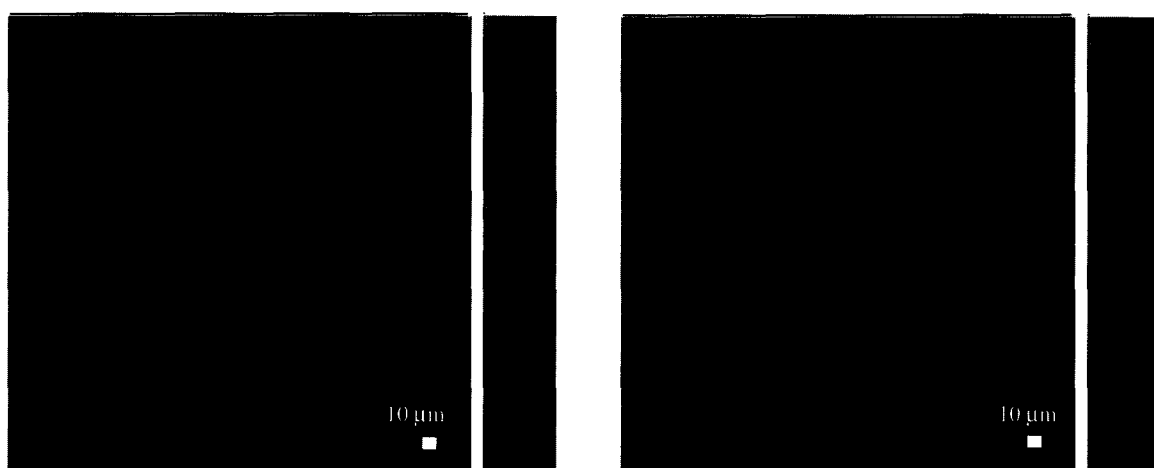
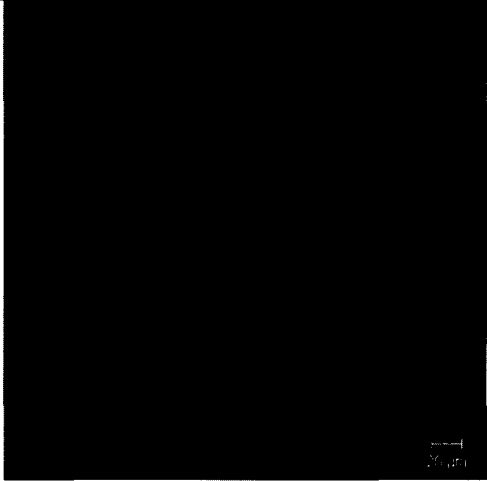
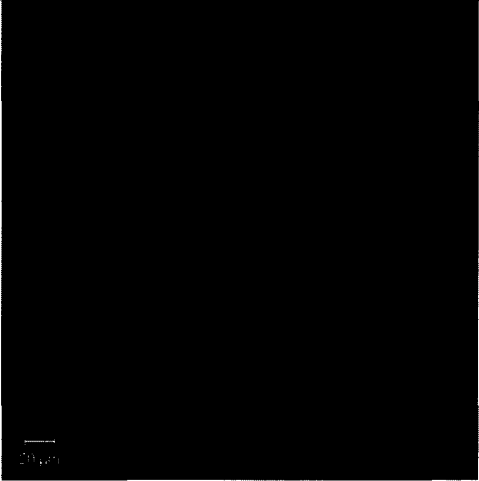
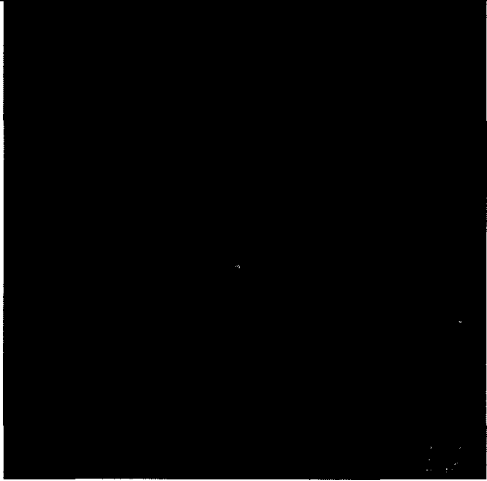
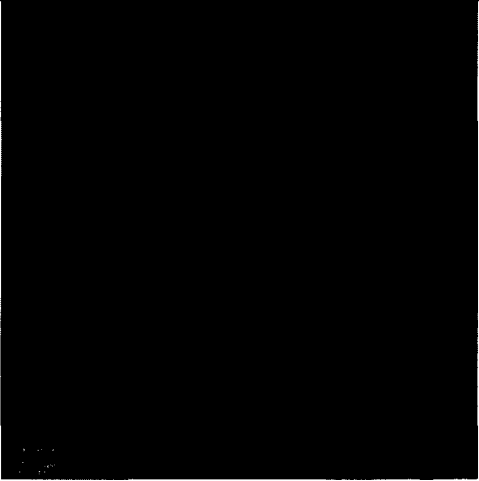


Figure 3-16 Visualization of actin filaments (red) and DAPI (blue) in tubules formed on patterned RGDS only. Cells cultured on only RGDS were not observed to form tubules with continuous lumens. Scale bar = 10 μ m. Red lines shows region of cross-section.

Cell-surface Markers and Protein Expression

After 2 days, cells cultured on restricted patterns of PEG-RGDS only or PEG-RGDS and PEG-VEGF were visualized for expression of VEGFR1, VEGFR2, ephA7, PECAM, fibronectin, and laminin. Expression of angiogenic markers at 2D after seeding was visualized via confocal microscopy, which suggested higher expression on cells forming tubules on thin lines (Figure 3-17), and quantification confirmed a statistically significant increase in angiogenic marker expression on tubules formed on thin lines. Quantification of pixel intensity per cell shows that restricted spreading and subsequent tubule formation of HUVECs on thin lines corresponds to increased levels of expression of ephA7 by 1.4-fold, VEGFR1 by 12.3-fold, VEGFR2 by 1.5-fold, and laminin by 2.4-fold as compared to cells spread on wide lines (Figure 3-18, $p < 0.05$). The accelerated formation of endothelial tubes on thin lines may be related to these higher levels of angiogenic marker expression, allowing cells to react to angiogenic signaling sequestered in the matrix. The ability to pattern PEG hydrogels allows control of tissue organization while patterned presentation of ligands contributes to activation of angiogenic pathways. Spatial restriction of angiogenic factors and integrin ligands on PEG hydrogels accelerate and tightly control the angiogenic response in these scaffolds.

	Thin Line	Wide Line
VEGFR1	 A	 B
EphA7 Red VEGFR2 Green	 C	 D

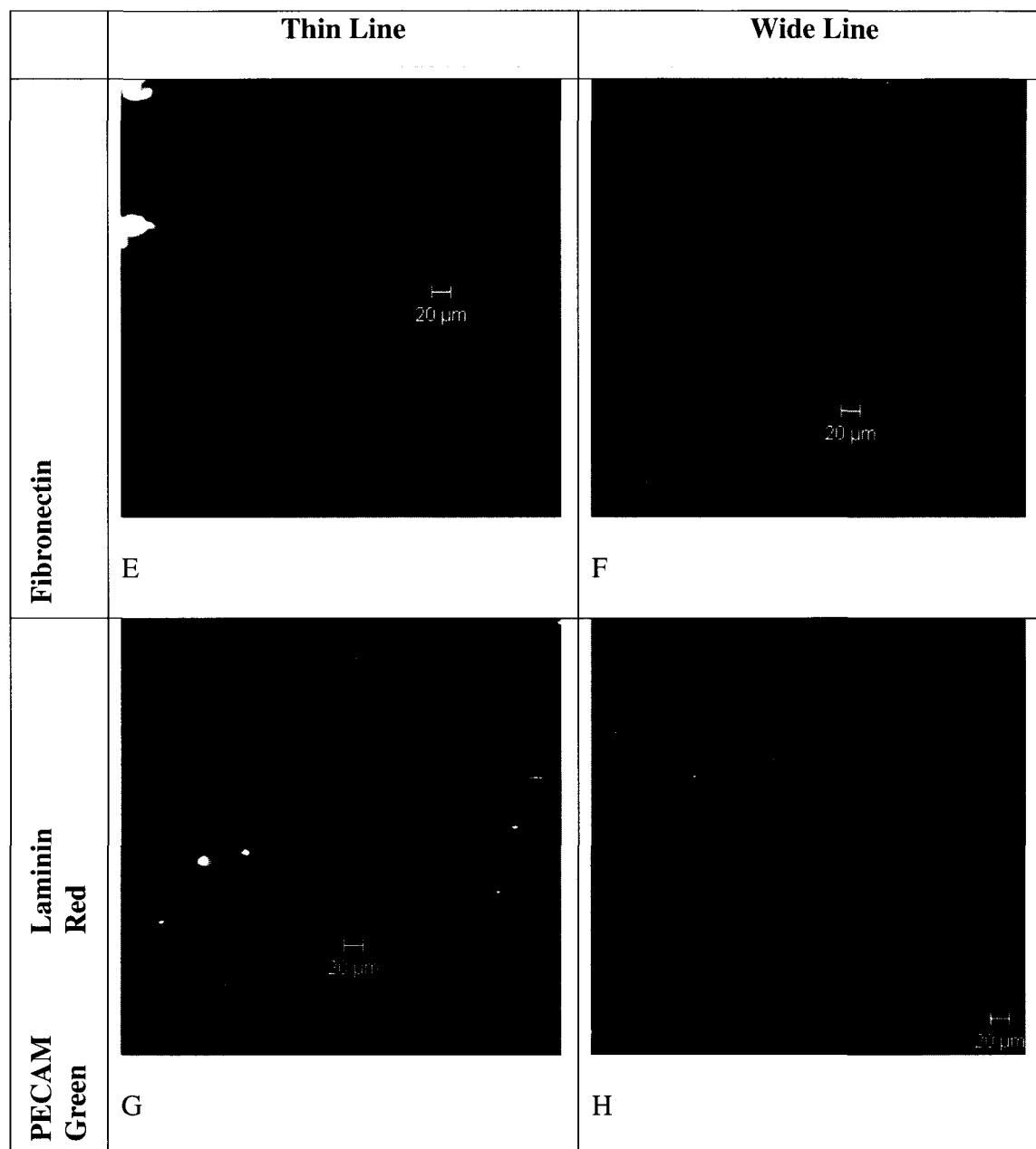


Figure 3-17 Confocal images of fluorescent immunocytochemistry. Cells on both thin and thick patterned lines on the same sample were fixed at day 2 and stained either for A & B) VEGFR1 (white), C&D) VEGFR2 (green), and EphA7 (red) or E & F) fibronectin (white), G & H) laminin (red), and PECAM (green). Background signals arise from incorporated eosin Y, which was used as the photoinitiator; the background signal was subtracted before quantification.

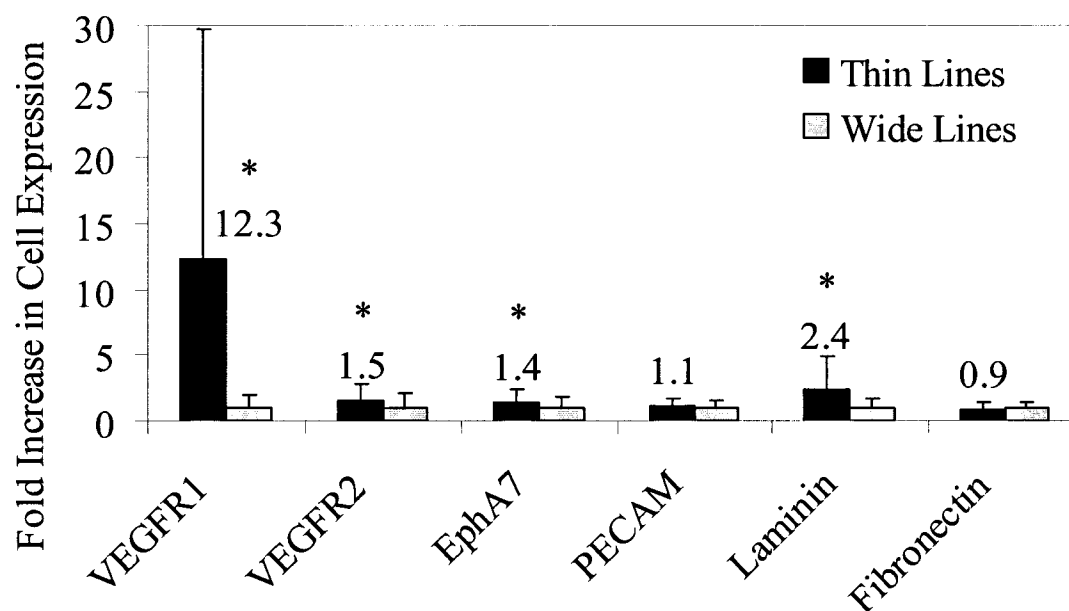


Figure 3-18 Analysis of protein expression of six angiogenic proteins and cell surface receptors expressed by endothelial cells on patterned lines at Day 2. Fluorescent immunocytochemistry images were analyzed for intensity of pixels in images to quantify expression of angiogenic cell surface receptors and proteins. Increased expression was determined for VEGFR1, VEGFR2, EphA7, and Laminin. * $p < 0.05$ using Student's T-test comparison between thin and wide lines within each marker category.

DISCUSSION AND CONCLUSIONS

The work presented in this work demonstrates the ability to pattern PEG hydrogels which allows control of tissue organization while patterned presentation of ligands contributes to activation of angiogenic pathways. Spatial restriction of angiogenic factors and integrin ligands, in this case VEGF and RGDS, on PEG hydrogels accelerates and tightly controls the angiogenic response in these scaffolds. The reported work illustrates that patterning localization of integrin ligands and signaling factors not only allows a more engineered, highly organized design for a vascularized engineered tissue, but also actively accelerates tubulogenesis and upregulates angiogenic genes within endothelial cells.

Combining tools of growth factor localization via photopolymerization in PEG hydrogels and novel Laser Scanning Lithography as a photolithographic alternative, this work presents the design of tightly regulated tissue engineering matrices which support endothelial tubulogenesis along specified boundaries, allowing design of highly organized tissues. Micron-level spatial restriction of endothelial cell attachment to extracellular matrix and availability of localized biochemical signaling accelerates endothelial tubule formation from 30 days to 2 days and upregulates expression of VEGF receptor 1 (VEGFR1), VEGF receptor 2 (VEGFR2), ephA7, and laminin within 2 days.

Recent developments of several technologies have made possible the promise of design and creation of tissue engineering matrices with high levels of tissue organization “preprogrammed” to ensure extracellular matrix-mimetic niches for metabolically active cells. Covalently attaching RGDS and VEGF to PEGDA hydrogel matrices promoted

endothelial cell fate determination towards tubulogenesis. Spatially restricting cell integrin ligands and angiogenic signals on physiologically-relevant PEGDA matrices through patterning “pushed” endothelial cells into a tubulogenic response. Two- and three-dimensional capillary networks patterned throughout PEGDA hydrogels are hypothesized to allow the culture of functional engineered tissues larger than 200 μm , the current oxygen diffusion limit for implanted tissues. Additionally, by restricting immobilization of VEGF, physiological responses to this growth factor will remain localized, leading to an expected, engineered tissue response.

Chapter 4 An Immobilized VEGF Fragment, PEG-KLTWQELYQLKYKGI, Promotes Microvasculature Formation in Poly(ethylene glycol) Diacrylate Hydrogels

INTRODUCTION

Many approaches of promoting microvascularization utilize signaling moieties, most often growth factor proteins, either released from or attached to a tissue engineering matrix. The use of growth factor proteins has inherent disadvantages, such as immunogenicity and loss of bioactivity. Although fibronectin was originally used for cell attachment to matrices, many researchers found the simplicity of the Arg-Gly-Asp (RGD) peptide sequence, the bioactive integrin ligand derived from fibronectin [Ruoslahti 2003], to be advantageous in matrix design. Similarly, it could be beneficial to use a shorter bioactive peptide sequence derived from a growth factor protein if it could confer the same bioactivity and cellular response.

A synthetic 15-amino acid peptide, based on a region of the vascular endothelial growth factor (VEGF) binding interface, has been shown to possess similar biological activity to that of the VEGF protein. This peptide, called QK, was based on the region of VEGF that binds to VEGFR-1 domain 2. The VEGF binding region, Phe-17-Tyr-25, forms an α -helix conformation in its native bound state. D'Andrea synthesized the exact peptide sequence in the binding domain, but found that the peptide did not form an α -helix in water, most likely from the lack of surrounding sequences that would stabilize the bioactive conformation. The unstructured VEGF15 peptide did not display bioactivity. To stabilize the α -helix conformation, alterations in amino acid sequence

were included; this designed peptide was called QK (Figure 4-1). The α -helix of the sequence was considered a necessity for bioactivity, as the tertiary structure of the sequence determined ligand-receptor binding [D'Andrea 2005]. The sequences of the investigated physiological VEGF binding region and the QK peptide are compared below (Table 4-1).



Figure 4-1 Conformational structure of QK in water from [D'Andrea 2005]. The designed peptide assumes an α -helix conformation, which is requisite for its bioactivity.

Table 4-1 Peptide sequence comparison of VEGF15, which is the exact VEGFR1 binding sequence found in VEGF165, and QK, which is the peptide with some amino acid substitutions to ensure an α -helix conformation in water.

VEGF15	Ac-KVKFMDVYQRSYCHP-amide
QK	Ac-KLTWQELYQLKYKGI-amide

In D'Andrea's studies, QK was able to bind and activate both KDR (VEGFR-2) and Flt-1 (VEGFR-1) receptors *in vitro*. In a proliferation assay, similar bioactivity levels were found between 1 mol VEGF and 385 mol QK. This result suggests that the

signaling triggered by QK-receptor binding is lower than that of VEGF-receptor binding, and that a 385-fold increase in activated receptors is required. Alternatively, QK-receptor binding could be more transitory, thus requiring more available ligand. One reason for the much-lower bioactivity of QK compared to VEGF could be its small size. D'Andrea et al. reported that its small size most likely prevents it from binding to two VEGF receptors at once, which is accepted as the standard method for receptor dimerization and subsequent signal pathway transduction. Despite its size, QK was shown to activate ERK1/2, which is a required cell signaling pathway step in VEGF-modulated angiogenesis. ERK1/2 was activated to different levels depending on dosage of QK, and QK and VEGF activation was additive. These results suggest that the larger number of QK molecules needed to initiate an angiogenic response does not saturate the available VEGF receptors on the cell surface, and therefore the cell is able to respond to QK signaling, even though many more QK molecules are required. Additionally, D'Andre et al. showed that QK induced tubulogenesis within 11 d in a Matrigel model. Human endothelial cells and other undefined human cells were cultured on Matrigel, with QK added in culture medium every 3 d. On day 11, cells were fixed, and tubules were visualized by CD31/PECAM-1 staining and subsequently quantified. QK also increased the tubulogenic response to VEGF, when cells were treated with both concurrently. D'Andrea et al. showed that QK could cause VEGF receptor dimerization and subsequent activation despite its small molecular weight [D'Andrea 2005]. This novel, bioactive VEGF-mimicking peptide is another promising option to promote and control angiogenesis in tissue engineering matrices because it shows similar bioactivity to VEGF yet provides the advantages of a peptide, including smaller size, ease of use in chemical

reactions, smaller likelihood to trigger an immune response, and ability to be more easily synthesized with variations allowing tuning of a biomimetic matrix system.

The use of poly(ethylene glycol) diacrylate (PEGDA) hydrogels as matrices allows the fine tuning of matrix-cell interactions. Results presented in Chapter 2 show that incorporation of peg-modified peptide RGDS and protein VEGF confers bioactivity upon the PEG hydrogel, promoting angiogenic activity. In the current work, RGDS and the novel QK peptide were covalently incorporated into PEG hydrogels, promoting an angiogenic response similar to RGDS and VEGF. This new system provides an alternative to the use of growth factor proteins in angiogenic signaling and is the first to use a bioactive peptide sequence derived from an angiogenic growth factor to induce microvascularization in engineered matrices.

MATERIALS AND METHODS

Cell Culture

Human umbilical vein endothelial cells (HUVEC, Cambrex/Lonza, Walkersville, MD) were used between passages 2 and 6 and cultured as previously described (Chapter 2). Cells were maintained in VEGF-free endothelial cell growth medium (EGM-2 media, Cambrex/Lonza). Before 3D encapsulation, HUVECS were labeled with Celltracker Red CMTPX (Molecular Probes). 50 μ g Celltracker Red was dissolved in 4 μ l DMSO and diluted in cell media for a final concentration of 5 μ g/ml. HUVECs were incubated in the prepared media for 45 min at 37°C. Labeling was visually confirmed via fluorescence microscopy, and labeling media was replaced with normal EGM-2 medium (without VEGF). Cells were washed with phosphate buffered saline (PBS) before enzymatic lifting using trypsin/EDTA and subsequent encapsulation as described below.

Preparation and Purification of Poly(ethylene glycol) Diacrylate (PEGDA)

Poly(ethylene glycol) diacrylate was synthesized as previously described (Chapter 2). In brief, PEG (Fluka/Sigma, MW = 6000 Da) was reacted with acryloyl chloride (Sigma) in anhydrous dichloromethane (DCM; Sigma) with triethyl amine (TEA; Sigma) under argon overnight at 25°C. PEGDA was purified via phase separation, and the organic phase containing PEGDA was dried and filtered. PEGDA was precipitated, filtered, and dried overnight and under vacuum, then characterized by ^1H -NMR, and stored at -20°C under argon until use.

Preparation and Purification of PEG-succinimidyl carbonate (PEG-SMC)

PEG-SMC was prepared and purified as previously described (Chapter 2). In brief, 3.4 kDa PEG was monoacrylated by reacting with acryloyl chloride. The filtered, purified product was then reacted with disuccinimidyl carbonate (Sigma). Purified PEG-SMC was characterized by ^1H -NMR and MALDI-TOF and stored at -80°C under argon until use.

Preparation and Purification of PEG-QK

The angiogenic peptide Ac-KLTWQELYQL[K(Ac)]Y[K(Ac)]GI-amide was designed to react with PEG-SCM at the first lysine (K) residue only, by protecting all other free amines with acetyl groups (represented by Ac). QK (MW=2036 Da, Aapptec, Louisville, KY) was dissolved in DMSO at a concentration of 7.4 mM. N,n -diisopropylethylamine (DIPEA, Sigma, 2 mol per mol PEG) was added to the solution to act as a base catalyst. Acryloyl-PEG-succinimidyl ester (PEG-SCM, Laysan, MW=3400 Da) was similarly dissolved at a concentration of 1.5 mM. PEG-SCM was added dropwise to QK in a 10:1 molar ratio with slow mixing and allowed to react for 4 d at 25°C . The product was precipitated in cold isopropanol and dried overnight. PEG-QK was then lyophilized and stored at -80°C under argon until use. Conjugation was characterized by MALDI-TOF (MS Autoflex, solvent: methanol).

Preparation and Purification of PEG-RGDS

The cell-adhesive peptide RGDS (American Peptide, Sunnyvale, CA) was dissolved in DMSO at a concentration of 30 mM. DIPEA was added to the solution to act as a base catalyst. Acryloyl-PEG-N-hydroxysuccinimide (PEG-SCM, Laysan, MW=3400 Da) was similarly dissolved at a concentration of 30 mM. PEG-SCM was added dropwise to RGDS in a 1:1 molar ratio with slow mixing and allowed to react for 4 d at 25°C. The product was dialyzed against DI H₂O for 8 h using a membrane with a 3500 Da molecular weight cutoff (Spectrum Laboratories, Rancho Dominguez, CA). PEG-RGDS was then lyophilized and stored at -80°C under argon until use. Conjugation was characterized by gel permeation chromatography (GPC) using a PLgel column (5 μ m, 500 Å, Polymer Laboratories, Amherst, MA), 0.1% ammonium acetate in DMF solvent, and evaporative light scattering (ELS) detector (Polymer Laboratories), run against unreacted PEG-SCM for comparison.

Synthesis of Collagenase-Degradable PEG-PQ-PEG

A collagenase-sensitive peptide (PQ) GGGPQGIWGQGK was prepared on a peptide synthesizer (Aapptec, Louisville, KY) using standard Fmoc chemistry. The peptide was cleaved from the resin using 95% trifluoroacetic acid (TFA), 2.5% triisopropylsilane (TIPS) in water and precipitated in ether. The peptide was reacted with PEG-SCM (Laysan, MW=3400 Da) in a 2:1 ratio (PEG-SCM:PQ) in DMSO and DIPEA (2 mol per mol PEG) for 4 d at 25°C to generate a PEG-diacrylate derivative with PQ in the polymer backbone. PEG-PQ-PEG was dialyzed against DI H₂O for 8 h using a

membrane with a 3500 Da molecular weight cutoff (Spectrum Laboratories), and conjugation was confirmed via GPC with ELS detection as described previously.

Synthesis of PEG-VEGF

PEG-VEGF was synthesized as previously described in detail (Chapter 2). In brief, VEGF₁₆₅ (Sigma) was reacted with acryloyl-PEG-SMC in sterile 50 mM sodium bicarbonate buffer (pH 8.5, 0°C) for 4 d. PEG-VEGF was then lyophilized under sterile conditions and stored in HEPES buffered saline (HBS) with 0.1% bovine serum albumin (BSA) at 4°C until use. Conjugation was confirmed via Western blot as previously described in detail (Chapter 2).

Bioactivity Assay

Bioactivity of PEG-QK was determined by measuring its pro-mitotic effect on endothelial cells. HUVECs were seeded at 1.05×10^3 cells/cm² in EGM-2 medium without VEGF on Day 1. On Day 4, medium was replaced with EGM-2 medium without VEGF and FGF, with an addition of either 0.13 pmol/ml VEGF (positive control), 50 pmol/ml QK, 50 pmol/ml PEG-QK, or no VEGF (negative control). The levels of QK were chosen to correspond with the bioactivity levels reported in D'Andrea's original paper on the peptide, which showed that the bioactivity of 1 mol VEGF was equal to that of 385 mol QK [D'Andrea 2005]. This medium was replaced after 4 h with EGM-2 without VEGF and FGF. On Day 6, cells were treated with a Hoechst 33342 dye (Bis-

Benzimide, Sigma), which labels cell nuclei. Hoechst dye was added at a concentration of 5 $\mu\text{g/ml}$ in EGM-2 without VEGF and FGF, and cells were incubated with this media for 1 h. Fluorescent images were taken immediately of each well, with 4-6 images per well, using a fluorescent microscope with excitation = 350 nm, emission = 460 nm. Cell nuclei were quantified using ImageJ. Statistical differences between groups were analyzed using ANOVA, followed by Tukey's Least Significant Difference post hoc analysis, with $p < 0.05$ considered statistically significant.

Formation of PEGDA Hydrogels

Hydrogels were formed as previously described in detail (Chapter 2). In brief, 6 kDa PEGDA was dissolved in HEPES buffered saline (HBS) in a 10% w/v solution and sterile filtered. Photoinitiator, 10 $\mu\text{L/mL}$ of 300 mg/mL 2,2-dimethoxy-2-phenylacetophenone in N-vinylpyrrolidone (NVP), was added to the solution. The polymer solution was pipetted into molds and crosslinked through exposure to long wavelength ultraviolet light (B-200SP UV lamp, UVP, 365 nm, 10 mW/cm^2) for 30 s. After crosslinking, the mold was removed, and the PEGDA hydrogel slab was placed in sterile PBS with 0.1% sodium azide until further use.

Surface Modification of PEGDA Hydrogels

Hydrogel slabs were soaked for 1 h in sterile PBS to remove sodium azide. 5 mm diameter circles were punched from PEGDA hydrogel slabs. A polymer solution consisting of 173 nmol/mL PEG-QK, 30 μ mol/mL PEG-RGDS, 1 μ mol/mL eosin Y, and 3.95 μ L/mL NVP was prepared. From this solution, 10 μ L was pipetted onto the top surface of the gel, completely covering the surface. The gel and polymer solution were exposed to a 532 nm laser at 30 mW/cm² for 30 s. Positive control hydrogels were made with 420 pmol/mL PEG-VEGF instead of PEG-QK, and negative control hydrogels contained PEG-RGDS only. The surface-modified gel was then soaked in sterile PBS for 1 d to allow non-reacted polymer, excess photoinitiator, and residual sodium azide to diffuse from the gel.

Quantification of Surface-Immobilized QK, VEGF, and RGDS

Hydrogel disks were modified with either PEG-QK, PEG-VEGF, or PEG-RGDS, and then soaked to allow unbound peg-modified factor to diffuse from the hydrogel. The amount of PEG-QK bound to the hydrogel was determined by measuring the absorbance of PEG-QK in the soak solution after hydrogel modification. The absorbance of PEG-QK, which includes a tryptophan amino acid residue, was measured at 280 nm spectrophotometrically (Vivian) and compared to prepolymer solution standards. An ELISA assay was used to determine the amount of VEGF that was covalently immobilized on positive control hydrogel surfaces as previously described by measuring the amount of PEG-VEGF removed by soaking (Chapter 2). A ninhydrin assay was used

to quantify the amount of covalently-linked PEG-RGDS on the surface of the gels, as previously described (Chapter 2).

Endothelial Tubule Formation

HUVECs were seeded (8.5×10^4 cells/cm²) onto gels with either PEG-RGDS and PEG-QK, PEG-RGDS and PEG-VEGF, or only PEG-RGDS covalently attached to the surface. HUVEC tubulogenic response on the gels was monitored and EGM-2 medium changed every other day. Three experimental groups were observed: QK- and RGDS-modified hydrogels cultured in EGM-2 medium (without soluble VEGF), VEGF- and RGDS-modified hydrogels cultured in EGM-2 medium (without soluble VEGF), and RGDS-modified hydrogels cultured in EGM-2 medium (without soluble VEGF). Images were taken of each entire gel and merged using Photoshop Elements software. Tubules were traced using Adobe Illustrator software, and length of each tubule was calculated in ImageJ software (NIH, Bethesda, Maryland). The total sum of tubule length per area was calculated for each sample. Data from separate experiments was pooled, and ANOVA followed by Tukey's Least Significant Difference post hoc analysis was performed to determine significant differences between groups, with $p < 0.05$ considered statistically significant. All data are presented as mean \pm standard deviation.

In some samples, cells were permeabilized with 0.1% Tween-20 for 30 min, blocked with BSA for 30 min, then treated with Alexafluor 488-conjugated phalloidin (10 U/mL, Molecular Probes) and DAPI (2 μ M, Invitrogen, Carlsbad, California) for 45 min to label cell actin filaments and nuclei, and visualized using confocal microscopy

(Zeiss Live5, Plan-Apochromat 20x objective with 0.8 numerical aperture and digital zoom of 1 or 2, for Alexafluor 488 phalloidin: excitation = 489 nm, emission BP filter = 500-525 nm; for DAPI: excitation = 405 nm, emission BP filter = 415-480 nm, pinhole = 7 μ m). Tubules stained with phalloidin/DAPI were captured via z-stack images.

Formation of Three-dimensional Proteolytically Degradable PEG Hydrogels

Collagenase-degradable hydrogels with encapsulated HUVEC cells (3 x 10⁷ cells/mL, labeled with Celltracker Red) were prepared. Briefly, PEG-PQ-PEG (0.1 g/mL), acryloyl-PEG-RGDS (3.5 μ mol/mL), and acryloyl-PEG-QK (152 nmol/mL or 760 nmol/mL) were mixed with a cell suspension and photocrosslinked by exposing to long wavelength UV (365 nm, 10 mW/cm²) for 7 min, using Irgacure 2959 as the photoinitiator (0.3% w/v). Two concentrations of PEG-QK were investigated; the lower corresponds to the bioactivity levels of comparative positive control PEG-VEGF hydrogels; the second is five times higher. As previously noted, D'Andrea et al. found that 385 mol QK had equal bioactivity to 1 mol VEGF in a proliferation assay [D'Andrea 2005]. As a positive control, hydrogels were crosslinked with incorporation of PEG-VEGF (400 pmol/mL) instead of PEG-QK, and as a negative control, hydrogels were prepared with PEG-RGDS only.

Time lapse Study of Endothelial Tubulogenesis in Three-dimensional Degradable PEG Hydrogels

Constructs were transferred to a confocal microscope (Zeiss Live5, Thornwood, NY) with a stage chamber providing a regulated environment (37°C and 5% CO₂). No additional proteolytic enzymes or protease inhibitors were added to the culture. Z-stack images were collected every hour for 60 h using the Multi Time Series macro (Zeiss), Plan-Apochromat 20x objective with 0.8 numerical aperture, and excitation wavelength = 532 nm, emission bandpass (BP) filter = 560-675 nm, and pinhole = 7 µm. Time lapse movies were analyzed for tubule formation, cell migration, and cell-cell contact formation. For tubule formation, tubules were traced at 22 h and 32 h time points and quantified. Total tubule length per viewing field was analyzed. For cell migration quantification, the movement of three randomly selected cells per viewing field was tracked using Logger Pro software, which allows the tracing and quantification of cell paths through timeframe progression. For cell-cell contact formation quantification, the number of all cell-cell contacts formed within the viewing field was counted by timeframe progression using Zeiss LSM5 Image Browser. The number of cell-cell contacts formed was normalized by the number of cells present in the first frame analyzed. ANOVA, followed by Tukey's Least Significant Difference, was performed to determine significant differences between groups, with $p < 0.05$ considered statistically significant.

Zymography Analysis of MMPs Present in 3D Time Lapse Culture Medium

At the end of the time lapse observation period, culture medium was collected from each experimental group. The medium was run on a 10% gelatin zymography gel (Biorad) under SDS denaturing conditions. After electrophoresis, the gel was removed and placed in renaturing buffer (Triton X-100, 2.5%) for 30 min to allow MMP activity at the final location on the gel. The gel was then transferred to zymogram developing buffer overnight (50 mM Tris base, 40 mM Tris-HCl, 0.2 M NaCl, 5 mM CaCl₂, 0.02% Brig 35). The gel was stained with Coomassie blue to determine the molecular weights of present MMPs by viewing areas of gel degradation.

RESULTS

Polymer Characterization

Conjugation of QK to acryloyl-PEG-SMC was confirmed by MALDI-TOF, which showed a distribution of PEG-QK species around 5000-7000 Da, which corresponds to one acryloyl-PEG molecule per QK, with the distribution due to the polydispersity of the acryloyl-PEG-SMC used in the reaction. Each species is about 44 Da different from the next species, which corresponds to the molecular weight of one ethylene glycol repeat in the PEG chain. Additionally, the peptide QK was not detected by MALDI-TOF at its molecular weight of 2036 Da, suggesting complete reaction of all peptide in the synthesis reaction. Conjugation of RGDS to acryloyl-PEG-SMC was confirmed via GPC, which showed the product PEG-RGDS to have a higher molecular weight and hydrodynamic size than PEG-SMC. Conjugation of PEG-PQ-PEG was similarly confirmed via GPC. Conjugation of VEGF to acryloyl-PEG-SMC was confirmed via Western blot.

Bioactivity of PEG-QK Determined by Pro-mitotic Effects

Bioactivity of PEG-QK was measured by its pro-mitotic effects on endothelial cells. Proliferation was measured by counting cell number after treatment with bioactive media containing VEGF, QK, PEG-QK, or no VEGF (Control). PEG-QK increased endothelial cell number 1.27 ± 0.02 fold and VEGF increased endothelial cell number 1.25 ± 0.05 fold, compared to a 1.09 ± 0.10 fold increase in response to unpegylated QK.

The apparent low bioactivity of unpegylated QK may be due to its low solubility in cell medium. PEG-QK appears to have sufficient solubility in water for ease of use. The PEG-QK and VEGF results were not statistically different from each other and are in range of VEGF proliferation expected results [Zisch 2003]. Both VEGF, as the positive control, and PEG-QK promoted a proliferation response that was statistically higher than the No VEGF control, with ** $p < 0.01$ between PEG-QK and Control as well as VEGF and Control, and * $p < 0.05$ between PEG-QK and QK as well as VEGF and QK (Figure 4-2).

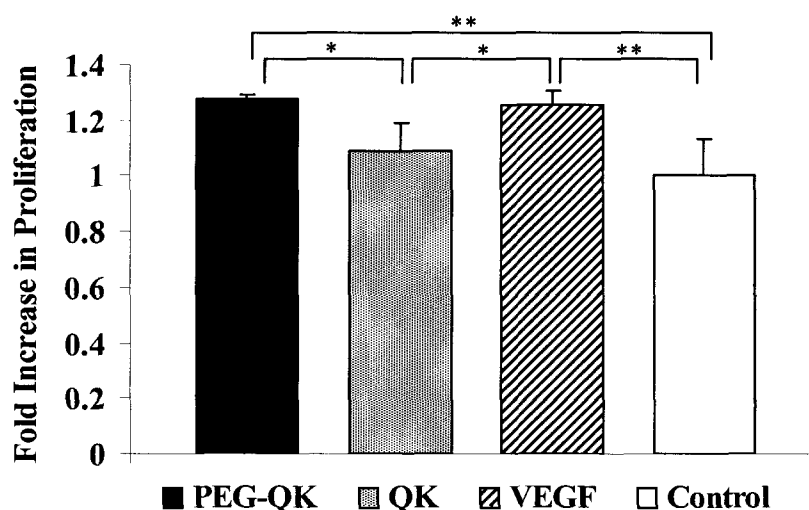


Figure 4-2 Bioactivity of PEG-QK was determined by measuring its pro-mitotic effects on endothelial cells. PEG-QK showed statistically similar results to VEGF in promoting cell proliferation, as determined by cell number after treatment. Cells were treated with EGM-2 medium without VEGF and FGF, with added PEG-QK, QK, or VEGF for 4 h. Cells were then cultured in EGM-2 medium without VEGF and FGF for 2 d. Cells were stained with Hoechst 33342 nuclear dye and imaged. Cell number was analyzed, and ANOVA, followed by Tukey's Least Significant Difference post-hoc analysis showed significant differences between experimental groups (* $p < 0.05$, ** $p < 0.01$).

Quantification of PEG-QK, PEG-VEGF, and PEG-RGDS on the Surface of Hydrogels

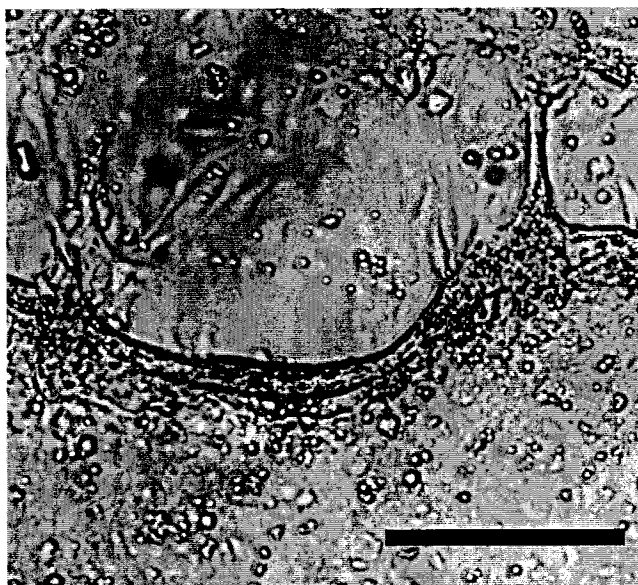
PEG-QK hydrogels had an average of 2.59 ± 1.17 nmol/cm² PEG-QK on the surface. PEG-VEGF hydrogels had an average of 4 ± 0.84 pmol/cm² PEG-VEGF on the surface. Although added amounts were calculated to equalize bioactivity levels between gels, it appears that more PEG-QK was successfully attached to the surface, leading to a 1.7 fold increase in bioactivity level on the PEG-QK gels as compared to the PEG-VEGF gels. All hydrogels had an average of 8.0 ± 2.1 nmol/cm² PEG-RGDS on the surface. Levels of PEG-RGDS were appropriate for long-term cell attachment and equal between all experimental groups.

Surface-immobilized VEGF Promotes Tubulogenesis

In previous work, PEG-VEGF promoted endothelial tubulogenesis on the surface of hydrogels by day 30, with tubules appearing as early as day 19 on some hydrogels (Chapter 2). In contrast, PEG-QK promoted endothelial tubulogenesis after only 5 d in culture, with extensive branching networks of endothelial tubes on hydrogels modified with PEG-QK and PEG-RGDS. Control hydrogel surfaces modified with PEG-VEGF and PEG-RGDS or only PEG-RGDS allowed HUVEC attachment and growth, but did not promote tubulogenesis by this early time point. Hydrogels modified with PEG-RGDS and PEG-QK promoted significantly more tubulogenesis at day 5 than those modified with PEG-RGDS and PEG-VEGF or PEG-RGDS alone (Figure 4-3, Figure 4-4, Figure 4-5; $p < 0.05$). Endothelial cells grown on hydrogels modified with PEG-QK and PEG-RGDS, cultured without VEGF in the medium, formed tubules totaling

$395 \pm 302 \mu\text{m}/\text{mm}^2$, while cells on hydrogels modified with PEG-RGDS and PEG-VEGF, cultured without VEGF in the medium, formed tubules totaling $72 \pm 62 \mu\text{m}/\text{mm}^2$, and cells on hydrogels modified with PEG-RGDS only, cultured without VEGF in the media, formed tubules totaling $117 \pm 200 \mu\text{m}/\text{mm}^2$. Levels of tubulogenesis on hydrogels with PEG-VEGF and PEG-RGDS were not significantly different than PEG-RGDS only. By day 15, some endothelial tubules on PEG-QK hydrogels had regressed (total tubule length/area = $286 \pm 145 \mu\text{m}/\text{mm}^2$). Additionally, by this time point, there were more tubules on PEG-VEGF ($535 \pm 82 \mu\text{m}/\text{mm}^2$) and PEG-RGDS ($519 \pm 704 \mu\text{m}/\text{mm}^2$) hydrogels, although there were no significant differences between groups at day 15. It is likely that the early tubulogenic response from PEG-QK was followed by tubule regression because the endothelial tubules were not supported by mural cells to encourage maturation of the endothelial tubule network. The addition of mural cells, such as pericytes, may act to prevent regression of early tubes formed in response to PEG-QK [Jain 2003].

A



B

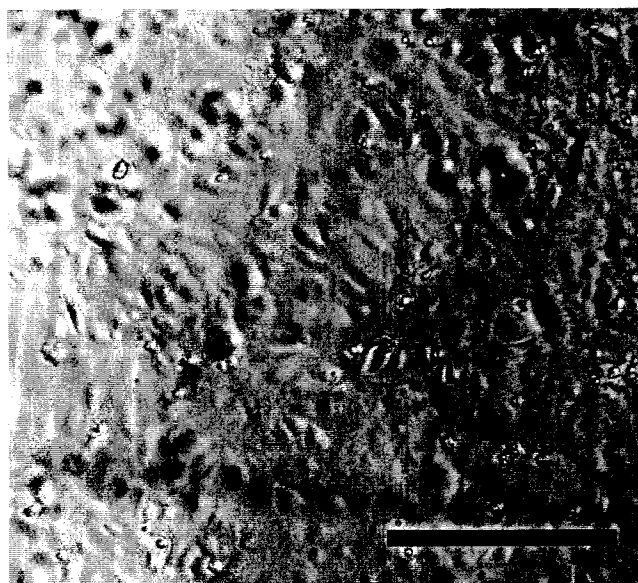


Figure 4-3 A) Branching endothelial tubule networks formed on the surface of hydrogels modified with RGDS and QK at 5 d. B) Fewer tubules formed on hydrogels modified with RGDS only at 5 d. Scale bar = 250 μ m.

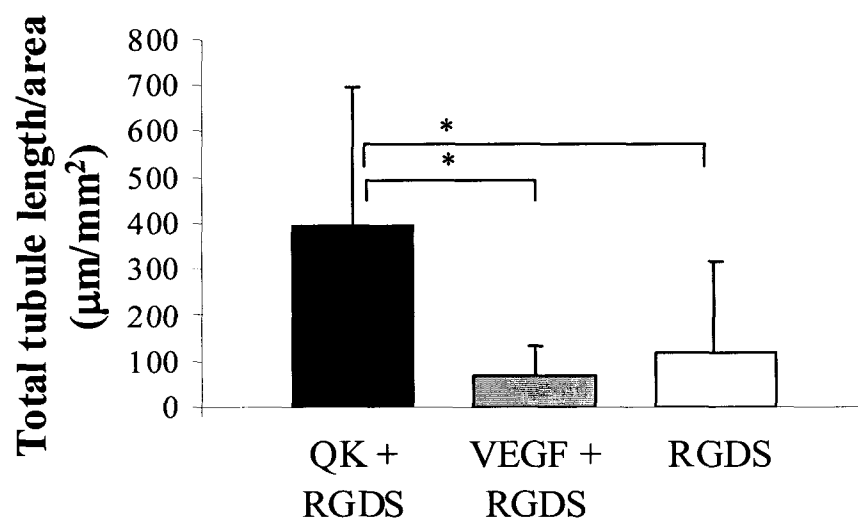


Figure 4-4 Surface endothelial tubule formation at day 5 on the surface of modified PEGDA hydrogels. PEG-QK promoted an acceleration of tubule formation compared to PEG-VEGF. * $p < 0.05$ between groups, following ANOVA and Tukey's Least Significant Difference analysis.

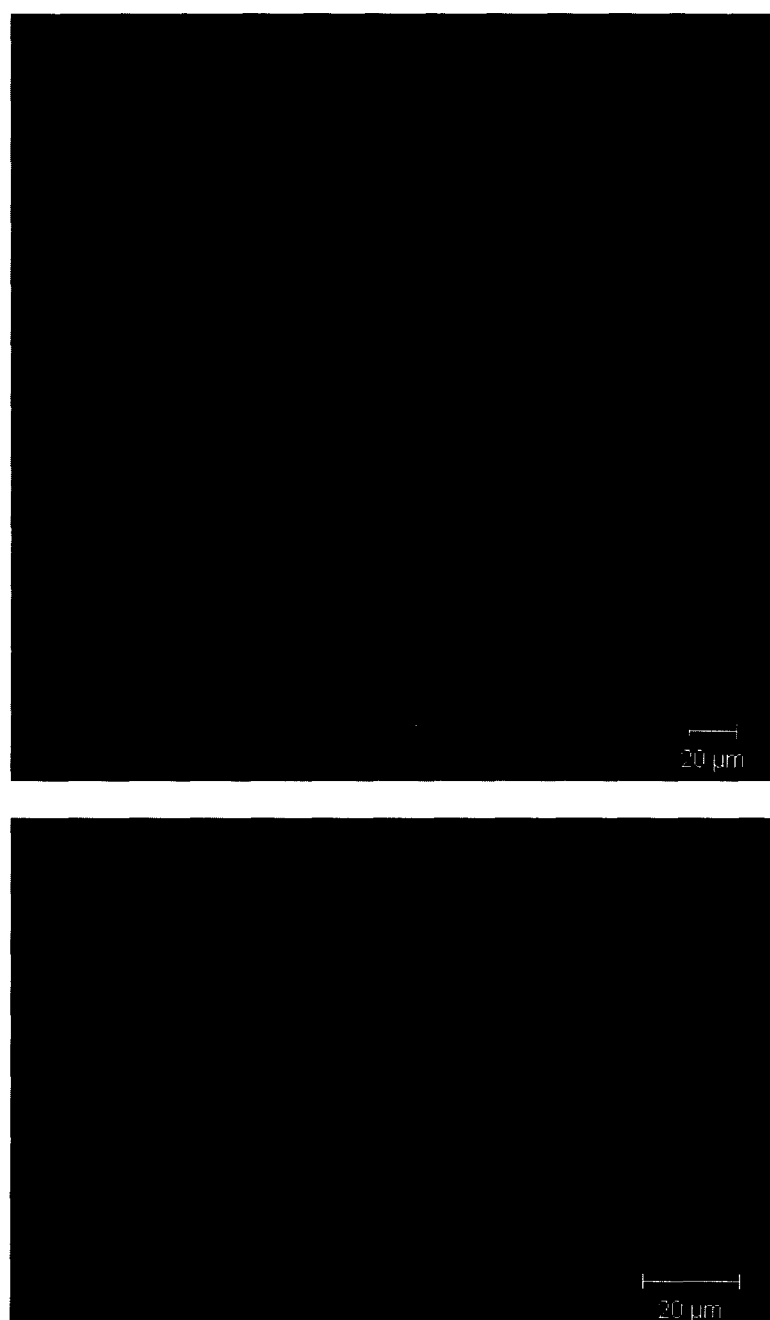


Figure 4-5 Confocal images of tubule networks on the surface of PEG-QK gels. Cells were labeled with phalloidin (red) and DAPI (blue) to visualize actin cytoskeleton and nuclei, respectively. Tubules were confirmed to rise above the plane of spread cells on the hydrogel surface. Low levels of DAPI and phalloidin are seen in background from spread cells.

Immobilized QK in 3D Collagenase-Degradable Hydrogels Promotes Tubulogenesis and Cell-Cell Contact Formation

In 3D PEG hydrogels with immobilized QK, endothelial cells exhibited extensive angiogenic behavior, as observed by time lapse confocal microscopy. Between 17-35 h after encapsulation, HUVECs formed elongated multiple-cell structures in hydrogels with RGDS and QK or RGDS and VEGF homogeneously and covalently bound to the matrix but less so in hydrogels with RGDS only (Figure 4-6, Figure 4-7, Figure 4-8, and Figure 4-9).

Figure 4-6 Time series of confocal images illustrating cell behavior in 3D collagenase-degradable PEG hydrogels. White arrows point to cell migration, cell-cell contact formation, and tubule formation. Yellow arrows and lines show path of cell migration and network formation. Cellular migration, cell-cell contact formation, and branching tube formation inside collagenase-degradable PEGDA hydrogels modified with PEG-QK (152 nmol/ml) and RGDS. Scale bar = 50 μm .

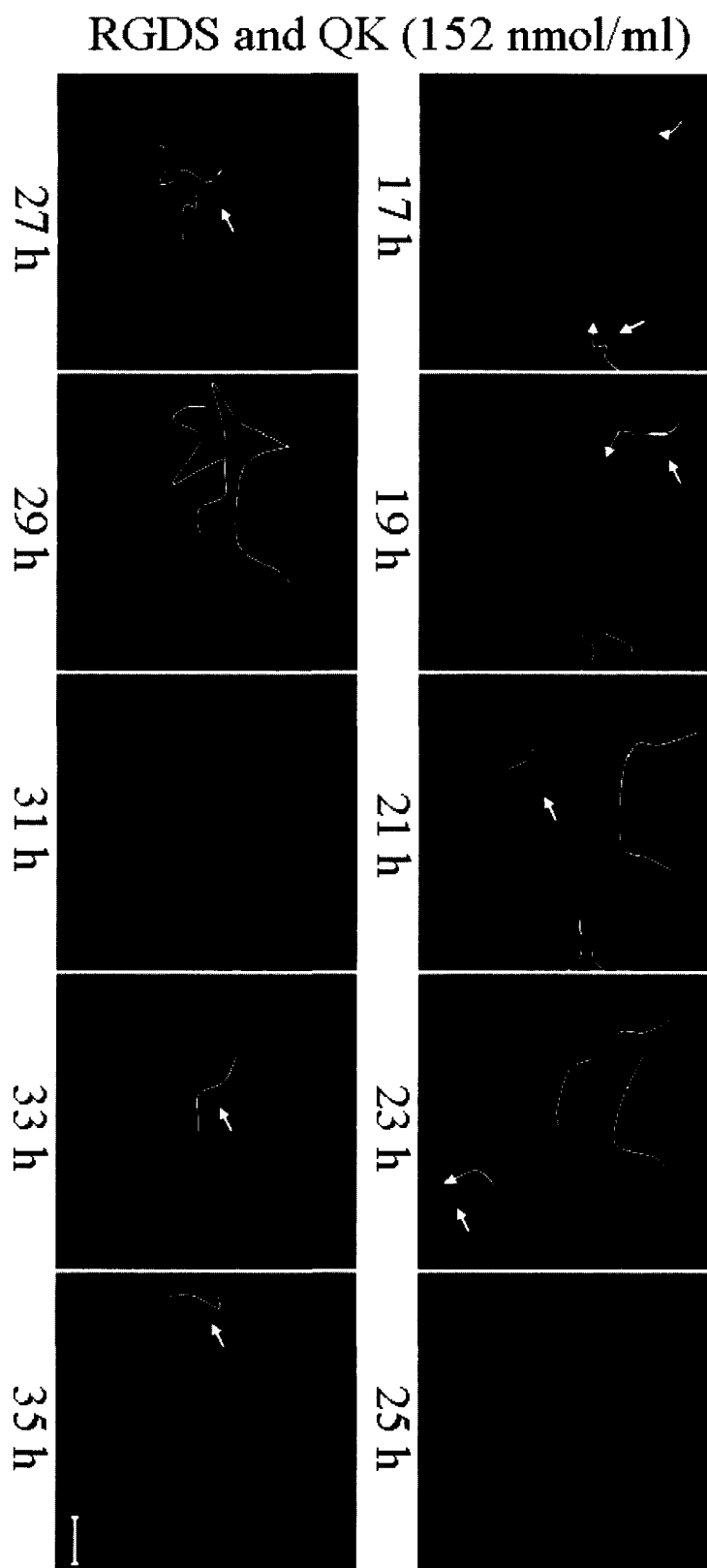


Figure 4-7 Time series of confocal images illustrating cell behavior in 3D collagenase-degradable PEG hydrogels. White arrows point to cell migration, cell-cell contact formation, and tubule formation. Yellow lines show path of network formation. Angiogenic activity in response to a 5-fold increase in attached PEG-QK. Scale bar = 50 μ m

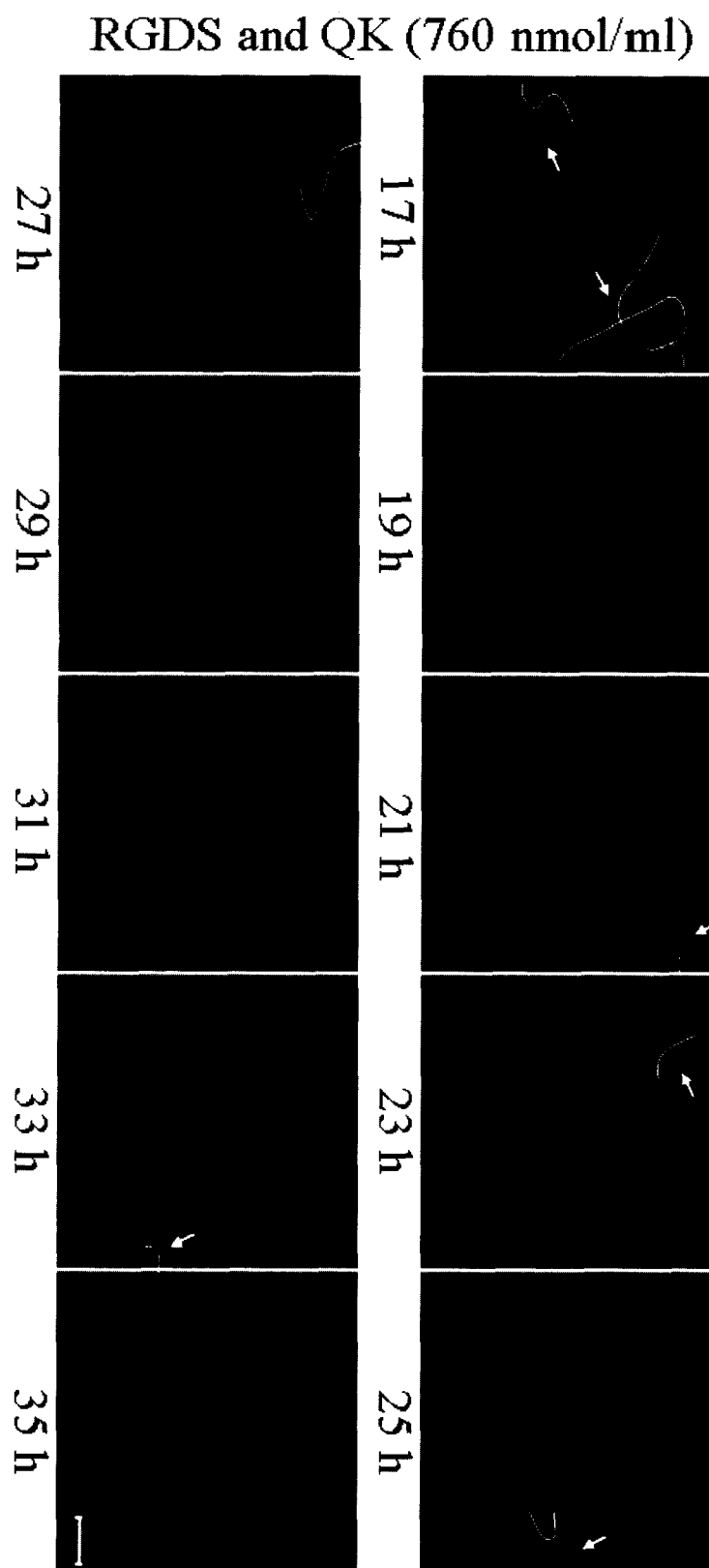


Figure 4-8 Time series of confocal images illustrating cell behavior in 3D collagenase-degradable PEG hydrogels. White arrows point to cell migration, cell-cell contact formation, and tubule formation. Yellow arrows and lines show paths of cell migration and network formation. Angiogenic activity in response to PEG-VEGF (400 pmol/ml). Scale bar = 50 μ m

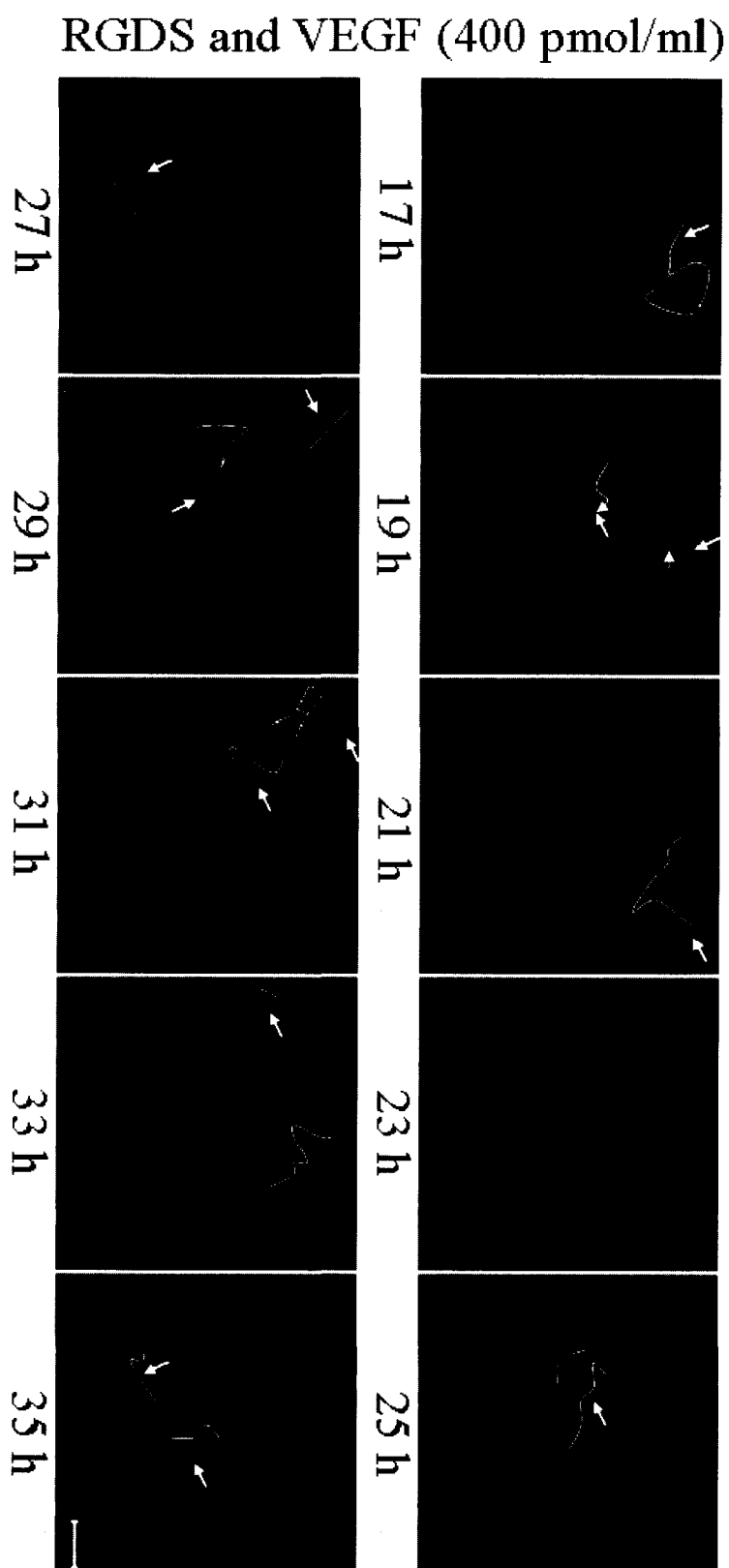
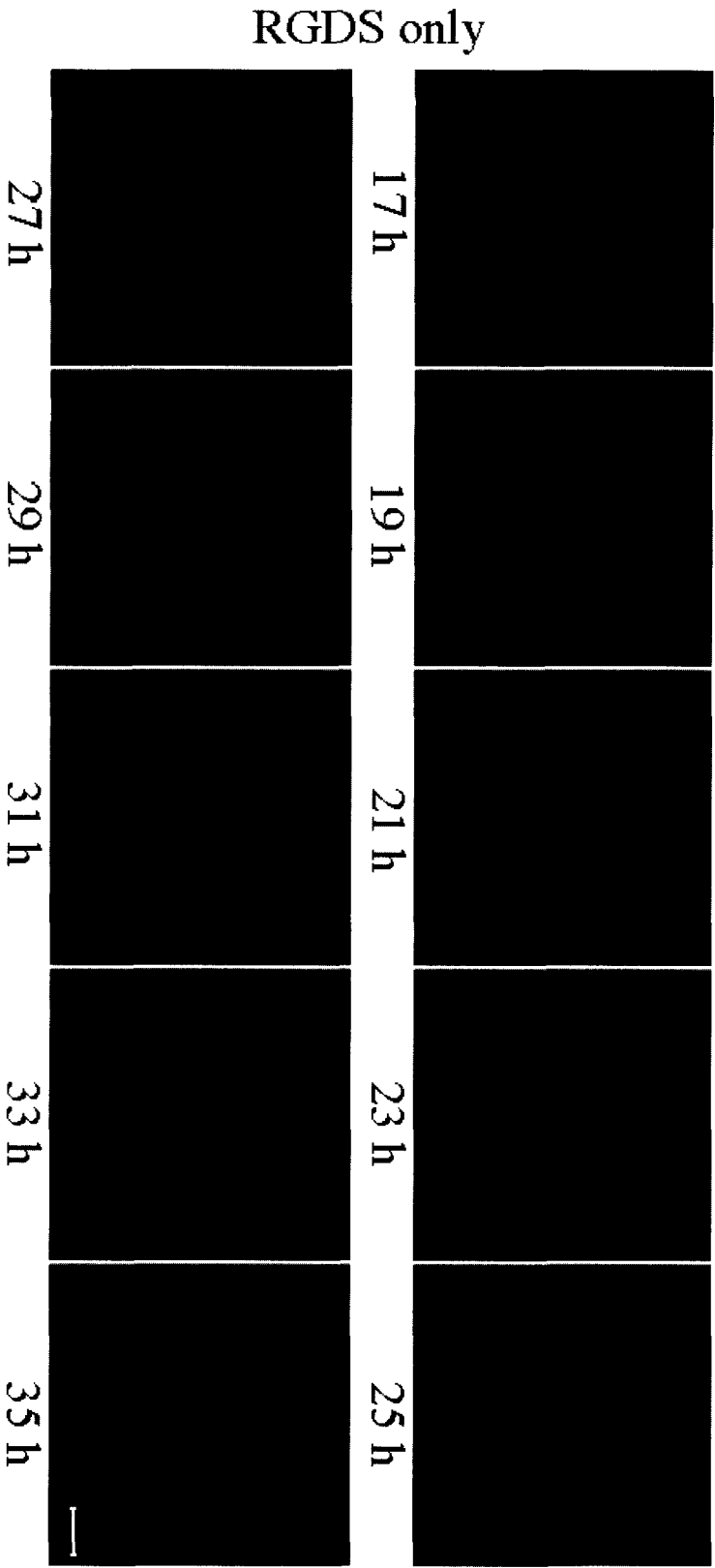


Figure 4-9 Time series of confocal images illustrating cell behavior in 3D collagenase-degradable PEG hydrogels. Less cellular activity in hydrogels modified with RGDS only. Scale bar = 50 μm .



Total tubule length per area was significantly higher in QK and VEGF hydrogels compared to RGDS-only hydrogels (Figure 4-10, $p < 0.05$). Cell-cell contact number was normalized to the number of cells in the initial frame of the time lapse data. Cells in QK-modified hydrogels formed 1.2 times more cell-cell contacts than cells in hydrogels with RGDS only and showed similar trends to cell-cell contact formation in hydrogels with VEGF and tubulogenesis results (Figure 4-11). Quantification of cell migration did not show an increase in cell migration in QK or VEGF hydrogels as compared to RGDS only. Both migration and cell-cell contact formation through surface projections are fundamental behaviors during angiogenesis [Ausprunk 1977]. While migration was not affected by the introduction of QK or VEGF in this study, endothelial cells formed tubule networks in QK and VEGF hydrogels, most likely through an increase in proliferation and organization, instead of migration. Additionally, the small increase in cell-cell contact in QK and VEGF hydrogels suggests that another cellular activity, such as cellular self-organization, may be responsible for the increase in tubule network length. Recent findings support this hypothesis, as several pathways exist after VEGFR2 dimerization, leading to specific cell responses (Figure 4-12) [Siekman 2008]. While one pathway leads to cell migration and actin remodeling, which would be required in cell-cell contact formation, a separate pathway leads to proliferation, tubule formation, and gene expression. In fact, the bifurcation of signaling pathways is essential in sprouting angiogenesis, in which some cells must migrate, while others remain in the pre-existing tubule structure to proliferate and allow the tube to grow [Siekman 2008].

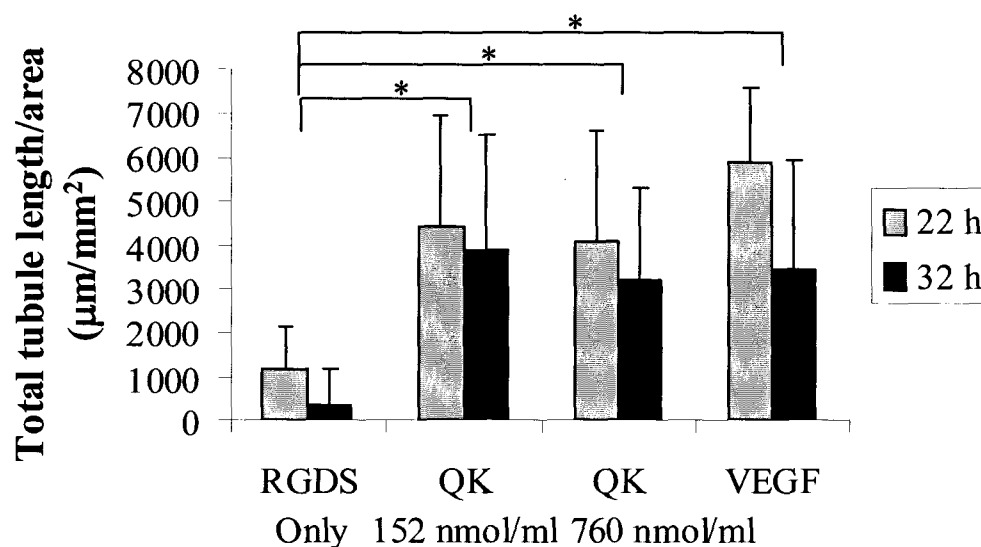


Figure 4-10 PEG-QK and PEG-VEGF promote endothelial tubule network formation in 3D collagenase-degradable hydrogels, but PEG-RGDS does not. Asterisk signifies statistical significance of $p < 0.05$ between QK groups and RGDS as well as VEGF and RGDS. Comparisons were made between results from the same time point (22 h v 22 h and 32 h v 32 h). The drop in tubule length within the VEGF experimental group between 22 h and 32 h was also statistically significant ($*p < 0.05$). The drops in tubule length in the QK groups were not statistically significant.

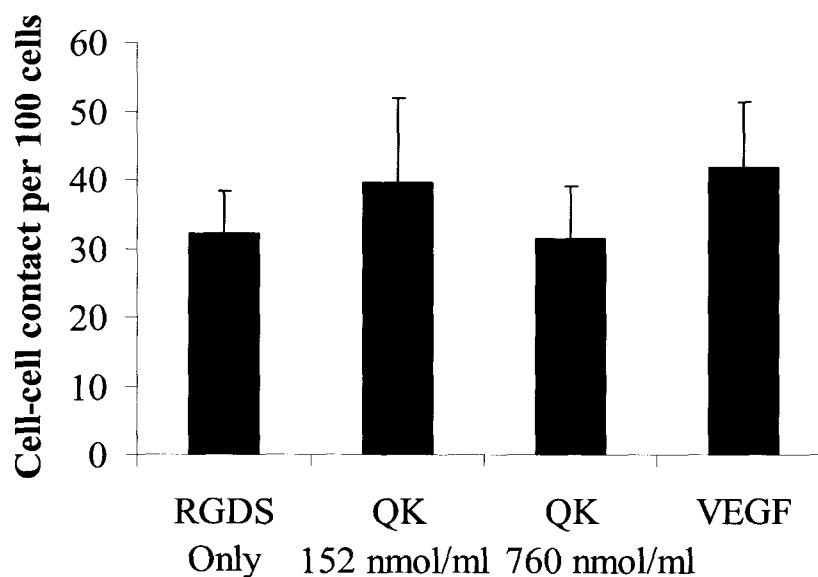


Figure 4-11 Cell-cell contact formation may respond to inclusion of QK or VEGF. Results of cell-cell contact formation follow trends of tubule length, suggesting a relationship between the two. No group had significantly more cell-cell contacts formed during the experimental observation from 2-32 h.

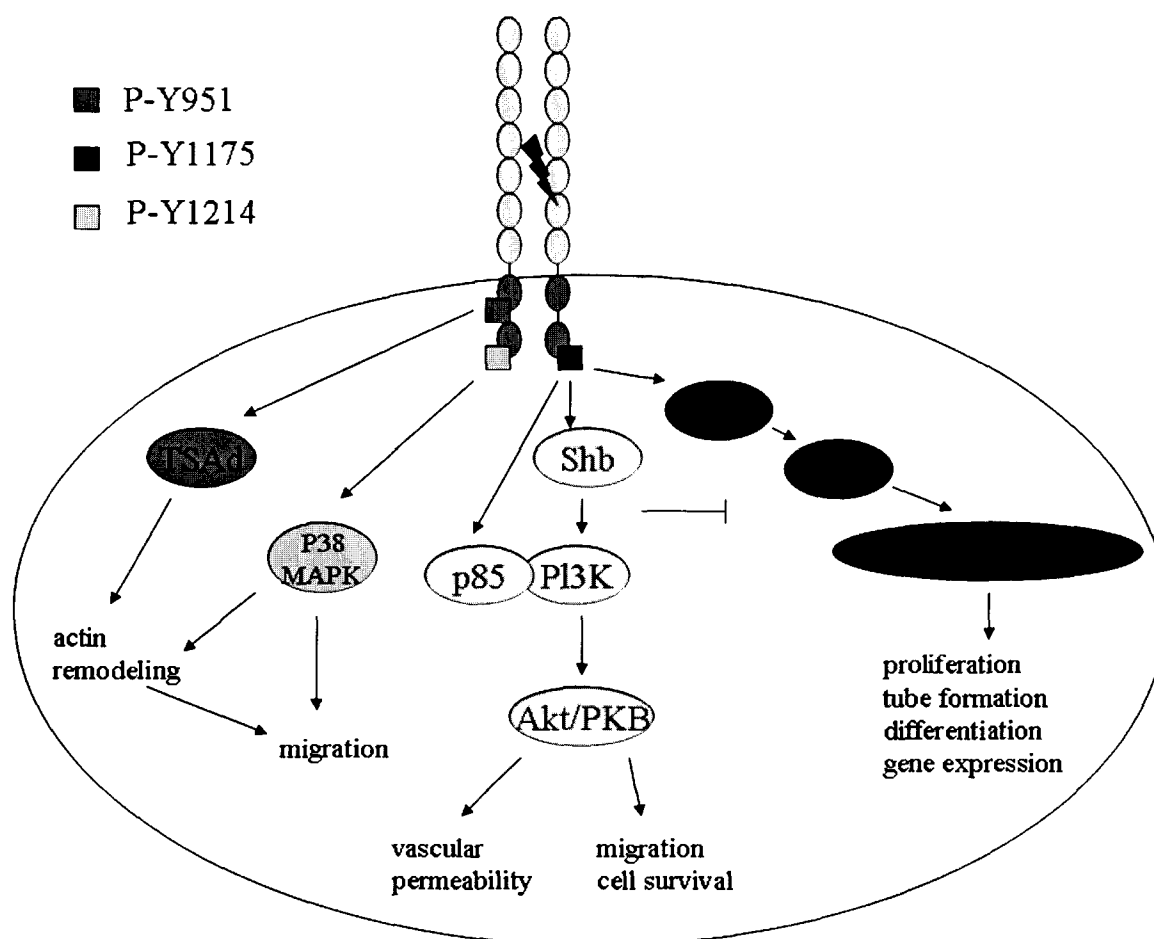


Figure 4-12 Several downstream pathways exist after VEGFR-2 dimerization. Phosphorylation of specific tyrosine residues determines which pathways are activated. Activation of the pathway for gene expression, differentiation, proliferation, and tube formation, as observed with PEG-QK, is the result of phosphorylation of Y1175, the most important tyrosine residue [Siekman 2008]. Other pathways lead to migration and actin remodeling, which would be responsible for cell-cell contact formation. Adapted from [Siekman 2008].

Time lapse confocal microscopy showed endothelial tubes regressing after 44 h for QK and 54 h for VEGF hydrogels, most likely due to the absence of mural cells, such as pericytes, that stabilize forming capillaries. HUVEC migratory behavior in QK hydrogels continued until the study ended, suggesting that the covalently-bound QK retained bioactivity throughout the study and was able to induce angiogenesis:

endothelial cell-cell contact formation, cellular self-organization, and endothelial tubule network formation.

Zymography Analysis of MMPs Present in 3D Time lapse Culture Medium

Zymography analysis of the culture medium from the observed collagenase-degradable hydrogels showed the presence of both MMP-2 and MMP-9. These MMPs correspond to those found during angiogenesis and are also able to cleave the PQ sequence in the collagenase-degradable hydrogels. Both pro-MMP forms and active forms were present in the medium in all experimental groups (Figure 4-13).

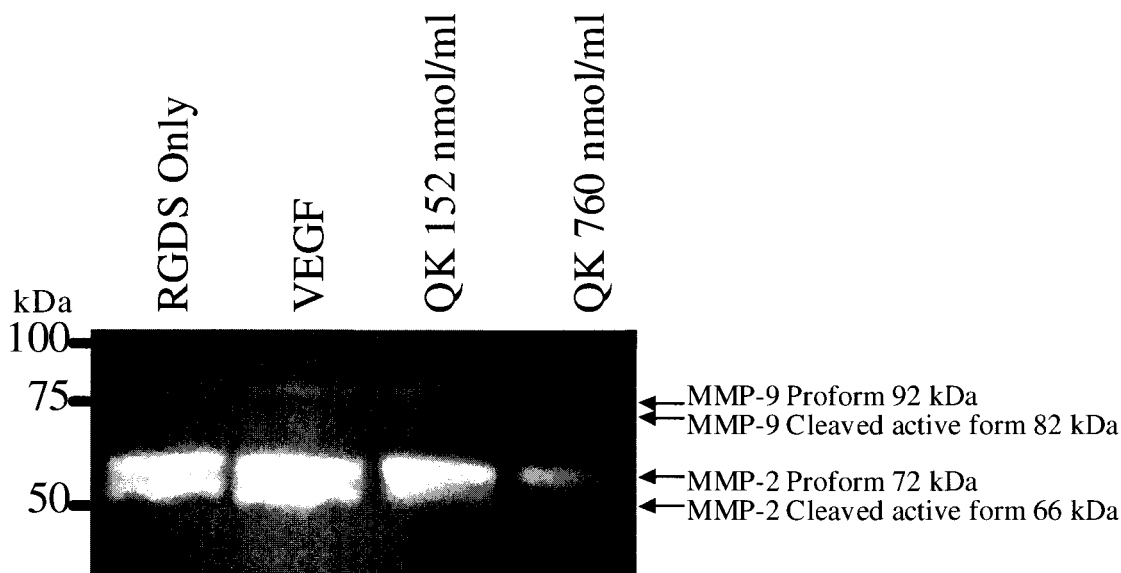


Figure 4-13 Zymogram of MMPs present in culture medium from 3D collagenase-degradable hydrogels with encapsulated endothelial cells. MMPs were run on a gelatin gel, thereby allowing visualization of pro- and active forms of MMP-2 and MMP-9, both of which are active during angiogenesis.

MMP amounts were not quantified, and thus, there may be more in hydrogels with QK or VEGF. The presence of MMP-2 and -9 in all experimental groups correlates with results of cell migration and cell-cell contact formation, in which experimental groups did not differ significantly from one another. These results further support that the increase in tubule formation is most likely due to cellular self-organization, that is, the ability to retain long-lasting cell-cell contacts to form long networks of tubules, and that the increase in tubule formation is most likely not due to an increase in MMP activity in this experimental environment.

DISCUSSION AND CONCLUSIONS

D'Andrea et al. made a useful discovery when they found that a synthesized peptide mimicking the VEGF region that binds VEGF receptors, with some amino acids altered to guarantee an α -helix conformation, would bind to and activate VEGF receptors responsible for the induction of angiogenesis. Their experiments showed that their 15-amino-acid peptide, QK, could promote endothelial cell proliferation and tubulogenesis in a Matrigel assay when added to culture medium.

D'Andrea did not examine the effects of sequestering QK in a matrix. Because PEG hydrogels have been shown to support angiogenic activity when modified with bioactive peptides and proteins, they were used as a matrix material to examine the angiogenic effects of covalently linked QK. This work showed that QK retains bioactivity when linked to a 3.4 kDa PEG chain, as shown by its effects on endothelial proliferation. Additionally, PEG-QK induced a significant tubulogenic response on the surface of PEG hydrogels. When covalently linked into a three-dimensional proteolytically-degradable hydrogel network, PEG-QK also promoted a significant increase in tubule network formation compared to hydrogels without an angiogenic signaling factor. The activity of PEG-QK was compared to that of PEG-VEGF in 2D and 3D. Studies show that PEG-QK induced an accelerated angiogenic response on the surface of hydrogels compared to PEG-VEGF, with tubule networks appearing as early as day 5 on QK-modified hydrogels. Three-dimensional time lapse results show that covalently linked QK promoted statistically similar levels of tubule formation as PEG-VEGF as measured at 22 h and 32 h. PEG-QK did not promote significant levels of cell

migration or cell-cell contact formation. These activities are promoted through a separate cell-signaling pathway, which PEG-QK may not activate. Additionally, D'Andrea et al. showed that QK activates ERK1/2, and current reported results are in agreement that the activities promoted by PEG-QK, proliferation and tube formation, are commonly attributed to the ERK1/2 pathway. Zymography results confirm that both MMP-2 and MMP-9 were activated in three-dimensional hydrogels. These enzymes are necessary for initiation of angiogenic activity *in vivo* [Roy 2006]. Presence of MMP-2 and MMP-9 did not appear to be dependent on the presence of PEG-QK, however, as these enzymes were also detected in cell culture medium from RGDS-only controls. Because MMP-2 and MMP-9 activity is considered requisite for angiogenesis, their presence in all experimental groups suggests that the collagenase-degradable hydrogels are a favorable environment for angiogenic activity and may encourage low levels of angiogenic activity, which can be increased via QK or VEGF signaling. These results suggest that the covalent incorporation of the angiogenic peptide QK could be used to promote angiogenesis in tissue engineered matrices.

The current work shows the success of incorporating a covalently-linked 15-amino acid biomimetic peptide into a tissue engineering matrix to promote angiogenesis. This novel work may lay the foundation for other similar studies in promoting desired cellular behaviors. Published work in the field of matrix modification has concentrated on incorporating full proteins into scaffold materials to promote cellular behaviors, with the one exception of ECM-mimetic peptides to promote cell adhesion. There is no known current published research in which bioactive peptides are incorporated into tissue engineering matrices to promote angiogenesis. Indeed, it appears that all studies

incorporating peptides use ECM-mimetic peptides to promote cell adhesion or protein attachment to ECM proteins (e.g. collagen binding peptides). Due to the popularity of incorporating small cell adhesion peptides, it is possible to imagine the possibilities of using biomimetic angiogenic peptides for therapy. There may be clear advantages to incorporating a small peptide instead of a large protein. First, the use of a synthesized peptide allows more flexibility of engineered design for desired bioactivity without the requirement for modifying protein expression in bacterial production. QK was synthesized to allow only one PEG chain per peptide. The native VEGF protein dimer can be modified with up to approximately 50 PEG chains, leading to a distribution of reaction products. Excess PEG chains may cause steric hindrance during ligand-receptor binding. Additionally, smaller peptides may be easier to incorporate into bioactive scaffolds, as diffusion into a scaffold may be faster and more complete. This finding could specifically be used in three-dimensional photopatterning of collagenase-degradable hydrogels, in which the hydrogel is first formed, followed by diffusion of the bioactive moiety into the hydrogel, subsequent photocrosslinking, and removal of uncrosslinked factors. Furthermore, this work shows that the bioactive QK peptide retains its bioactivity in reaction conditions containing organic solvents, in this case DMSO. Native proteins characteristically lose bioactivity in such solvents. This characteristic allows more workability using QK than VEGF in chemical formulations. Additionally, it is unlikely that the body would mount an immune response to a 15-amino-acid peptide. Therefore, PEG-QK bioactivity may be prolonged compared to PEG-VEGF *in vivo* and should be studied in the future.

PEG-QK has been shown to promote angiogenesis in PEG hydrogels, without the use of sequestered growth factor proteins. Just as most researchers have come to agree that it is more advantageous to include cell-adhesive peptides rather than full-sized ECM proteins in engineered matrices, this novel work introduces the use of a covalently linked angiogenic peptide, PEG-QK, as a comparable and possibly more favorable angiogenic factor than PEG-VEGF for covalent incorporation in scaffolds to promote angiogenesis.

Chapter 5 Conclusions and Future Directions

THESIS SUMMARY

The difficulty of incorporating microvascular networks within engineered tissues currently acts as a roadblock to the advancement of the tissue engineering field. In the body, capillary networks act to transport oxygen, nutrients, and waste to cells, and most cells are within $\sim 100\ \mu\text{m}$ of a blood capillary [Sieminski 2005]. Microvascular networks form in the body during angiogenesis, in which endothelial cells respond to secreted growth factors to migrate, proliferate, and form endothelial tubes [Keck 1989], which are later supported by mural cells [Betsholtz 2005]. The research reported in this thesis has explored several novel methods to promote and control angiogenic responses from endothelial cells in engineered matrices.

The objectives of the work were additive. First, studies were performed to determine the feasibility of covalently linking an angiogenic growth factor protein, vascular endothelial growth factor (VEGF), to poly(ethylene glycol) (PEG) hydrogel scaffolds to promote angiogenic behavior by endothelial cells. Modified hydrogels were characterized, and cellular responses were observed by light and confocal microscopy. Cellular behavior was tracked over days on the surface of hydrogels and over hours within three-dimensional collagenase-degradable hydrogels. Next, research was focused on the feasibility of micron-scale patterning of PEG-VEGF on the surface of hydrogels and its effect on cellular response. Several methods were tried, and Laser Scanning Lithography proved to be a desirable patterning technique to restrict VEGF immobilization to micron-scale patterns. Cellular response was observed via light and

confocal microscopy as well as immunocytofluorescence techniques to study changes in expression of angiogenic markers in response to restriction of spreading and signaling. Finally, a biomimetic peptide was incorporated into the PEG hydrogel system to explore the feasibility of using a short bioactive peptide instead of a full-size protein to promote angiogenesis. Studies of cellular response to the covalently-linked peptide mirrored those used to characterize PEG-VEGF. The additive nature of these studies allowed a continual metamorphosis of potentially valuable angiogenesis-promoting techniques using biocompatible PEG hydrogels.

CONCLUSIONS

Several specific aims were explored to improve the process of microvascularization of engineered tissue constructs. Microvascularization was induced on the surface of and within PEG hydrogels, as these matrices act as biocompatible scaffolds which allow specific material modifications to tightly control cellular behavior.

First, vascular endothelial growth factor was covalently linked to PEG hydrogels (Chapter 2). Signaling by VEGF is considered the rate-limiting step in angiogenesis [Ferrara 2003]. Results show that covalently linking PEG chains to VEGF does not negate its bioactivity. This work was the first to show that VEGF need not be cleaved from a matrix to promote angiogenic activity. Covalently linked VEGF was shown to promote endothelial tubulogenesis on the surface of PEG hydrogels by 30 d. Additionally, covalently linked VEGF was shown to promote angiogenic activity, including cell migration and cell-cell contact within 3D collagenase-degradable

hydrogels. Current published ideas about VEGF signaling suggest that VEGF must be internalized by VEGF receptors to induce a signaling cascade [Santos 2007]. Results in this thesis point to a possible alternate mechanism of VEGF signaling, in which VEGF is not internalized to the nucleus. This research shows that angiogenesis can be triggered by VEGF sequestered in the matrix, which allows the design of a controlled, engineered system that can promote local angiogenesis without the worry of unwanted systemic angiogenesis from cleaved, diffused VEGF. This result could lead to new therapeutics in which sequestered PEG-VEGF is delivered to an infarcted area of the heart or to a wound-healing site requiring angiogenic stimuli. Whereas direct injection of VEGF would increase the risk of systemic vascular permeability, leading to hypertension [Elcin 2006], a matrix-controlled angiogenic stimulus could potentially act at the local site, with increased longevity of bioactivity. Limitations of incorporating PEG-VEGF into matrices for tissue engineering applications exist. Mainly, these studies found that PEG-VEGF and endothelial cells alone cannot promote a stable three-dimensional microvascular network. It will be necessary to incorporate additional signaling growth factors and cells to stabilize the initial angiogenic response.

Secondly, VEGF signaling was further restricted by using Laser Scanning Lithography to pattern specific areas of VEGF attachment (Chapter 3). This work shows that micron-scale patterning can be used to control the location of capillary formation and accelerate the tubule formation response. This work showed that the restriction of RGDS and VEGF to thin lines (less than 70 μm wide) promoted endothelial tubule formation by day 2. Cells attached to wide lines did not form tubules by day 2, as expected from results from Chapter 2. Additionally, results show that the patterning of both VEGF and

RGDS promote endothelial tubules forming with lumens by day 2, whereas patterning of RGDS only did not produce any tubules with observed lumens, further suggesting that signaling from VEGF increased the angiogenic response of the patterned cells.

Immunocytofluorescence characterization of the cellular response on these hydrogels showed an increase in VEGFR1, VEGFR2, EphA7, and laminin expression on tubules formed on thin lines as compared to cells spread on wide lines. The increased availability of angiogenic cell surface receptors VEGFR1, VEGFR2, and EphA7 suggest that endothelial cells underwent changes in angiogenic cell-signaling pathways and gene expression in response to the restriction of spreading. Similarly, increased expression of laminin also suggests that cells on thin lines were participating in tubulogenesis to a higher degree than those allowed to remain spread. Interestingly, both VEGFR1 and VEGFR2 were upregulated, even though these tend to play protagonist roles in angiogenesis. Whereas VEGFR2 is the main signaling receptor, VEGFR1 often acts as a “decoy receptor” to bind VEGF, thus preventing its interaction with VEGFR2. In upregulating both receptors, cells seem to be trying to respond in a controlled manner to the external stimulus of spatially restricted attachment, perhaps in an effort to prevent a pathologically aggressive angiogenic response. Longer culture periods would be required to show the long-term effects of restrictions in spreading and to determine whether upregulation of either VEGFR1 or VEGFR2 remains for a longer period. The major limitation in this technique is variability of final pattern dimensions, however, this could be addressed by using more automation during the focusing step, in which a preset focal plane could be determined, or by switching to two-photon excitation, in which excitation occurs only at one plane, instead of a cone of excitation as provided by confocal

microscopy. These methods may be useful in defining micron-level control of cellular behavior in multi-cell engineered tissues. Specifically, the work presented could be used to specifically pattern the location of capillary networks within a metabolically active engineered tissue.

Lastly, results were presented from the novel use of PEG-QK, a peg-reacted biomimetic peptide derived from the receptor-binding region of VEGF (Chapter 4). This work reports the first time that an angiogenic peptide was used in a tissue engineered scaffold to promote microvascular network formation. PEG-QK was shown to retain bioactivity, as determined by its pro-mitotic effects on endothelial cells. Furthermore, PEG-QK was shown to promote an accelerated tubulogenic response on the surface of PEG hydrogels, as it promoted extensive tubule networks by day 5. Incorporation of PEG-QK in 3D collagenase-degradable hydrogels promoted endothelial tubule network formation statistically similar to that of PEG-VEGF. D'Andrea et al. showed that QK triggered an angiogenic cell signaling cascade that was not dependent on the molecule binding two receptors concurrently, as QK is too small to do this [D'Andrea 2005]. Similarly, the results in this thesis suggest that alternative angiogenic signaling pathways may be involved. Specifically, PEG-QK was shown to activate cell proliferation and tubulogenesis, but not increased migration or cell-cell contact. D'Andrea et al. did not characterize the migration and cell-cell contact formation characteristics of cells treated with soluble QK, and thus, these results are the first to show that PEG-QK, and possibly QK, may promote a functional subset of VEGF-induced angiogenic behaviors. These results may point to different signaling pathways that lead to similar end results of microvasculature formation. The use of only PEG-QK and endothelial cells led to a

preliminary endothelial tube network that regressed. Stabilization of such microvascular networks is required for a functional tissue engineering use. Stabilization could be coerced either through incorporation of additional growth factors and mural cells, or allowing host-graft anastomosis, in which host cells could provide stabilization of endothelial tubes. The use of a biomimetic peptide to promote angiogenesis in a matrix allows additional control of cell-matrix interactions by highly restricting the cell's interaction with a biochemical signal to only a short signaling peptide sequence, instead of several domains of a full-size dimeric protein. Results suggest that this restriction affects the cell's response. Further modification of the peptide sequence may reintroduce cellular behavior of migration and cell-cell contact formation. This result might be able to point to specific receptor-ligand binding domains responsible for separate, related cell behaviors. This work lays the foundation for the explorative use of other biomimetic peptides to promote desired cellular behavior.

FUTURE DIRECTIONS

The results of this thesis point to additional questions that could be determined by future research. First, these *in vitro* studies, specifically those involving PEG-VEGF and PEG-QK, warrant continued investigation using *in vivo* models in order to move them closer to clinical use. Secondly, the two-dimensional patterning studies should be expanded to three-dimensions, using novel 3D patterning techniques, allowing the formation of three-dimensional microvascular networks within bulk hydrogels. Finally, the biological signaling involved in these new biomimetic-ECM environments could be

explored; as these systems differ from those found in the body, but appear to promote similar angiogenic behaviors.

Results from Chapter 2 showing that covalently-linked PEG-VEGF promotes an angiogenic response by endothelial cells could point to new biological cellular signaling pathways involved in angiogenesis. Current research suggests that VEGF must be internalized to promote angiogenic signaling [Santos 2007]. Biologists could use covalently-linked PEG-VEGF to determine if angiogenic pathways are altered when VEGF is not internalized. Similarly, future studies could explore whether VEGF is cleaved by enzymes in undiscovered regions to release it from the multiple PEG chains attaching it to the PEG matrix. Since the completion of the work described in this thesis, PEG-VEGF has been used within the research group in a murine *in vivo* assay. Results show that it promotes increased microvascularization in collagenase-degradable hydrogels without encapsulated cells when implanted in the cornea. In this case, surrounding capillaries are attracted to the hydrogel by released VEGF and form microvascular networks within the hydrogel in response to the diffused VEGF and the covalently-linked VEGF present (Figure 5-1) [Moon 2009].

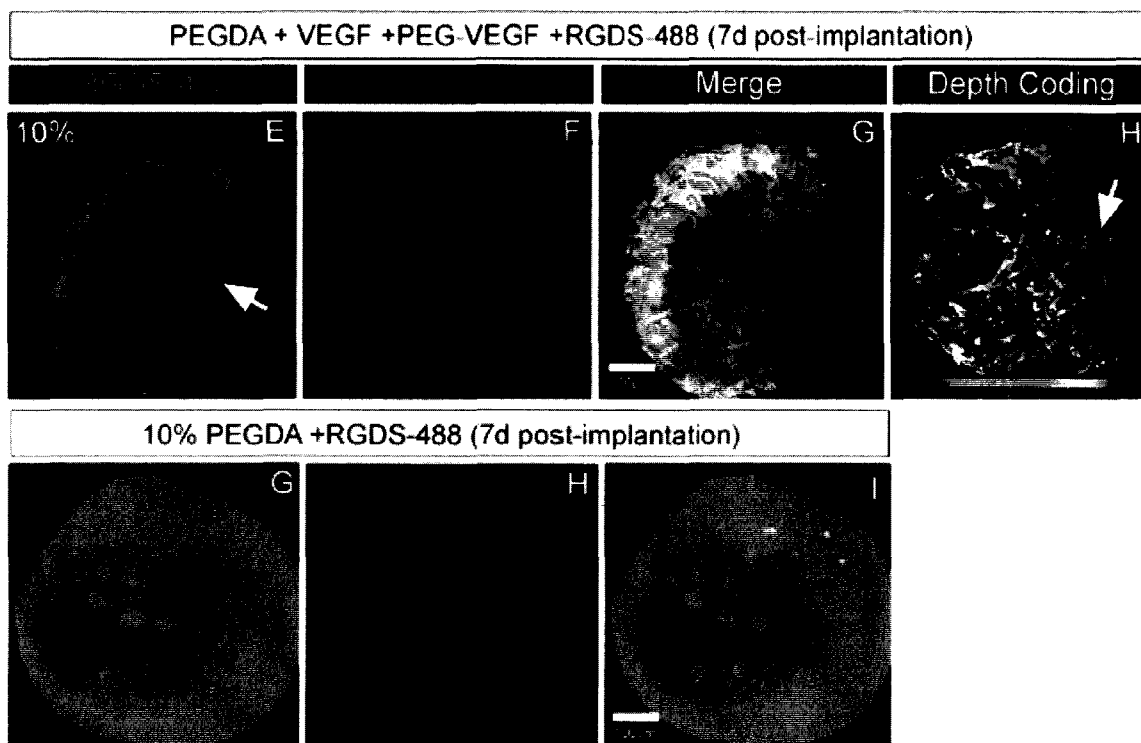


Figure 5-1 PEG-VEGF has been used in a murine cornea model based on work reported in this thesis. Results show that the incorporation of released VEGF and PEG-VEGF in collagenase-degradable hydrogels promotes infiltration of surrounding capillaries from the cornea limbus. Microvasculature is visualized by using genetically altered mice with fluorescent endothelial cells. From [Moon 2009].

Findings from Chapter 3 show that micron-scale patterning of VEGF allows precise bottom-up design of engineered matrices. Patterning could be used to create intricate control of cell placement and behavior. Specific integrin ligands could be patterned to promote designed co-cultures of cells on and within PEG hydrogels. Furthermore, three-dimensional patterning using two-photon excitation will allow the patterning of PEG-VEGF or PEG-QK within bulk hydrogels to design three-dimensional microvascular networks to support metabolically active cells performing tissue functions. Precise spatial control of tissue function within functional engineered tissues could lead to the development of highly intricate engineered organs and organ substructures, such as those found in the kidney, liver, and pancreas.

Finally, studies from Chapter 4 showing that covalently-linked PEG-QK promotes angiogenesis in PEG hydrogels *in vitro* could be expanded to *in vivo* models. PEG-QK hydrogels could be investigated in murine cornea models such as those reported using PEG-VEGF. *In vivo* models can be used to show whether the newly formed microvasculature is functional, by observing red blood cell or fluorescently-labeled dextran transport. Further, the biological cell signaling pathways involved in PEG-QK angiogenic signaling could further explain the cellular behavior in which endothelial tubule networks were formed without an increase in cell migration. A more complete understanding of the biological signaling pathways could support or suggest variations in using PEG-QK in engineered matrices to promote microvasculature formation. Additionally, studies incorporating both endothelial cells and supporting mural cells, such as pericytes, would show whether tubules formed by PEG-QK could be stabilized and maintained for functional transport.

The need for organ transplants has risen steadily in the past decade (U.S. Organ Procurement and Transplantation Network 2007). Tissue engineering of functional tissues and organs could meet demands of quantity and increase quality of tissue transplantation by incorporating techniques to reduce tissue rejection. One major limitation in tissue engineering is providing microvascular networks throughout engineered tissue for transport of nutrients, oxygen, and waste. Future studies should build upon the foundation provided by the work reported in this thesis. The research methods and findings reported show that several techniques may be used alone or in conjunction to improve microvascularization of tissue engineered constructs. Research on incorporation of PEG-VEGF and PEG-QK into hydrogel scaffolds, either as covalent

surface modification, covalent bulk incorporation, or as patterned surface modification, may provide tools for future clinically successful, therapeutic, vascularized engineered tissues.

References

- . "www.advancedbiohealing.com." from www.advancedbiohealing.com.
- . "carticel.com." from carticel.com.
- . "estrellamountain.edu." from estrellamountain.edu.
- . (2000). The Bantam Medical Dictionary. The Bantam Medical Dictionary. New York, Bantam Books.
- . (2007). U.S. Organ Procurement and Transplantation Network 2007 Annual Report.
- Aimes, R.T. and Quigley, J.P. (1995). "Matrix metalloproteinase-2 is an interstitial collagenase. Inhibitor-free enzyme catalyzes the cleavage of collagen fibrils and soluble native type I collagen generating the specific 3/4- and 1/4-length fragments." J Biological Chemistry 270(11): 5872-6.
- Atala, A., S.B. Bauer, et al. (2006). "Tissue-engineered autologous bladders for patients needing cystoplasty." Lancet 367(9518): 1241-6.
- Ausprunk, D.H. and J. Folkman. (1977). "Migration and proliferation of endothelial cells in preformed and newly formed blood vessels during tumor angiogenesis." Microvasc Res 14(1): 53-65.
- Barrett, A.J., N.D. Rawlings, et al. (1998). Handbook of Proteolytic Enzymes. Academic Press, San Diego.
- Behrens, P., T. Bitter, et al. (2006). "Matrix-associated autologous chondrocyte transplantation/implantation (MACT/MACI)--5-year follow-up." Knee 13(3): 194-202.
- Betsholtz, C. and H. Gerhardt. (2005). "Role of pericytes in vascular morphogenesis." Mechanisms of Angiogenesis. M. Clauss. Basel, Switzerland, Birkhauser Verlag: 115-125.
- Borges, J., F.T. Tegtmeier, et al. (2003). "Chorioallantoic membrane angiogenesis model for tissue engineering: a new twist on a classic model." Tissue Eng 9(3): 441-50.
- Brogi, E., T. Wu, et al. (1994). "Indirect angiogenic cytokines upregulate VEGF and bFGF gene expression in vascular smooth muscle cells, whereas hypoxia upregulates VEGF expression only." Circulation 90(2): 649-52.

- Chen, R.R., E.A. Silva, et al. (2007). "Spatio-temporal VEGF and PDGF delivery patterns blood vessel formation and maturation." *Pharm Res* 24(2): 258-64.
- Cliff, W. J. (1963). "Observations on healing tissue: A combined light and electron microscopic investigation." *Trans. Roy. Soc. London Ser. B* 246: 305-25.
- Conn, H., R. Harmel, et al. (1972). "New method for oxygen content in blood based on acrylamide polymerization." *Surg Forum* 23(0): 195-7.
- D'Andrea, L.D., G. Iaccarino, et al. (2005). "Targeting angiogenesis: structural characterization and biological properties of a de novo engineered VEGF mimicking peptide." *Proc Natl Acad Sci USA* 102(40): 14215-20.
- DeLong, S.A., A.S. Gobin, et al. (2005). "Covalent immobilization of RGDS on hydrogel surfaces to direct cell alignment and migration." *J Control Release* 109(1-3): 139-48.
- DeLong, S.A., J.J. Moon, et al. (2005). "Covalently immobilized gradients of bFGF on hydrogel scaffolds for directed cell migration." *Biomaterials* 26(16): 3227-34.
- de Vries, C., J.A. Escobedo, et al. (1992). "The fms-like tyrosine kinase, a receptor for vascular endothelial growth factor." *Science* 255(5047): 989-91.
- Dike, L.E., C.S. Chen, et al. (1999). "Geometric control of switching between growth, apoptosis, and differentiation during angiogenesis using micropatterned substrates." *In Vitro Cell Dev Biol Anim* 35(8): 441-8.
- Dike, L.E. and D.E. Ingber. (1996). "Integrin-dependent induction of early growth response genes in capillary endothelial cells." *J Cell Sci* 109 (Pt 12): 2855-63.
- Elcin, A.E. and Y.M. Elcin. (2006). "Localized angiogenesis induced by human vascular endothelial growth factor-activated PLGA sponge." *Tissue Eng* 12(4): 959-68.
- Enholm, B., K. Paavonen, et al. (1997). "Comparison of VEGF, VEGF-B, VEGF-C and Ang-1 mRNA regulation by serum, growth factors, oncoproteins and hypoxia." *Oncogene* 14: 2475-83.
- Fernandez, B. (2005). "Arterialization, coronariogenesis, and arteriogenesis." *Mechanisms of Angiogenesis*. M. Clauss. Basel, Switzerland, Birkhauser Verlag: 53-64.
- Ferrara, N. and T. Davis-Smyth. (1997). "The biology of vascular endothelial growth factor." *Endocr Rev* 18(1): 4-25.

- Ferrara, N., H. P. Gerber, et al. (2003). "The biology of VEGF and its receptors." *Nat Med* 9(6): 669-76.
- Ferrara, N. and W.J. Henzel. (1989). "Pituitary follicular cells secrete a novel heparin-binding growth factor specific for vascular endothelial cells." *Biochem Biophys Res Commun* 161(2): 851-8.
- Folkman, J. and M. Klagsbrun. (1987). "Angiogenic factors." *Science* 235(4787): 442-7.
- Gerhart, H. (2005). "How do endothelial cells orientate?" *Mechanisms of Angiogenesis*. Clauss, M. Basel, Switzerland, Birkhauser Verlag: 3-13.
- Gitay-Goren, H., S. Soker, et al. (1992). "The binding of vascular endothelial growth factor to its receptors is dependent on cell surface-associated heparin-like molecules." *J Biol Chem* 267(9): 6093-8.
- Gobin, A.S. and J.L. West. (2002). "Cell migration through defined, synthetic ECM analogs." *Faseb J* 16(7): 751-3.
- Hahn, M., J. Miller, et al. (2005). "Laser scanning lithography for surface patterning on hydrogels." *Advanced Materials* 17: 2939-42.
- Hahn, M.S., M.K. McHale, et al. (2007). "Physiologic pulsatile flow bioreactor conditioning of poly(ethylene glycol)-based tissue engineered vascular grafts." *Ann. Biomedical Engr* 35(2): 190-200.
- Harris, J.M. and S. Zalipsky. (1997). *Poly(ethylene glycol): Chemistry and biological applications*. Washington DC: American Chemical Society.
- Helm, C.L., A. Zisch, et al. (2007). "Engineered blood and lymphatic capillaries in 3-D VEGF-fibrin-collagen matrices with interstitial flow." *Biotechnol Bioeng* 96(1): 167-76.
- Houck, K.A., D.W. Leung, et al. (1992). "Dual regulation of vascular endothelial growth factor bioavailability by genetic and proteolytic mechanisms." *J Biol Chem* 267(36): 26031-7.
- Ingber, D.E. (1990). "Fibronectin controls capillary endothelial cell growth by modulating cell shape." *Proc Natl Acad Sci* 87(9): 3579-83.
- Jain, R.K. (2003). "Molecular regulation of vessel maturation." *Nat Med* 9(6): 685-93.
- Jain, R.K., P. Au, et al. (2005). "Engineering vascularized tissue." *Nat Biotechnol* 23(7): 821-3.

- Kane, R.S., S. Takayama, et al. (1999). "Patterning proteins and cells using soft lithography." *Biomaterials* 20(23-24): 2363-76.
- Keck, P.J., S.D. Hauser, et al. (1989). "Vascular permeability factor, an endothelial cell mitogen related to PDGF." *Science* 246(4935): 1309-12.
- Landua, A.J. and J. Awapara. (1949). "Use of modified ninhydrin reagent in quantitative determination of amino acids by paper chromatography." *Science* 109(2833): 385.
- Lazarous, D.F., M.S. Shou, et al. (1996). "Comparative effects of basic fibroblast growth factor and vascular endothelial growth factor on coronary collateral development and the arterial response to injury." *Circulation* 94(5): 1074-82.
- Leslie-Barbick, J.E., J.J. Moon, et al. (2009). "Covalently-immobilized vascular endothelial growth factor promotes endothelial cell tubulogenesis in poly(ethylene glycol) diacrylate hydrogels." *Journal of Biomaterials Science: Polymer Edition* 20: 1763-79.
- Leung, D.W., G. Cachianes, et al. (1989). "Vascular endothelial growth factor is a secreted angiogenic mitogen." *Science* 246(4935): 1306-9.
- Liu Tsang, V., A.A. Chen, et al. (2007). "Fabrication of 3D hepatic tissues by additive photopatterning of cellular hydrogels." *Faseb J* 21(3): 790-801.
- Lobb, R.R., M.E. Key, et al. (1985). "Partial purification and characterization of a vascular permeability factor secreted by a human colon adenocarcinoma cell line." *Int J Cancer* 36(4): 473-8.
- Lutolf, M.P., J.L Lauer-Fields, et al. (2003). "Synthetic matrix metalloproteinase-sensitive hydrogels for the conduction of tissue regeneration: engineering cell-invasion characteristics." *Proc Natl Acad Sci* 100: 5413-8.
- Mann B.K., A.T. Tsai, et al. (1999). "Modification of surfaces with cell adhesion peptides alters extracellular matrix deposition." *Biomaterials*. 20(23-24): 2281-6.
- Marston, W.A., J. Hanft, et al. (2003). "The efficacy and safety of Dermagraft in improving the healing of chronic diabetic foot ulcers: results of a prospective randomized trial." *Diabetes Care* 26(6): 1701-5.
- Mazue, G., F. Bertolero, et al. (1991). "Preclinical and clinical studies with recombinant human basic fibroblast growth factor." *Ann NY Acad Sci* 638: 329-40.
- Mazue, G., F. Bertolero, et al. (1992). "Experience with the preclinical assessment of basic fibroblast growth factor (bFGF)." *Toxicol Lett* 64-65 Spec No: 329-38.

- Mazue, G., A.J. Newman, G. et al. (1993). "The histopathology of kidney changes in rats and monkeys following intravenous administration of massive doses of FCE 26184, human basic fibroblast growth factor." *Toxicol Pathol* 21(5): 490-501.
- Moon, J.J., M.S. Hahn, et al. (2008). "Micropatterning of poly(ethylene glycol) diacrylate hydrogels with biomolecules to regulate and guide endothelial morphogenesis." *Tissue Eng Part A*. 15(3): 579-85.
- Moon, J.J., S. Lee, et al. (2007). "Synthetic biomimetic hydrogels incorporated with ephrin-A1 for therapeutic angiogenesis." *Biomacromolecules* 8(1): 42-9.
- Moon, J.J., J.E. Saik, et al. (2009). "Biomimetic collagenase-sensitive hydrogels with vasculo-conductive properties." *Nature Materials* In review.
- Muller, Y.A., B. Li, et al. (1997). "Vascular endothelial growth factor: crystal structure and functional mapping of the kinase domain receptor binding site." *Proc Natl Acad Sci* 94(14): 7192-7.
- Nillesen, S.T., P.J. Geutjes, et al. (2007). "Increased angiogenesis and blood vessel maturation in acellular collagen-heparin scaffolds containing both FGF2 and VEGF." *Biomaterials* 28(6): 1123-31.
- Padmavathi, N.Ch., P.R. Chatterji. (1996). "Structural characteristics and swelling behavior of poly(ethylene glycol) diacrylate hydrogels." *Macromolecules* 29: 1976-9.
- Pepper, M.S., N. Ferrara, et al. (1991). "Vascular endothelial growth factor (VEGF) induces plasminogen activators and plasminogen activator inhibitor-1 in microvascular endothelial cells." *Biochemical and Biophysical Research Communications* 181(2): 902-6.
- Pertovaara, L, A. Kaipainen, et al. (1994). "Vascular endothelial growth factor is induced in response to transforming growth factor in fibroblastic and epithelial cells." *J Biol Chem* 269(9): 6271-4.
- Peters, M.C., P.J. Poverini, et al. (2002). "Engineering vascular networks in porous polymer matrices." *J Biomed Mater Res* 60(4): 668-78.
- Plouet, J., J. Schilling, et al. (1989). "Isolation and characterization of a newly identified endothelial cell mitogen produced by AtT-20 cells." *Embo J* 8(12): 3801-6.
- Pötgens A.J., N.H. Lubsen, et al. (1994). "Covalent dimerization of vascular permeability factor/vascular endothelial growth factor is essential for its biological activity. Evidence from Cys to Ser mutations." *J Biol Chem* 269(52): 32879-85.

- Roberts, M.J., M.D. Bentley, et al. (2002). "Chemistry for peptide and protein PEGylation." *Adv Drug Deliv Rev* 54 (4): 459-76.
- Robinson C.J. and S.E. Stringer. (2001). "The splice variants of vascular endothelial growth factor (VEGF) and their receptors." *J Cell Sci.* 114(Pt 5): 853-65.
- Roy, R., B. Zhang, et al. (2006). "Making the cut: protease-mediated regulation of angiogenesis." *Exp Cell Res* 312(5): 608-22.
- Ruoslahti, E. (2003). "The RGD story: a personal account." *Matrix Biology* 22: 459-65.
- Santos, S.C.R., C. Miguel, et al. (2007). "VEGF and VEGFR-2 (KDR) internalization is required for endothelial recovery during wound healing." *Experimental Cell Research.* 313: 1561-74.
- Senger, D.R., D.T. Connolly, et al. (1990). "Purification and NH₂-terminal amino acid sequence of guinea pig tumor-secreted vascular permeability factor." *Cancer Res* 50(6): 1774-8.
- Siekman, A., L. Covassin. (2008). "Modulation of VEGF signaling output by the Notch pathway." *BioEssays* 30: 303-13.
- Sieminski, A.L., R.P. Hebbel, et al. (2005). "Improved microvascular network in vitro by human blood outgrowth endothelial cells relative to vessel-derived endothelial cells." *Tissue Eng* 11(9-10): 1332-45.
- Springer, M.L., A.S. Chen, et al. (1998). "VEGF gene delivery to muscle: potential role for vasculogenesis in adults." *Mol Cell* 2(5): 549-58.
- Sutherland, R.M., B. Sordat, et al. (1986). "Oxygenation and differentiation in multicellular spheroids of human colon carcinoma." *Cancer Res* 46(10): 5320-9.
- Unemori, E.N., N. Ferrara, et al. (1992). "Vascular endothelial growth factor induces interstitial collagenase expression in human endothelial cells." *J Cell Physiol* 153(3): 557-62.
- van Hinsbergh, V.W., P. Koolwijk, et al. (2005). "The hemostatic system in angiogenesis." *Exs* 94: 247-66.
- Vincenti, V., C. Cassano, et al. (1996). "Assignment of vascular endothelial growth factor gene to human chromosome 6p21.3." *Circulation* 93: 1493-5.
- Wang, H.U., Z.F. Chen, et al. (1998). "Molecular distinction and angiogenic interaction between embryonic arteries and veins revealed by ephrin-B2 and its receptor Eph-B4." *Cell* 93(5): 741-53.

- West, J.L. and J.A. Hubbell. (1999). "Polymeric biomaterials with degradation sites for proteases involved in cell migration." *Macromolecules* 32: 241-4.
- Whitesides, G.M., E. Ostuni, et al. (2001). "Soft lithography in biology and biochemistry." *Annu. Rev. Biomed. Eng.* 3: 335-73.
- Zachary, I. (2005). *Signal Transduction in Angiogenesis. Mechanisms of Angiogenesis*. M. Clauss. Basel, Switzerland, Birkhauser Verlag: 267-300.
- Zisch, A.H., M.P. Lutolf, et al. (2003). "Cell-demanded release of VEGF from synthetic, biointeractive cell ingrowth matrices for vascularized tissue growth." *Faseb J* 17(15): 2260-2.